

Investigations on the function of *ten-1* during embryonic
development in *Caenorhabditis elegans*.

Inauguraldissertation

zur

Erlangung der Würde eines Doktors der Philosophie

vorgelegt der

Philosophisch-Naturwissenschaftlichen Fakultät

der Universität Basel

von

Ulrike Topf

aus Dresden, Deutschland

Basel, 2011

Genehmigt von der Philosophisch-Naturwissenschaftlichen Fakultät auf Antrag von

Prof. Ruth Chiquet-Ehrismann

Prof. Markus Affolter

Basel, den 14. 12. 2010

Prof. Dr. Martin Spiess
Dekan



Namensnennung-Keine kommerzielle Nutzung-Keine Bearbeitung 2.5 Schweiz

Sie dürfen:



das Werk vervielfältigen, verbreiten und öffentlich zugänglich machen

Zu den folgenden Bedingungen:



Namensnennung. Sie müssen den Namen des Autors/Rechteinhabers in der von ihm festgelegten Weise nennen (wodurch aber nicht der Eindruck entstehen darf, Sie oder die Nutzung des Werkes durch Sie würden entlohnt).



Keine kommerzielle Nutzung. Dieses Werk darf nicht für kommerzielle Zwecke verwendet werden.



Keine Bearbeitung. Dieses Werk darf nicht bearbeitet oder in anderer Weise verändert werden.

- Im Falle einer Verbreitung müssen Sie anderen die Lizenzbedingungen, unter welche dieses Werk fällt, mitteilen. Am Einfachsten ist es, einen Link auf diese Seite einzubinden.
- Jede der vorgenannten Bedingungen kann aufgehoben werden, sofern Sie die Einwilligung des Rechteinhabers dazu erhalten.
- Diese Lizenz lässt die Urheberpersönlichkeitsrechte unberührt.

Die gesetzlichen Schranken des Urheberrechts bleiben hiervon unberührt.

Die Commons Deed ist eine Zusammenfassung des Lizenzvertrags in allgemeinverständlicher Sprache: <http://creativecommons.org/licenses/by-nc-nd/2.5/ch/legalcode.de>

Haftungsausschluss:

Die Commons Deed ist kein Lizenzvertrag. Sie ist lediglich ein Referenztext, der den zugrundeliegenden Lizenzvertrag übersichtlich und in allgemeinverständlicher Sprache wiedergibt. Die Deed selbst entfaltet keine juristische Wirkung und erscheint im eigentlichen Lizenzvertrag nicht. Creative Commons ist keine Rechtsanwalts-gesellschaft und leistet keine Rechtsberatung. Die Weitergabe und Verlinkung des Commons Deeds führt zu keinem Mandatsverhältnis.

Acknowledgments

I am grateful to Prof. Ruth Chiquet-Ehrismann for the opportunity to do my Phd thesis in her lab and expanding my knowledge about *C. elegans*. Thanks for giving me the chance to develop my own ideas, experiments and independence.

I would like to thank my thesis committee members, Prof Markus Affolter and Dr. Joy Alcedo for their scientific input in the project.

Thanks to the teneurin subgroup, Daniela, Jan and Jonas for discussion about our mysterious protein.

A special thanks to Agnieszka Trzebiatowska for the introduction to the worm teneurin.

Furthermore, I would like to thank all past and present members of the Chiquet lab for nice working atmosphere.

Ich danke aus ganzem Herzen meinen Eltern und Großeltern, deren anhaltende Unterstützung und Bestätigung mir die Möglichkeit und Kraft gab auch noch diese langen vier Jahre meiner Doktorantenzeit glücklich durch zu stehen.

Finally, I am most grateful to Krzysiek for his continuous support, encouragement and understanding.

TABLE OF CONTENTS

Summary	7
1. Introduction.....	8
1.1. Teneurin family members have a conserved protein domain structure.....	8
1.2. Expression of teneurins	10
1.3. Function of teneurins	11
1.4. Teneurin mechanism of action – working model.....	13
1.5. <i>C. elegans</i> embryonic development.....	14
1.6. Cell-Matrix interaction during <i>C. elegans</i> development.....	17
1.7. Collagen Prolyl 4-hydroxylase (C-P4H)	22
2. Aim of the work.....	26
3. Results.....	27
3.1. Published Results	27
3.2. Submitted Results.....	39
3.3. Unpublished Results.....	82
3.3.1. High-throughput screen for genes genetically interacting with <i>ten-1</i>	82
3.3.2. Knock-down of <i>phy-2</i> in <i>phy-1</i> loss of function mutant increases collagen IV aggregation in muscle cells	85
3.3.3. Micro array analyses of <i>ten-1</i> mutants versus wild type	87
3.3.4. Generation and characterisation of antibodies against the intracellular domain specific for TEN-1L	91

4. Discussion	97
4.1. P4H functions in secretion of collagen IV from the muscles into the basement membrane.....	97
4.2. Identification of interaction partners of <i>ten-1</i> by RNA interference.....	98
4.3. Micro array analysis of <i>ten-1</i> deletion mutants	101
4.4. Insights into mechanism of action of TEN-1	102
5. Materials and Methods	105
5.1. High-throughput screen for genes interacting with <i>ten-1</i>	105
5.2. Generation of chemically competent HT115(DE3) bacteria.....	106
5.3. Generation of chemically competent ArcticExpress™(DE3)RIL bacteria.....	106
5.4. Cloning of <i>ten-1</i> ICD	106
5.5. Expression of TEN-1 ICD in ArcticExpress™ (DE3)RIL bacteria.....	107
5.6. Purification of TEN-1 ICD	107
5.7. Protein techniques	108
5.7.1. Protein extraction from worms	108
5.7.2. SDS page electrophoresis	109
5.7.3. Western Blot analysis	109
5.8. <i>C. elegans</i> antibody staining and microscopy.....	109
5.9. Isolation of total RNA from <i>C. elegans</i> and preparation of cDNA	110
5.10. List of primers	111
5.11. List of plasmids.....	111
5.12. List of bacteria strains.....	112

5.13. List of worm strains..... 112

6. Appendix..... 114

6.1. Summary of candidate genes and the observed phenotype..... 114

6.2. Abbreviations..... 117

7. References 119

Curriculum vitae..... 127

SUMMARY

Teneurins are a family of phylogenetically conserved proteins. Their most prominent site of expression is the nervous system. Investigations on the expression pattern in vertebrates and invertebrates also revealed the importance for teneurins at sites of morphogenesis during embryonic development. Nevertheless, the function of teneurins remains to be discovered. Teneurins are type II transmembrane proteins. The mechanism of action of teneurins involves the translocation of the intracellular domain into the nucleus. It is postulated that the release of the intracellular domain requires several proteolytic events in the extracellular part, the transmembrane domain and at the cytosolic part. The stimulus of these events is unclear, but there is evidence for homophilic interactions between the teneurins.

The advantage of *C. elegans* as a model organism to investigate the function and mechanism of action of teneurins is that the *C. elegans* genome codes only for a single ortholog of the vertebrate teneurins. Two different promoters give rise to at least two different transcript versions. The promoters show distinct patterns of activity in the mesoderm and in the ectoderm of the worm. Two independent deletion mutants are characterized as null mutations. Knock-down by RNAi and analysis of the null mutants revealed that *ten-1* is essential for embryonic development but also for postembryonic events like larval development and reproduction. Interestingly, investigations on potential genetic interaction partners of *ten-1* uncovered functional redundancy between *ten-1* and basement membrane associated genes coding for homologs of integrin, dystroglycan, laminin, nidogen and perlecan. Co-staining of chicken teneurin and laminin in some tissues during embryonic development might point to an evolutionary conserved function of teneurins associated with the basement membrane.

In this study I used a genome wide approach to obtain a comprehensive list of potential genetic interaction partners of *ten-1*. I characterized the interaction with *phy-1* in more detail. *phy-1* is conserved among the phyla and codes for the catalytical domain of the collagen-modifying enzyme prolyl 4-hydroxylase. I found that loss of *phy-1* in the *ten-1* null mutant background enhances embryonic lethality significantly. Worms die during late elongation because of loss of connectivity between muscles, epidermis and the separating basement membrane. In addition, I present evidence that the function of PHY-1 modifying basement membrane collagen IV is conserved also in *C. elegans*.

1. INTRODUCTION

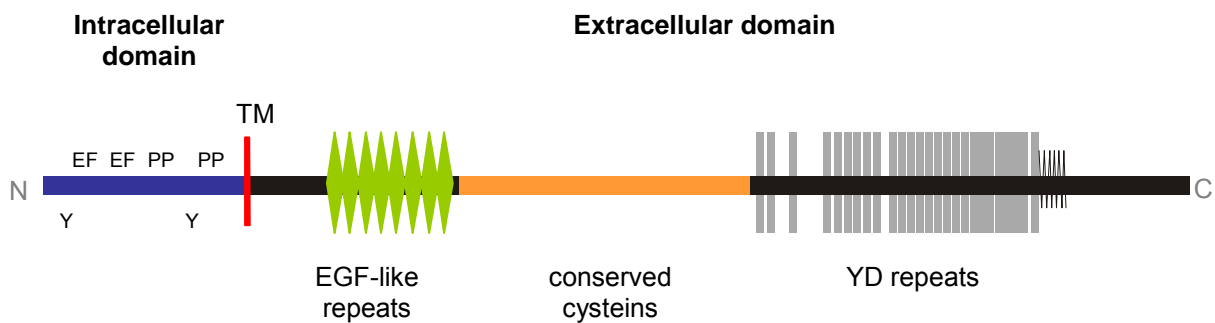
1.1. Teneurin family members have a conserved protein domain structure

The teneurins are a family of transmembrane proteins phylogenetically conserved in metazoan (Minet and Chiquet-Ehrismann, 2000). They were first discovered in *Drosophila* in an attempt to find the homolog of the extracellular matrix protein tenascin in arthropods. Two novel proteins were found and named ten-m for “tenascin-like protein major” and ten-a for “tenascin-like protein accessory” (Baumgartner and Chiquet-Ehrismann, 1993; Baumgartner et al., 1994). Further studies showed that apart of a structural similarity in the EGF like repeats teneurins are an independent family with distinct protein domains and function not being related to tenascins. Independently ten-m was found by Levine and colleagues using novel antibodies against *Drosophila* phosphotyrosine containing proteins (Levine et al., 1994). Investigations in other organisms revealed conservation of teneurins in mouse, chicken and *C. elegans* (Ben-Zur and Wides, 1999; Drabikowski et al., 2005; Minet et al., 1999). Four teneurin paralogs were found in vertebrates and named teneurin-1,-2,-3 and -4. In *C. elegans* a sole ortholog encodes teneurin named *ten-1*.

Teneurins code for type II transmembrane proteins. They have a common protein domain structure (Figure 1A). Most highly conserved is the extracellular domain (ECD). It contains eight tenascin-like epidermal-growth-factor-like repeats. The for teneurins characteristic free cysteines in the second and fifth EGF-like repeat can form cross links with their counterparts on an adjacent molecule, resulting in the formation for teneurin dimers (Feng et al., 2002). The central part of unknown function contains 17 highly conserved cysteine residues. Towards the C-terminus are 26 YD repeats and a series of partial YD repeats are located. YD repeats were described before only in the cell wall proteins of a few prokaryotes (Minet and Chiquet-Ehrismann, 2000). Thus, the YD repeat domains in teneurins make the family unique in eukaryotes (Figure 1A). Using electron microscopy, the C-terminal half of the protein was found to form a large globular domain connected to the rod like EGF-like repeats. The C-terminal globular domain is glycosylated (Figure 1B). The intracellular domain (ICD) of teneurins is phylogenetically less conserved. Among the vertebrate teneurins the ICD contains highly conserved and unique features. This includes proline-rich stretches with characteristic SH3-binding sites, two EF-hand-like putative Ca^{2+} binding sites and putative phosphorylation sites (Figure 1A). The molecular functions of these domains are unknown (Tucker and

Chiquet-Ehrismann, 2006). The *C. elegans* teneurin gene is under the control of two alternative promoters giving rise to two transcript versions that differ only in the length of the ICD. The ICD contains a predicted bipartite nuclear localization signal which is partially on the ICD unique for TEN-1L and partially on the common part of the two predicted protein versions (Drabikowski et al., 2005). Vertebrate teneurins contain an arginine-lysine stretch at the analogous location.

A



B

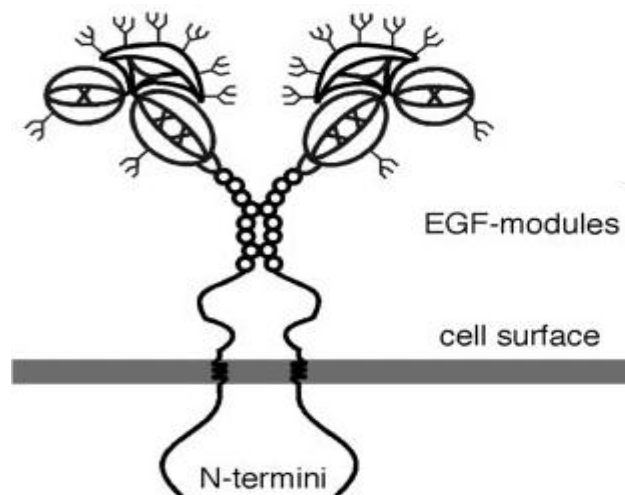


Figure 1. Teneurin protein structure. (A) Domain organization of vertebrate teneurins. The intracellular domain (ICD) contains EF-hand like motifs (EF), prolin-rich stretches (PP) and putative tyrosine phosphorylation sites (Y). Teneurins have a single trans-membrane domain (TM) and a large extracellular domain (ECD). The ECD contains EGF-like repeats (green), a region with conserved cysteins (orange) and condensed and relaxed YD repeats (grey). (B) Teneurins are type II transmembrane proteins that can dimerize through their EGF repeats. The C-terminus has a globular shape which can be intensively glycosylated. Picture is taken from (Feng et al., 2002).

1.2. Expression of teneurins

The name teneurin originates from their most prominent place of expression, the nervous system. Nevertheless, many studies showed also expression of teneurins in non-neuronal tissues uncovering the importance of teneurins during development (Tucker and Chiquet-Ehrismann, 2006; Tucker et al., 2007). The two promoters driving expression of the sole teneurin gene, *ten-1*, show distinct expression activity in *C. elegans*. The upstream promoter *ten-1a* is predominantly active in the pharynx, the somatic gonad precursor cells, the distal tip cells, the intestine and the vulva muscles and sex muscles (Drabikowski et al., 2005). This expression pattern was confirmed by expression of the long version of TEN-1, TEN-1L, fused to GFP (Trzebiatowska et al., 2008). The downstream promoter *ten-1b* is predominantly active in the ventral and dorsal hypodermis and in a subset of neurons including the nerve ring and the ventral nerve cord (Drabikowski et al., 2005). The *Drosophila*, *ten-a*, is found in the central nervous system (CNS), the eye and in muscle attachment sites (Baumgartner and Chiquet-Ehrismann, 1993; Fascetti and Baumgartner, 2002). In contrast, *Drosophila* *ten-m* is expressed in a subset of neurons and mainly in sites of morphogenesis like parasegments, morphogenetic furrow, wing pouch and leg and antennal discs (Baumgartner et al., 1994; Levine et al., 1994; Levine et al., 1997). In zebra fish, teneurins are found predominantly in the developing brain, somites and spinal cord (Mieda et al., 1999). Investigations on the expression pattern of teneurins in chicken uncovered that different teneurins are detected in distinct non-overlapping populations of neurons in the developing visual system (Minet et al., 1999; Rubin et al., 1999). Especially interesting is the expression of the avian teneurin-1 and teneurin-2 in alternating layers within the developing optic tectum (Rubin et al., 1999). The chicken teneurins are also expressed at sites of pattern formation most clearly seen in the chicken limb buds. There teneurin-2 is expressed in the apical ectodermal ridge and teneurin-4 is expressed in the zone of polarizing activity (Tucker et al., 2001; Tucker et al., 2000). In mouse, expression studies focused mostly on the developing nervous system. Each teneurin is expressed by a distinct subpopulation of neurons, but these populations often overlap (Zhou et al., 2003). Prominent sites of expression are: the pyramidal layer of the adult hippocampus, the dentate gyrus, the Purkinje cell layer in the cerebellum, the granule cell layer and the molecular layer (Tucker et al., 2007). As in chicken embryos, mouse teneurin-3 and teneurin-4 has been shown to be expressed in limb buds (Ben-Zur et al., 2000; Lossie et al., 2005).

1.3. Function of teneurins

Despite the extensive studies determining the sites of expression, little is known about the biological function of teneurins. One of the difficulties in analyzing the function of teneurin in vertebrates may be the genetic redundancy as well as splice variants increasing the number of possible protein versions. In this perspective *C. elegans* is an advantageous model organism to investigate teneurin function, since only one gene codes for teneurin. Knock-down by RNA interference (RNAi) using a probe common for both isoforms revealed that *ten-1* is essential for the embryonic development in *C. elegans*. Worms that hatched were misshaped and often arrested as early larvae. The lethality was most likely due to failure during migration of epidermal cells and subsequent enclosure defects during elongation. Specific knock-down of the *ten-1L* resulted in less penetrant embryonic lethality but worms reaching adulthood had defects in germ line development and formation of the somatic gonad. The phenotypes observed by knock-down could be confirmed in two deletion mutants, *ok641* and *tm651* (Drabikowski et al., 2005; Trzebiatowska et al., 2008). Both mutants are expected to be null mutants since an in-trans deletion did not enhance any of the phenotypes (Trzebiatowska et al., 2008). The deletions in the gene resulting in the mutant alleles are described in figure 2A. Recently, another allele for *ten-1* was isolated, *et5* (Morck et al., 2010). The allele corresponds to a C>T point mutation and introduces a stop codon downstream of the 8 EGF-repeats. Postembryonic phenotypes are more prominent in the null mutants. Worms arrest as larvae and animals reaching adulthood are sterile or burst through the vulva. Only about 5 % of the null mutants are embryonic lethal (Drabikowski et al., 2005). The mutant carrying the point mutation showed comparable embryonic lethality but reduced and milder postembryonic phenotypes (Morck et al., 2010). This result indicates an essential role of the EGF-repeats for the function of teneurin. For a summary of *ten-1* mutant phenotypes see figure 2B. In summary, knock-down and deletion mutant analysis of *ten-1* in *C. elegans* revealed an essential role for teneurin in morphogenesis.

Most functional data of vertebrate teneurins were generated using cell culture and biochemical assays. Neuronal outgrowth was shown for Nb2a cells expressing full-length teneurin-2 and for explanted chick dorsal root ganglia plated on teneurin-1 YD-repeats (Minet et al., 1999; Rubin et al., 1999). The ICD of teneurin-1 was shown to

interact with the adaptor protein CAP/Ponsin, which could represent a possible link to the actin cytoskeleton (Nunes et al., 2005).

Studies in other labs described some in vivo functions of vertebrate teneurins. In mice a point mutation near the C-terminus of teneurin-4 causes delays in gastrulation as well as neural tube defects prior to embryonic lethality (Lossie et al., 2005). Knock-out mice lacking teneurin-3 show abnormalities in mapping of ipsilateral projections, and exhibit deficits when performing visually mediated behavioural tasks (Leamey et al., 2007).

A



B

<i>ten-1</i> mutant alleles	Embryonic lethality in %	Larval arrest in %	Sterile/ bursting vulva in %	fertile adult in %
<i>ok641</i> ^(a)	6.4	32.1	16.7	44.8
<i>tm651</i> ^(a)	5.7	31.9	17.4	45.1
<i>et5</i> ^(b)	5.8	18.6	2.5	73.1

Figure 2. Summary of *ten-1* mutant alleles and mutant phenotypes. (A) Position of *ten-1* mutant alleles corresponding to the *ten-1* protein domain structure. *ten-1(tm651)* deletes 893 base pairs (bp) including the ICD of the TEN-1S, the transmembrane domain up to the first EGF repeat. The deletion causes a stop codon resulting in the loss of the entire extracellular domain. *ten-1(ok641)* is an in frame deletion of 2130 bp and affects the last three EGF repeats and part of the domain with the conserved cysteines. *ten-1(et5)* is a nucleotide (nt) substitution from C to T introducing a stop codon just downstream of the EGF repeats. (B) Summary of *ten-1* mutant phenotypes. Whereas the two deletion mutants are characterized as null mutants the nt substitution shows milder post-embryonic phenotypes and is a partial loss of function mutant. ^(a) (Trzebiatowska et al., 2008), ^(b) (Morck et al., 2010).

1.4. Teneurin mechanism of action – working model

There is evidence that the transmembrane protein teneurin undergoes proteolytic cleavage to initiate a signal transduction cascade. Indeed, it has been shown in different systems that the ICD of teneurins can be released and translocate to the nucleus. Transfection of the soluble ICD of teneurin-2 in HT1080 cells results in translocation of the ICD and colocalization with PML bodies (Bagutti et al., 2003). Investigations on chicken teneurin-1 showed nuclear localization in the developing brain using specific antibodies (Kenzelmann et al., 2008). Furthermore, using an N-terminal peptide antibody endogenous teneurin could be detected in the nuclei of *C. elegans* embryos and adult gut cells (Drabikowski et al., 2005). Nevertheless, the function of the ICD in the nucleus is unknown. A yeast two-hybrid screen revealed the interaction of teneurin-1 with the nuclear methyl CpG binding protein MBD1. This may be a link between teneurin signalling and transcriptional regulation. In the same screen the transcription factor Zic was found to interact with teneurin-1. This transcription factor family is implied in neuronal development and strengthens the idea of teneurins being important for neuronal development (Nunes et al., 2005).

The event triggering the release of the ICD is unknown. In vitro experiments suggest that teneurins promote homophilic cell-cell adhesion with an important role for the protein domains C-terminally of the EGF-like repeats (Rubin et al., 2002). On the other hand, there is evidence that teneurins may interact with components of the extracellular matrix. Thus, the induction of filopodia in neuroblastoma NB2A cells by teneurin-2 depends on the substrate and is more prominent on laminin than on poly-L-lysine (Rubin et al., 1999). Furthermore, chicken teneurin-2 was found to co-localize with laminin in the basement membrane of the optic cup and the heart endocardium (Tucker et al., 2001). Analysis of genetic interaction between *C. elegans ten-1* and laminin, *epi-1*, as well as nidogen, *nid-1*, resulted in synthetic lethality (Trzebiatowska et al., 2008). Loss of perlecan, *unc-52*, in *ten-1* mutant background affects the ipsilateral outgrowth of the pharyngeal neuron M2 (Morck et al., 2010).

Potential sites for proteolysis are conserved among the different teneurins [(Minet and Chiquet-Ehrismann, 2000) and unpublished data]. C-terminally of the transmembrane domain most teneurins contain a furin-like cleavage site. Indeed, for a recombinant avian teneurin-2 fusion protein, it was shown that this site is functional in vitro (Rubin et al., 1999; Tucker et al., 2001). In addition, unpublished data in *C.*

elegans confirm the functionality of the furin cleavage site also for *ten-1* (Drabikowski, personal communication). It implies that the extracellular domain is released into the extracellular milieu. Another conserved furin cleavage site is located at the very N-terminus. The release of an N-terminal peptide with neuromodular activity was reported (Wang et al., 2005). To release the ICD proteolytic cleavage needs to occur in the transmembrane region or close to it. Proteases responsible for this have not been identified. Candidate proteases are Site-2 protease, signal peptide peptidase (SPP) and SPP-like proteases since they have been shown to cleave type II transmembrane proteins (Kenzelmann et al., 2007). For a summary of the teneurin signalling model see figure 3.

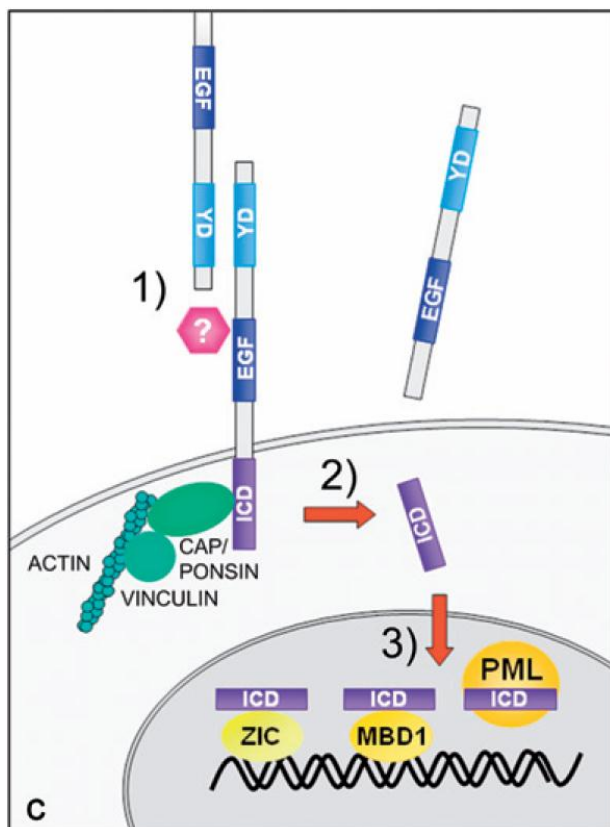


Figure 3. Teneurin signalling model. (1) An external stimulus triggers the shedding of teneurin. The stimulus could be a homophilic interaction or binding of an unknown ligand. (2) Several cleavage events result in release of the extracellular domain to the extracellular milieu and release of the intracellular domain (ICD) from the membrane. The ICD translocates to the nucleus. The ICD was found to interact with CAP/Ponsin which could provide a link to the actin cytoskeleton. (3) In the nucleus the ICD might influence transcription. Binding to ZIC and MBD1 was shown via a yeast-2-hybrid screen. In addition, teneurin was found to co-localize with PML bodies. (Kenzelmann et al., 2007).

1.5. *C. elegans* embryonic development

C. elegans morphogenesis is largely controlled by the development of the epidermis, a single epithelial layer that surrounds the worm (Chisholm and Hardin, 2005). The major epidermal precursor cells are generated after the 9th embryonic cell division. The 71 major epidermal cells form most of the epidermis, whereas an additional 11 minor epidermal cells form epidermal syncytia at the extreme head and tail. The

minor epidermal cells are smaller and born later, after the 10th round of division. Three main groups of epidermal cells are evident after the terminal divisions: dorsal epidermal cells, lateral or “seam” epidermal cells and ventral epidermal cells (Gendreau et al., 1994; Page et al., 1997). Dorsal epidermal cells undergo massive rearrangement and migration, known as dorsal intercalation, to form a single row across the dorsal midline (Williams-Masson et al., 1998). Shortly after this process is started, ventral epidermal cells start to migrate towards the ventral midline. Most important in this process, known as ventral enclosure, are the two “leading” cells. Ventral enclosure can be blocked by laser inactivation of these cells (Williams-Masson et al., 1997). Interestingly, *ten-1b* promoter is active in these cells. The loss of *ten-1* in the “leading” cells could be one explanation for the observed enclosure defects and embryonic lethality in the *ten-1* mutants or by knock-down experiments (Drabikowski et al., 2005).

Following the epidermal enclosure the embryo starts to elongate. The process of embryonic elongation is described in more detail in this section because elongation is affected in the most studied mutant of this thesis. Figure 4 presents an overview of the different stages of elongation. Elongation converts the bean-shaped embryo into the elongated shape of the worm and reflects the elongation of the epidermal cells (Priess and Hirsh, 1986). Early elongation, between comma and two-fold stage, is driven by actin microfilaments and microtubules within dorsal and ventral epidermal cells. Both filaments become highly organized in a circumferential pattern (Costa et al., 1997; Costa et al., 1998; Priess and Hirsh, 1986; Williams-Masson et al., 1997). Circumferential filament bundles (CFBs) do not persist after elongation is completed (Costa et al., 1997). Actomyosin-based contraction of epidermal cells has been shown to be crucial for elongation (Piekny et al., 2003; Wissmann et al., 1997). The contractile machinery is predominantly active in the lateral seam cells. The dorsal and ventral epidermal cells may not actively constrict but respond to seam-generated force. Most important for elongation is the connection of CFBs to adherens junctions (Chisholm and Hardin, 2005). Mutations in genes coding for the core proteins of the cadherin-catenin complex fail to elongate due to detachment of the CFBs (Costa et al., 1998). In addition, the claudin-like protein, which localizes to the adherens junctions and the epidermal spectrin cytoskeleton, is essential for epidermal elongation (Simske et al., 2003).

Elongation beyond the 2-fold stage requires muscle structures. Mutations causing an absence of muscle cells fail to elongate beyond the 2-fold stage. This phenotype is referred as the Pat, paralyzed arrest at 2-fold (Williams and Waterston, 1994). Myoblasts arise after the end of gastrulation and migrate to their final position in four longitudinal quadrants. Each quadrant forms a double row of muscle cells. In mid embryogenesis, the sarcomere components move to the cell membrane and form the sarcomere structure. At the same time attachment structures are assembled forming connections laterally between muscle cells and between muscles and the basal side of the epidermis (Hresko et al., 1994). The mechanism by which muscle function promotes epidermal elongation is not known. It was shown that muscles induce hemidesmosome-like trans-epidermal attachment structures (Hresko et al., 1999). Their molecular structure and function will be described in the following section. In addition, intermediate filaments connecting the apical and basal side of the epidermis are essential for late elongation (Ding et al., 2003; Woo et al., 2004). An importance for early elongation of these filaments has not been shown. Mutations in components of the attachment structures result in a weak pat phenotype (Chisholm and Hardin, 2005). Animals display initially normal muscle contraction, but with increased mechanical stress muscles detach from the epidermis. Another important role during late elongation plays the extracellular matrix of the basement membrane (bm) separating muscle cells from the epidermis. Lack of perlecan, UNC-52, causes elongation to block at the 2-fold stage (Hresko et al., 1994). Whereas lack of collagen IV leads to progressive muscle detachment and arrest of embryos at a 3-fold stage (Gupta et al., 1997).

After elongation is complete the epidermis secretes the cuticle of the first larval stage. Now the cuticle is responsible for holding the epidermal cells in place. Animals lacking cuticle collagens elongate normally but fail to maintain the elongated shape and retract (Priess and Hirsh, 1986). Similar defects are found when genes required for collagen processing or secretion are mutated (Novelli et al., 2004; Roberts et al., 2003).

In summary, elongation of the *C. elegans* embryo is an actively controlled process. Many morphogenetic events can be found also in other organisms. Almost all the molecular pathways are conserved, making *C. elegans* a tractable model for the study of morphogenetic processes.

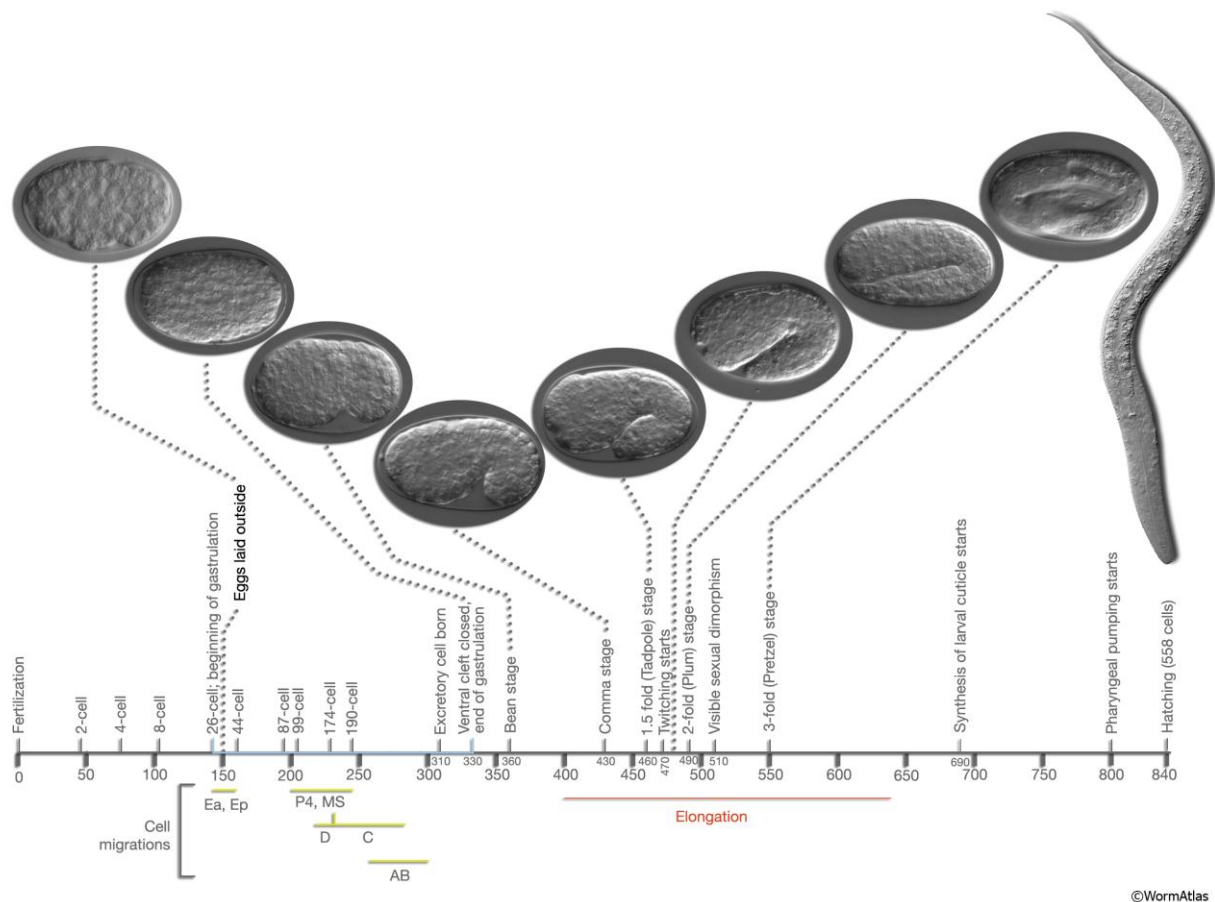


Figure 4. Overview of the embryonic development of *C. elegans* at a cultivation temperature of 20°C. Time scale is in minutes starting from time point 0 when the fertilization occurs. DIC images of important developmental changes are presented and named accordingly. The start of the cell migration coincides with the laying of the egg outside of the mother. The process of elongation starts around 400 min after fertilization and is finished around 650 min. During elongation the embryo reduces its circumference by the factor of three and increases in length by a factor of four. For detailed description see text. Picture is taken from (Hall and Altun, 2008).

1.6. Cell-Matrix interaction during *C. elegans* development

The nematode epithelium consists of polarized cells that form special cell – cell and cell – matrix junctions. These junctions contribute to cell integrity and make up the platform for cell shape changes (Labouesse, 2006). Many of the proteins involved have homologs in vertebrates, thus *C. elegans* is a suitable model organism to investigate their function and interplay. I will focus in this section on the cell – matrix junctions, their molecular content and their formation during development.

The epidermis possesses adhesion structures that connect its ventral and its dorsal side to distinct extracellular matrix surfaces. These junctional complexes are connected by intermediate filaments. The entire complex is called fibrous organelles (FO) and is a functional homolog of the vertebrate type I hemidesmosomes (HD) (Cox and Hardin, 2004; Ding et al., 2004; Labouesse, 2006). For an overview of the different complexes see figure 5. Similar structures are present in the pharyngeal marginal epithelial cells, rectum, vulva and areas of the epidermis that contact the mechanosensory touch neurons (Bercher et al., 2001; Cox and Hardin, 2004). Mammalian type I hemidesmosomes consist of a set of unique proteins. The membrane receptor $\alpha 6\beta 4$ -integrin connects to the basement membrane by binding to laminin-332, the cytolinker plakins, plectin and BP230, and another membrane receptor collagen XVII. The plakin family proteins connect the intermediate filaments, keratin-5 and keratin-14, indirectly with the $\alpha 6\beta 4$ -integrin. The integrin $\alpha 6$ subunit also interacts with CD151. BP180 weakly associates with laminin-332 (de Pereda et al., 2009; Jones et al., 1998). In *C. elegans* the membrane receptor connecting epidermis to the basement membrane is distinct from the mammalian integrin receptor. LET-805/myotactin is localized basally. It is a single-pass transmembrane protein with extracellular fibronectin type III repeats. The protein is predicted to be long enough to potentially reach the muscle membrane (Hresko et al., 1999). There is no ortholog of myotactin described in vertebrates. Two single transmembrane receptors, MUP-4 and MUA-3 are localized at the apical side. Both contain EGF repeats in their extracellular domain and they are weakly homologous to vertebrate matrilins (Bercher et al., 2001; Hong et al., 2001). All three receptors are predicted to associate with VAB-10A. VAB-10A is the sole ortholog of the two vertebrate plakins. It is generated by alternative splicing of the unique spectraplakin locus *vab-10*. VAB-10A is required to anchor intermediate filaments at FO (Bosher et al., 2003). The intermediate filaments IFA-2/MUA-6, IFA-3 and IFB-1 are associated with FO. They are more closely related to nuclear lamins (Dodemont et al., 1994), and form IFB-1/IFA-2 and IFB-1/IFA-3 heterodimers. Additionally, the ankyrin repeat-containing protein VAB-19 and the signalling adaptor EPS-8, which may physically interact with VAB-19, have been identified to localize to FO however, the molecular mechanism of attachment to the FO is still unclear (Ding et al., 2003; Ding et al., 2008).

The ECM in *C. elegans* is distinct from the one of mammals which might be a reason for the different needs of receptors (Labouesse, 2006). On the basal side of the epidermis, the myoblast-produced ECM includes laminin and collagen IV, which are

responsible for muscle polarization and adhesion to the epidermis. Whether they influence FO formation is unclear (Graham et al., 1997; Gupta et al., 1997; Huang et al., 2003). In *C. elegans* the perlecan homolog UNC-52 appears to be most important for FO formation (Spike et al., 2002). It is produced in the epidermis and is predicted to bind to myotactin (Hresko et al., 1994). In addition, the ECM protein HIM-4 is required in regions where the epidermis contacts the uterus and mechanosensory axons (Vogel and Hedgecock, 2001). The amount of secreted UNC-52 has been shown to be essential for FO formation. Thus, loss of its chaperone CRT-1 reduces UNC-52 protein level by 50%. This minor reduction results in disorganized FO pattern and detachment of muscles in a compromised VAB-10A background (Zahreddine et al., 2010).

Hemidesmosomes have long been considered as stable, structural entities. Several studies have challenged this opinion (Zhang and Labouesse, 2010). Cell culture experiments suggest that HDs undergo active disassembly and reassembly. The HD proteins BP180 and β 4-integrin have dynamic properties, especially during in vitro keratinocyte migration and wound healing in scratch assays (Geuijen and Sonnenberg, 2002; Tsuruta et al., 2003). Moreover, HDs disassemble rapidly during carcinoma invasion (Rabinovitz et al., 2004). The dynamic nature of HDs remains to be confirmed in vivo. *C. elegans* is a suitable model to study hemidesmosome-like structures, since they indeed undergo dynamic changes during development. FOs are assembled prior to embryonic elongation around the comma stage (Zhang and Labouesse, 2010). Initially, they form a punctuated structure along the anterior-posterior axis. They get progressively oriented in parallel, circumferential stripes when muscle cells start to contract (Labouesse, 2006). VAB-10A and myotactin are essential for this assembly. Thus, these proteins are not necessary for initial localization of VAB-19 and intermediate filaments but seem to become essential for the maturation of FOs. Consequently, in strong loss of function VAB-10A or myotactin mutants, embryos die due to loss of epidermal integrity and detachment of muscles and cuticle. VAB-19 has shown to be most important during reorganization of FOs during late embryogenesis (Ding et al., 2003). Loss of its function causes misslocalization of myotactin, VAB-10A, intermediate filaments and its adaptor protein EPS-8 (Ding et al., 2008). The exact mechanism of assembly of *C. elegans* FOs remains to be elucidated. It might be more complex than assembly of the mammalian HDs since assembly has to be co-ordinately regulated basally and apically of the epidermis (Zhang and Labouesse, 2010).

Progress has been made on post-translational modification of components of the FOs. A recent study identified two kinases, PAK-1 and PIG-1, in a genetic screen for genes interacting together with *vab-10A*. The role of phosphorylation needs to be investigated but could give further validation of in vitro experiments showing phosphorylation of mammalian β 4-integrin (Zahreddine et al., 2010). Additionally, modification by the small ubiquitin-like modifier SUMO contributes to the turn-over of FOs. Specifically, the modification of IFB-1 has been demonstrated to be essential (Kaminsky et al., 2009).

Investigations on the control of FOs component levels were performed by a genetic screen for enhancers of the *vab-10A* phenotype. The E3-ubiquitin ligase EEL-1 negatively regulates LET-805 expression via an indirect mechanism. Increased membrane receptor expression might result in stronger adhesion of the epidermis to the ECM. This could result in frictions during elongation and subsequent rupture of epidermis (Zahreddine et al., 2010). Interestingly, similar observations have been made in zebra fish, where the increase of α 6-integrin results in abnormal HDs (Sonawane et al., 2009).

Taken together, *C. elegans* FOs, also molecularly distinct have many features in common with mammalian HDs. Knowledge of the nematode FOs will thus greatly contribute to the understanding of vertebrate HDs.

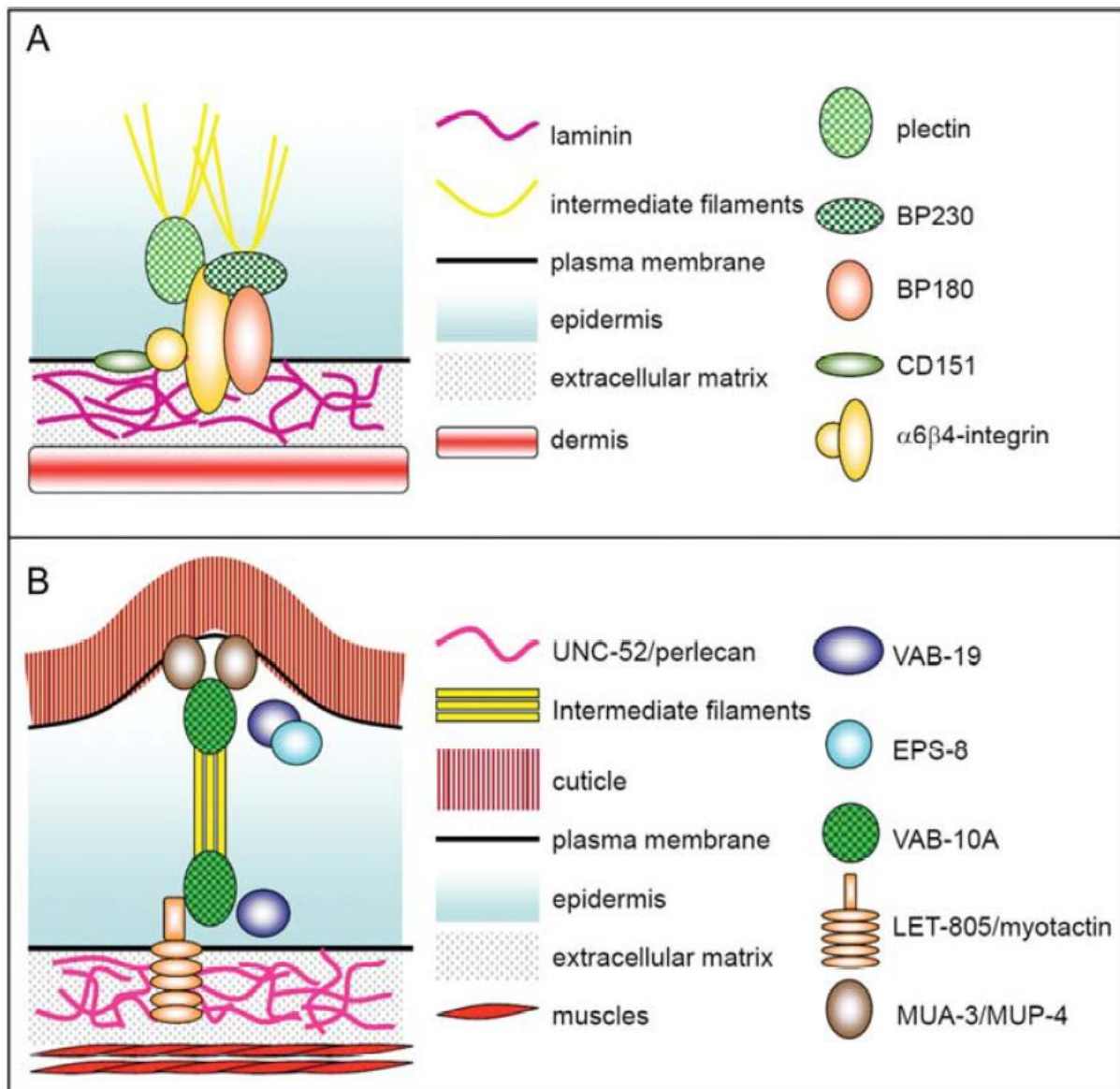
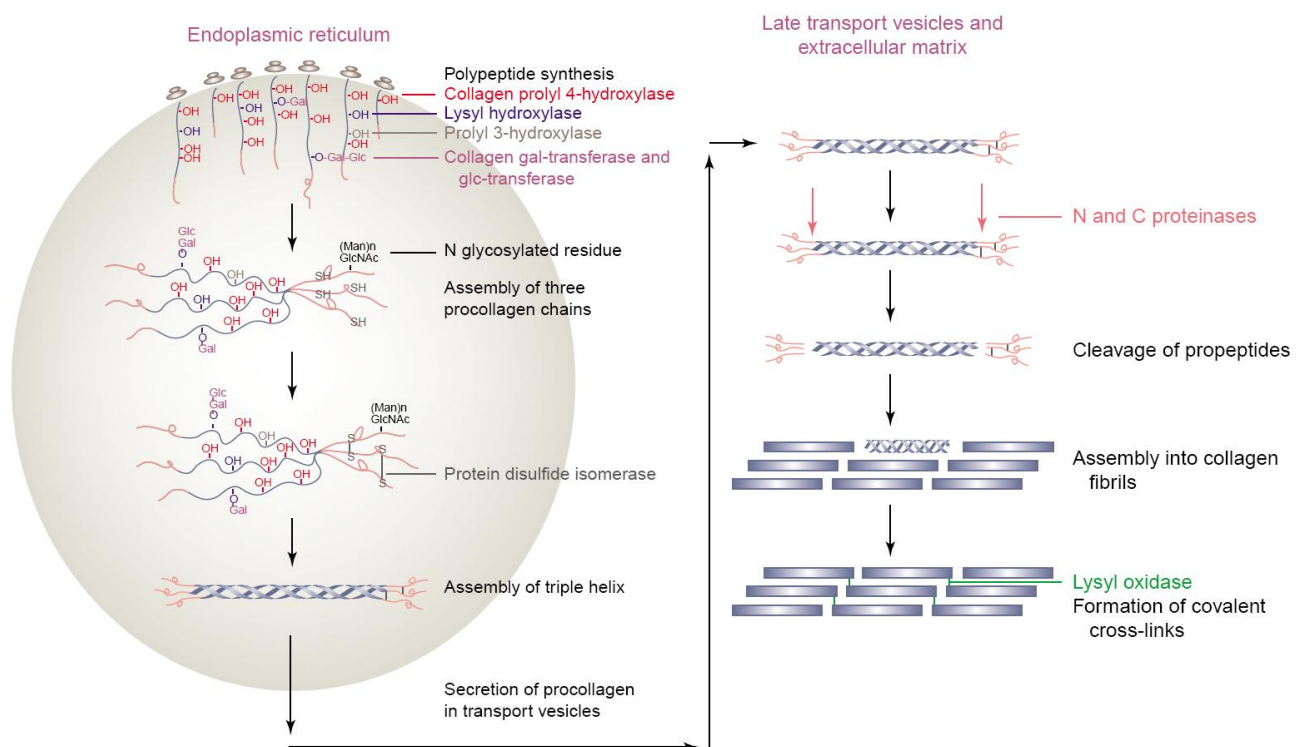


Figure 5. Model of vertebrate type I hemidesmosomes and the homologous structure of *C. elegans* fibrous organelles. (A) Type I hemidesmosomes connect intermediate filaments of the epidermal cells basally to the extracellular matrix via the transmembrane protein $\alpha6\beta4$ -integrin. (B) Fibrous organelles connecting the epidermis on the basal side to the basement membrane and muscle cells via the transmembrane receptor LET-805/ myotactin and apically to the extracellular matrix of the cuticle via the receptors MUA-3 and MUP-4. For description of the single components see text. Figure is taken from (Zhang and Labouesse, 2010).

1.7. Collagen Prolyl 4-hydroxylase (C-P4H)

Collagens are the most abundant proteins in mammals. Procollagen is synthesized by ER membrane bound ribosomes and secreted into the lumen of the endoplasmic reticulum (ER). There procollagen undergoes several steps of maturation which depend on the type of collagen produced. First the signal peptide is cleaved off. Second, certain proline and lysine residues are hydroxylated to 4-hydroxyproline, 3-hydroxyproline, and hydroxylysine by prolyl-hydroxylases and lysyl-hydroxylases, respectively. Some of the hydroxylysine residues and asparagine residues at the C-terminus become modified by glycosylation. Three propeptides are recognized at their C-terminus and associate. The formation of intra- and intermolecular disulfide bonds stabilize the structure which is tighter associated in a zipper-like principle towards the N-terminus. The procollagen molecules are transported from the ER to the Golgi. The N- and C-terminal peptides are cleaved off and the triple helices begin spontaneously to assemble into collagen fibrils. The fibrils are stabilized by formation of covalent crosslinks by oxidation of lysine and hydroxylysine residues (Myllyharju



TRENDS in Genetics

and Kivirikko, 2004). For summary see figure 6.

Figure 6. Overview of post-translational modification, secretion and formation of triple helix of pro-collagen. For description see text. Figure is taken from (Myllyharju and Kivirikko, 2004).

The initial modification by hydroxylation of residues is an essential step to ensure stability of the triple helix under physiological conditions (Fessler and Fessler, 1978). I will concentrate here on the collagen modifying enzyme prolyl 4-hydroxylase since I found the gene for this enzyme to genetically interact with *ten-1*. The C-P4H is conserved among the phyla (Friedman et al., 2000). In general it consists of an alpha domain which has the catalytic activity and a beta domain serving as protein disulfide isomerase (PDI). For the proper function, the enzyme requires vitamin C as a cofactor. In vertebrates three genes code for the hydroxylase subunit, alpha (I), (II) and (III). The three isoenzymes have unique alpha subunits combined with the same beta subunits (Myllyharju and Kivirikko, 2004) (figure 7). An essential function for the vertebrate P4H-alpha (I) subunit was identified. Mice lacking the gene are embryonic lethal due to insufficient modification of type IV collagen and subsequent instability of basement membranes (Holster et al., 2007). The *C. elegans* genome contains four genes coding for the catalytic alpha subunit: *phy-1*, -2, -3 and -4.1. *phy-1* and *phy-2* are the most similar to the vertebrate genes (figure 8A) (Friedman et al., 2000; Keskiaho et al., 2008; Myllyharju et al., 2002; Riihimaa et al., 2002; Winter and Page, 2000). PHY-1 and PHY-2 form together with two identical beta subunits (PDI) a tetrameric enzymatic complex. Both alpha subunits can also form a dimer with the beta subunit, but the PHY-2 – PDI-2 complex is only detectable at very low abundance (figure 7) (Myllyharju et al., 2002). A summary of the expression and loss of function phenotypes is presented in figure 8B. *phy-1* and *phy-2* share a similar expression pattern (Myllyharju et al., 2002; Shen et al., 2005). Both genes are expressed throughout the development of the worm and predominantly in the hypodermis, the tissue of cuticle collagen production. Homozygous inactivation of either *phy-1* or *phy-2* prevents assembly of the tetrameric enzyme complex. In the absence of *phy-2*, *phy-1* compensates this loss and *phy-2* null mutants have a wild type phenotype at physiological conditions. Interestingly, under hypoxic conditions the same *phy-2* mutant is almost completely embryonic lethal, suggesting an essential role for *phy-2* under stress situations (Shen et al., 2005). Loss of *phy-1* function causes a dumpy phenotype, indicating that *phy-2* is not able to fully compensate the loss of *phy-1*. The dumpiness of the animal is due to insufficient modification of collagen incorporated in the cuticle. An essential function for the P4H in the modification of basement membrane collagens has not been reported, although double mutants of *phy-1* and *phy-2* are embryonic lethal. The main reason for this lethality is that after elongation no sufficient cuticle can be secreted and the

worms explodes (Winter and Page, 2000). Some groups reported that double mutants can also arrest during the elongation process pointing to an additional function of P4H (Friedman et al., 2000). *phy-3* and *phy-4.1* are quite distinct from *phy-1* and *phy-2* (Figure 8A). *phy-3* in combination with PDI-2 does not show any enzymatic activity in vitro, although in combination with PDI-1 it shows low activity. The *phy-3* mRNA is detected in the embryo, the L4 larvae and the adult nematode. Expression in the later stages is restricted to the spermatheca. The *phy-3* null mutant appears phenotypically wild type. Interestingly, in null mutant embryos the 4-hydroxyproline content was remarkably reduced. The authors argued that the reduction affected collagens of the egg shell (Riihimaa et al., 2002). *phy-4.1* is shown to form tetramers with PDI-2 as well as dimers. Its expression is restricted to the pharyngeal gland, the lumen of the pharynx and the excretory duct. In vivo enzymatic experiments suggest that *phy-4.1* is involved in modification of other proline rich proteins than collagens (Keskiäho et al., 2008).

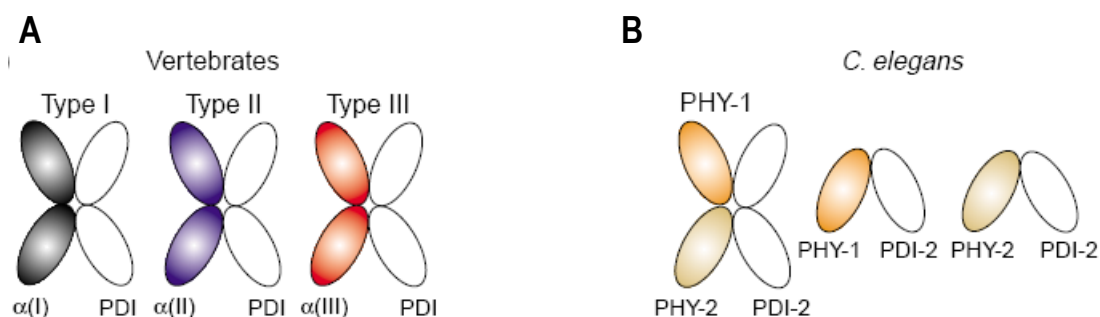
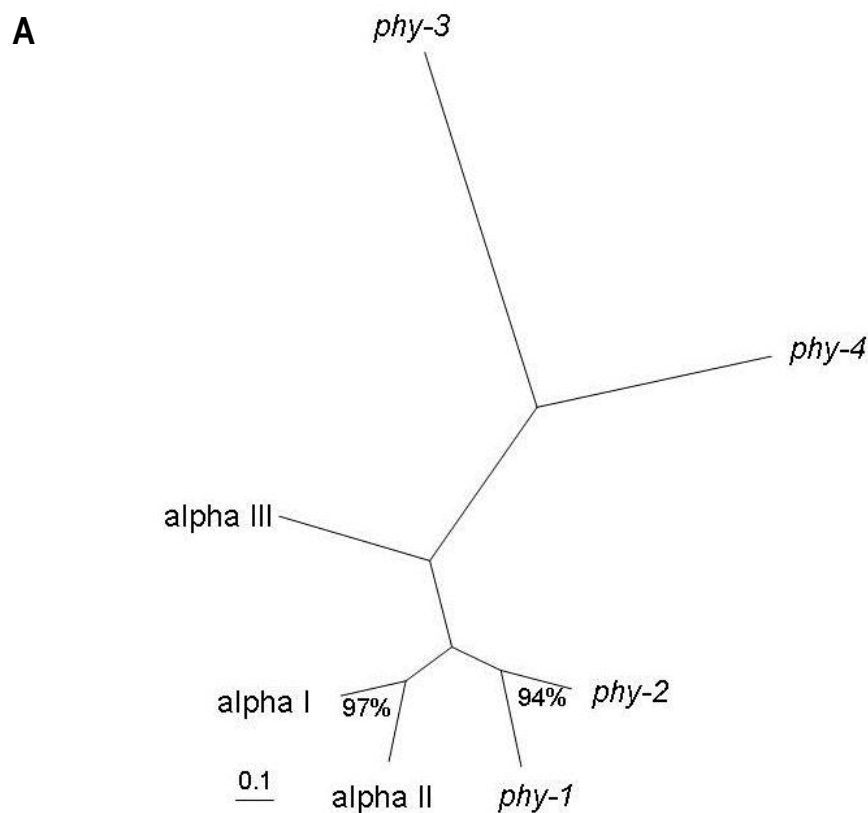


Figure 7. Domain composition of prolyl 4-hydroxylase in vertebrates vs. *C. elegans* (A) In vertebrates three genes code for the hydroxylase subunit, alpha (I), (II) and (III). The three isoenzymes have unique alpha subunits combined with the same beta subunits. (B) *phy-1* and *phy-2* code for the hydroxylase subunit in *C. elegans* and are the most similar to the vertebrate hydroxylase subunits. PHY-1 and PHY-2 form together with two identical beta subunits a tetrameric enzymatic complex. Both alpha subunits can also form a dimer with the beta subunit. (Myllyharju and Kivirikko, 2004)



B

Expression pattern	genotype	phenotype
	<i>phy-1</i> Δ	mild dumpy
	<i>phy-2</i> Δ	wild type
	<i>phy-3</i> Δ	wild type
	<i>phy-4</i> Δ	wild type
	<i>phy-1;phy-2</i> Δ	embryonic lethal
	<i>phy-1;phy-3</i> Δ	dumpy

Figure 8. (A) Phylogenetic tree of the catalytic subunit of the vertebrate and the *C. elegans* prolyl 4-hydroxylase. *phy-1* and *phy-2* are the most similar to the vertebrate P4H alpha subunit whereas *phy-3* and *phy-4* are most distinct from the vertebrate genes. (B) Summary of expression pattern, and knock-out phenotype of the *C. elegans* P4H genes *phy-1*, -2, -3 and -4 under physiological conditions. *phy-1* appears the most important gene in these conditions. *Phy-1* and *phy-2* show overlapping expression in the epidermis (blue). *phy-2* and *phy-3* are both expressed in the spermatheca (yellow). For references see text.

2. AIM OF THE WORK

The work described in this dissertation was done to investigate functions of the single ortholog of vertebrate Teneurins, *ten-1*, in the model organism *C. elegans*.

The aim of the thesis was to identify *ten-1* interacting genes using a genome wide RNA interference screening for suppressors and enhancers of the *ten-1* mutant phenotype. Successfully confirmed interactions were further analyzed by epistatic analysis. The final aim was to dissect the mechanisms underlying the genetic interaction data and thus gain new insights into the molecular function of teneurins.

3. RESULTS

3.1. Published Results

Caenorhabditis elegans teneurin, *ten-1*, is required for gonadal and pharyngeal basement membrane integrity and acts redundantly with integrin *ina-1* and dystroglycan *dgn-1*.

Trzebiatowska, A., Topf, U., Sauder, U., Drabikowski, K. and Chiquet-Ehrismann, R. (2008). *Mol Biol Cell* 19, 3898-908.

My contribution:

I performed the final experiment of knock-down of *epi-1* by RNA interference and performed the immunohistochemistry of staining worms with anti collagen IV antibodies to visualize the basement membrane and confirming the loss of integrity of gonadal basement membrane. Finally, I was involved in preparing the manuscript for the revised version.

Caenorhabditis elegans Teneurin, *ten-1*, Is Required for Gonadal and Pharyngeal Basement Membrane Integrity and Acts Redundantly with Integrin *ina-1* and Dystroglycan *dgn-1*

Agnieszka Trzebiatowska,* Ulrike Topf,* Ursula Sauder,[†] Krzysztof Drabikowski,* and Ruth Chiquet-Ehrismann*

*Friedrich Miescher Institute for Biomedical Research, Novartis Research Foundation, CH-4058 Basel, Switzerland; and [†]Microscopy Center, Pharmazentrum, University of Basel, CH-4056 Basel, Switzerland

Submitted January 14, 2008; Revised June 27, 2008; Accepted July 1, 2008
Monitoring Editor: Jean E. Schwarzbauer

The *Caenorhabditis elegans* teneurin ortholog, *ten-1*, plays an important role in gonad and pharynx development. We found that lack of TEN-1 does not affect germline proliferation but leads to local basement membrane deficiency and early gonad disruption. Teneurin is expressed in the somatic precursor cells of the gonad that appear to be crucial for gonad epithelialization and basement membrane integrity. *Ten-1* null mutants also arrest as L1 larvae with malformed pharynges and disorganized pharyngeal basement membranes. The pleiotropic phenotype of *ten-1* mutant worms is similar to defects found in basement membrane receptor mutants *ina-1* and *dgn-1* as well as in the mutants of the extracellular matrix component laminin, *epi-1*. We show that the *ten-1* mutation is synthetic lethal with mutations of genes encoding basement membrane components and receptors due to pharyngeal or hypodermal defects. This indicates that TEN-1 could act redundantly with integrin INA-1, dystroglycan DGN-1, and laminin EPI-1 in *C. elegans* development. Moreover, *ten-1* deletion sensitizes worms to loss of nidogen *nid-1* causing a pharynx unattached phenotype in *ten-1;nid-1* double mutants. We conclude that TEN-1 is important for basement membrane maintenance and/or adhesion in particular organs and affects the function of somatic gonad precursor cells.

INTRODUCTION

Teneurins are large transmembrane proteins that play important roles in cell signaling and cell adhesion (Tucker and Chiquet-Ehrismann, 2006; Tucker *et al.*, 2007). Teneurins are phylogenetically conserved among metazoans and they were described in several species, including *ten-1* in *Caenorhabditis elegans* (Drabikowski *et al.*, 2005), *ten-m/odz* and *ten-a* in *Drosophila* (Baumgartner *et al.*, 1994; Levine *et al.*, 1994; Fascetti and Baumgartner, 2002; Rakovitsky *et al.*, 2007), zebrafish (Mieda *et al.*, 1999), and in chicken (Minet *et al.*, 1999; Tucker *et al.*, 2000; Tucker *et al.*, 2001; Rubin *et al.*, 2002) and mouse (Oohashi *et al.*, 1999; Ben-Zur *et al.*, 2000; Zhou *et al.*, 2003). In vertebrates, the four teneurin paralogs were named teneurin-1 to -4, *ten-m1* to -*m4*, or *odz-1* to -4.

The extracellular domain of all teneurins is composed of eight tenascin-type EGF-like repeats, a region of conserved cysteines, and YD repeats that are also found in a few bacterial proteins (Minet and Chiquet-Ehrismann, 2000). The

intracellular domain contains proline-rich stretches and putative tyrosine phosphorylation sites but is less conserved than the extracellular part and cannot be aligned in a linear way between the phyla. Teneurins are thought to interact in a homophilic manner (Oohashi *et al.*, 1999; Rubin *et al.*, 2002; Bagutti *et al.*, 2003; Leamey *et al.*, 2008) and to date, no other ligand has been identified.

The name "teneurins" refers to their high expression in the developing and adult nervous system (Mieda *et al.*, 1999; Oohashi *et al.*, 1999; Otaki and Firestein, 1999; Ben-Zur *et al.*, 2000; Tucker *et al.*, 2000; Rubin *et al.*, 2002; Zhou *et al.*, 2003). In the developing mouse cortex, all teneurins are expressed in distinctive gradients and may be required for neocortical patterning (Li *et al.*, 2006). Several reports point out their role in the development of visual pathways. Leamey *et al.* (2008) have found that teneurins are up-regulated in visual versus somatosensory areas of the neocortex. Moreover, expression of different teneurins is largely nonoverlapping and can be found in interconnected regions of the developing visual system (Rubin *et al.*, 1999, 2002; Kenzelmann *et al.*, 2008; Leamey *et al.*, 2008). For instance, teneurin-1 staining is found in the tectofugal pathway, and teneurin-2 is primarily expressed in the thalamofugal pathway. In addition, teneurins were shown to promote neurite outgrowth in vitro (Minet *et al.*, 1999; Rubin *et al.*, 1999) and in vivo (Leamey *et al.*, 2008), suggesting an important function for teneurins in axon guidance and target recognition. Recently, the first vertebrate teneurin knockout was described (Leamey *et al.*, 2007). Teneurin-3 regulates eye-specific patterning in the

This article was published online ahead of print in *MBC in Press* (<http://www.molbiolcell.org/cgi/doi/10.1091/mbc.E08-01-0028>) on July 16, 2008.

Address correspondence to: Ruth Chiquet-Ehrismann (Ruth.Chiquet@fmi.ch).

Abbreviations used: BM, basement membrane; DIC, differential interference contrast; L1, first larval stage; L2, second larval stage; L3, third larval stage; L4, fourth larval stage; Pun, pharynx unattached; SGP, somatic gonad precursor cells.

visual system, and the knockout mice show impaired binocular vision.

Beside prominent expression in the nervous system, teneurins are also found in nonneuronal tissues. They are expressed in alternating parasegments in the fly embryo, as well as in cardiac cells, muscle attachment sites, and the tracheal system in *Drosophila* (Baumgartner and Chiquet-Ehrismann, 1993; Baumgartner *et al.*, 1994). In the chicken teneurins are found in limb buds, branchial arches, and somites (Tucker *et al.*, 2000, 2001), and in *C. elegans* *ten-1* is expressed in gonadal somatic cells, pharynx, and muscles (Drabikowski *et al.*, 2005). Teneurin expression in each of these tissues is often associated with pattern formation and cell migration.

The *in vivo* function of teneurins is mainly inferred from studies of *C. elegans* and *Drosophila* mutants. Mutation of the fly *ten-m* gene causes embryonic lethality due to the fusion of adjacent denticle belts (Baumgartner *et al.*, 1994; Levine *et al.*, 1994). Moreover, defects in the ventral nerve cord, cardiac cells and eye patterning are found in late *ten-m* mutant embryos (Levine *et al.*, 1994; Kinel-Tahan *et al.*, 2007). Similar defects in cuticle and eye development have been observed for the second *Drosophila* teneurin gene, *ten-a* (Rakovitsky *et al.*, 2007). In *C. elegans*, deletion in the *ten-1* gene causes a pleiotropic phenotype, including gonad disorganization, nerve cord defasciculation, and defects in distal tip cell migration and axonal pathfinding (Drabikowski *et al.*, 2005).

The single teneurin ortholog in *C. elegans*, *ten-1*, is under control of alternative promoters giving rise to two protein variants. The isoforms differ only in their intracellular domains. Their expression patterns are complex but mostly nonoverlapping: TEN-1 long (TEN-1L) is found mainly in the mesoderm, including pharynx, somatic gonad, and various muscles and neurons, and TEN-1 short (TEN-1S) is predominantly expressed in some hypodermal cells and in a subset of neurons (Drabikowski *et al.*, 2005).

We report here the role of TEN-1 in gonadal basement membrane maintenance, as well as in epidermal and pharyngeal development. Mutation of the *ten-1* gene leads to gonad rupture and sterility. Germ cell leakage from the gonads has also been reported for basement membrane mutants, e.g., integrin α *ina-1*, dystroglycan *dgn-1*, and laminin α B *epi-1* (Baum and Garriga, 1997; Huang *et al.*, 2003; Johnson *et al.*, 2006). Furthermore, the genetic interactions between *ten-1*, *ina-1*, *dgn-1*, *epi-1*, and *nid-1* suggest that teneurin, integrin, and dystroglycan have related and partly redundant functions in *C. elegans* development.

MATERIALS AND METHODS

General Methods and *C. elegans* Strains

C. elegans strains were maintained at 20°C as described (Brenner, 1974). The following strains were used in this study: wild-type N2, variety Bristol, CH120: *cle-1(cg120)* I, CB444: *unc-52(e444)* II, VC518: *ten-1(ok641)* III; TM0651: *ten-1(tm651)* III; NG39: *ina-1(gm39)* III; NG144: *ina-1(gm144)* III; CB189: *unc-32(e189)* III; CX2914: *nDf16/dpy-17(e164) unc-32(e189)* III; CH119: *nid-1(cg119)* V; CH121: *dgn-1(cg121)/dpy-6(e14) unc-115(mi481)* X. The *tm651* deletion removes nucleotides R13F6: 3661-4550 of the *ten-1* coding sequence.

The following GFP marker strains were used: RU7: *kdEx7[ten-1::gfp]*; RU97: *ten-1(ok641) kdEx45 [F36A3, III]*; JK2049: *qls19 [lag-2::gfp]*; S80747: *buls1[pie-1::GFP::PGL-1]* (gift of Susan Strome, University of California, Santa Cruz, CA); IM253: *urEx131 [lam-1::gfp]* (gift of William Wadsworth, Robert Wood Johnson Medical School, Piscataway, NJ); CH1878: *dgn-2(ok209) dgn-3(tm1092) dgn-1(cg121)*; *cgEx308 [DGN-1::GFP]* (gift of James Kramer, Northwestern University Medical School, Chicago, IL).

Double mutant worms were maintained as [*ten-1(ok641);ina-1(gm144)*]; *kdEx45*], [*ten-1(ok641/+);nid-1(cg119)*], [*ten-1(ok641);dgn-1(cg121/+)*]; *kdEx45*] or [*ten-1(ok641/+);dgn-1(cg121)*]; *cgEx308*] strains and genotyped by PCR for the phenotypic analysis.

Constructs and Plasmids

The translational *Pten-1a::GFP::TEN-1L* minigene reporter construct was generated by cloning *SpeI*-*HindIII* cDNA fragment and *HindIII*-*XhoI* genomic fragment of TEN-1 long variant into p123T vector (Mo Bi Tec, Goettingen, Germany). The following restriction sites were introduced into the primers: *SpeI* and *XhoI* flanking the *ten-1* coding sequence, *SacII* at the 5' end of the *ten-1a* promoter, and *Apal* downstream of the 3' UTR.

The long intracellular domain, transmembrane domain, and a short fragment of the extracellular part were amplified using 5'-AACAGTCTACCGAATCCCAACC-3' and 5'-ATAACTAGTATGTTCCAGCACAGGTAACCTACCACG-3' primers and cDNA from mixed stage N2 worms as a template. For the extracellular domain of *ten-1* we used 5'-GCTGAAATACCCACTCGCCAGC-3' and 5'-ATCTCGAGCTATTCAGATTTTCGGAACCTCC-3' primers and R06H12 cosmid as a template. The sequence encoding green fluorescent protein (GFP) was amplified from pPD117.01 vector and its *NcoI* site was mutated to CCTTGG. GFP was fused by PCR to the N-terminus of the *ten-1* cDNA fragment, which was cloned into *SpeI*-*NcoI* sites of *ten-1* minigene. Hemagglutinin (HA) tag was added at the C-terminus of *ten-1* coding sequence by PCR and cloned into *HpaI*-*XhoI* sites. The *Pten-1a::GFP::TEN-1L* construct contained 4235 base pairs of the *ten-1a* promoter and a 512-base pair sequence downstream of the stop codon. PCR fragments were generated with Pfu Turbo DNA polymerase (Stratagene, La Jolla, CA).

Transgenic Animals

Transgenic lines were generated as previously described (Mello *et al.*, 1991). The *Pten-1a::GFP::TEN-1L* plasmid was injected into *ten-1(ok641)* mutant worms. Injections of *GFP::TEN-1* minigene at low concentration (5 ng/ μ l) resulted in a very weak GFP fluorescence, mainly in the nervous system. Therefore, we injected the worms with high concentrations of the transgene (40 ng/ μ l) and obtained several lines giving stronger GFP fluorescence. We used pRF4 [*rol-6*] as a coinjection marker. This resulted in the line RU152: *kdEx121 [Pten-1a::GFP::TEN-1L]* used in this study.

RNA Interference

RNA-mediated interference (RNAi) was performed as described (Kamath and Ahringer, 2003). The K08C7.3 RNAi clone was obtained from the Ahringer feeding library. Wild-type and *ten-1(ok641)* synchronized L4 hermaphrodites were placed on RNAi plates and grown at 15°C for 72 h. Single adult worms were placed on fresh RNAi plates and allowed to lay eggs for 24 h. These plates were examined for 3 d to determine embryonic lethality and postembryonic phenotypes.

Immunostaining of *C. elegans* Larvae

C. elegans larvae were prepared as previously described (Finney and Ruvkun, 1990). Fixed animals were blocked overnight at 4°C in PBS containing 0.1% Triton X-100 (Triton) and 10% goat serum. Samples were incubated with an antibody against collagen IV LET-2 (NW68, kind gift of James Kramer) overnight at 4°C, washed in PBS containing Triton, and incubated with fluorescein conjugated goat anti-rabbit secondary antibody overnight at room temperature. Finally, fixed larvae were washed in PBS containing Triton and Hoechst, followed by PBS alone.

Electron Microscopy

Worms were washed in M9 and anesthetized in 8% ethanol in M9 for 5 min. They were placed in a fixative (2.5% glutaraldehyde, 1% paraformaldehyde in 0.1M sucrose, and 10 mM PBS, pH 7.4), cut open with a needle at both anterior and posterior ends, and fixed for 2 h. Worms were embedded in 2% agarose, cut into small blocks, and washed three times in PBS. Subsequently, pieces were fixed with a second solution (1% osmium tetroxide, 1.5% potassium ferrocyanide in PBS) for 2 h and washed three times in water. Worms were stained with 1% uranyl acetate for 1 h. Samples were dehydrated in ethanol (10 min in 50% ethanol, 10 min in 70% ethanol, 10 min in 90% ethanol, and 10 min in 100% ethanol) and acetone (10 min). Blocks with worms were embedded in Epon resin (Fluka, Buchs, Switzerland): first in Epon-acetone (1:1) for 1–2 h and then in pure resin for 2–4 h. Samples polymerized for 24–48 h at 60°C and in 60-nm sections were prepared with Ultratcut E. Sections were stained in uranyl acetate for 60 min and then 2 min in Millonig's lead acetate stain. Pictures were taken on Philips Morgagni 80 KV microscope (Eindhoven, The Netherlands).

Phenotypic Analysis

Young adult hermaphrodites were placed on separate plates and allowed to lay eggs for 24 h. The progeny were analyzed for embryonic and postembryonic phenotypes: lethality, larval arrest, sterility, and bursting at the vulva.

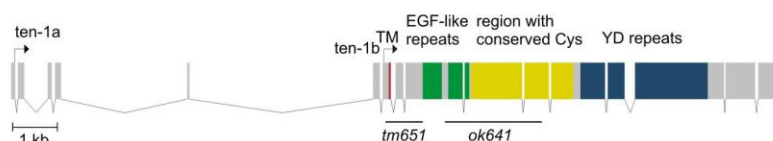
A. Trzebiatowska *et al.*

Figure 1. Genomic organization of *ten-1* gene and location of *tm651* and *ok641* deletions. Exons are depicted as boxes and introns are shown as lines. Expression of *ten-1* is regulated by alternative promoters: *ten-1a* and *ten-1b*, resulting in two type II transmembrane protein variants differing in the length of their

intracellular domain. Fragments of exons encoding different protein domains are labeled as follows: red, single transmembrane domain, green, EGF-like repeats in two groups, yellow, region of conserved cysteines, and blue, stretch of YD repeats. Black horizontal lines show the regions deleted in two *ten-1* mutants: *tm651* and *ok641*.

Time Course of Germline Development and Basement Membrane Breakdown

Synchronized, starved L1 larvae carrying the *GFP::PGL-1* marker were placed on bacteria plates. We scored the number of germ cells in 20 worms for each genotype at 0, 8, 12, 16, and 20 h. For the study of basement membrane integrity, we used synchronized worms carrying the *LAM-1::GFP* marker and analyzed 50–62 worms for each developmental stage.

Microscopy

Animals were mounted on 2% agarose pads in a drop of M9 buffer containing 25 mM sodium azide. Differential interference contrast (DIC) and fluorescence images were acquired with Z1 microscope (Zeiss, Jena, Germany) and Axio-Cam Mrm camera (Zeiss) using 63×/1.4 NA Plan-Apochromat objective (Zeiss) and AxioVision software.

RESULTS

Both *ten-1(ok641)* and *ten-1(tm651)* Are Functional Null Alleles

In our previous study we described the *ten-1* mutation, *ok641*, that carries an in-frame 2130-base pair deletion removing four EGF-like repeats and a large part of the conserved cysteines region (Drabikowski *et al.*, 2005). We now obtained another allele, *tm651*, lacking 890 base pairs and introducing a frameshift into the *ten-1* coding sequence (Figure 1). This deletion results in a loss of the transmembrane domain and the entire extracellular part. Therefore, *tm651* is most likely a null allele. Because phenotypes of both *ten-1* mutants show similar penetrance (Table 1), we assume that *ok641* represents a functional null allele as well.

To confirm this hypothesis, we created heterozygous worms carrying nDf16 deficiency in trans to *tm651* or *ok641* and investigated whether the mutant phenotypes became aggravated after complete removal of one copy of the *ten-1*

gene. The *ok641/nDf16* and *tm651/nDf16* worms displayed a similar range of defects to *ok641* and *tm651* homozygous animals, and the values observed were very close to those calculated under the assumption of *ten-1* mutants being null alleles (Table 2).

These data and the fact that *ok641* and *tm651* deletions affected protein regions that are common to both TEN-1 isoforms, suggested that there was no functional TEN-1 present in any of the *ten-1* mutants.

Gonads of *ten-1* Mutant Worms Burst Early in Development

Previous studies demonstrated that TEN-1 plays an important role in gonad development and function (Drabikowski *et al.*, 2005). Homozygous *ten-1(ok641)* worms are viable, but 15–20% are sterile or burst-through-the-vulva due to germ cell leakage in the middle of the gonad. Occasionally, gonads disintegrate completely and germ cells float in the pseudocoelom. We could rescue gonadal and vulval defects by expression of the *kdEx121* transgene encoding the long teneurin isoform under its own promoter (Table 1).

To determine the basis and the developmental stage of gonad bursting, we performed a time course experiment of germ cell proliferation in the early gonads of *ten-1(ok641)* mutants. We used worms carrying a P-granule GFP marker to distinguish between germ cells and somatic gonad precursor cells. Interestingly, we found that germ cells were released from the gonads of *ten-1* mutant already at the early L3 stage (Figure 2B). At the same time point, there were no germ cells present around the developing somatic gonad primordium in the wild-type worms (Figure 2A). A sharp DIC boundary surrounding the gonad was visible in the

Table 1. Phenotypes of *ten-1* deletion mutants

Genotype	Embryonic lethality (%)	Larval arrest (%)	Sterile and/or vulva defects (%)	Fertile adults (%)	n
Wild type	0.9	0	0	99.1	321
<i>ten-1(tm651)</i>	5.7	31.9	17.4	45.1	386
<i>ten-1(ok641)</i>	6.4	32.1	16.7	44.8	346
<i>ten-1(ok641), kdEx121</i>	1.2	5.5	7.2	86.1	165

Table 2. Embryonic lethality and larval arrest phenotypes appearing in the progeny of nDf16/*ten-1 unc-32* transheterozygotes

Genotype	Embryonic lethality (%)	Larval arrest (%)	Adults: total (%)	% Unc in adult worms	n
nDf16/ <i>ten-1(tm651) unc-32(e189)</i>	29.7	27.2	43.1	32.1	492
nDf16/ <i>ten-1(ok641) unc-32(e189)</i>	33.5	22.6	43.9	30.1	310
Expected value for nDf16/ <i>ten-1</i> ^a	29.5	24.0	46.5	33.3	

^a The calculated ratio of phenotypes expected if the *ten-1* mutants are null mutants.

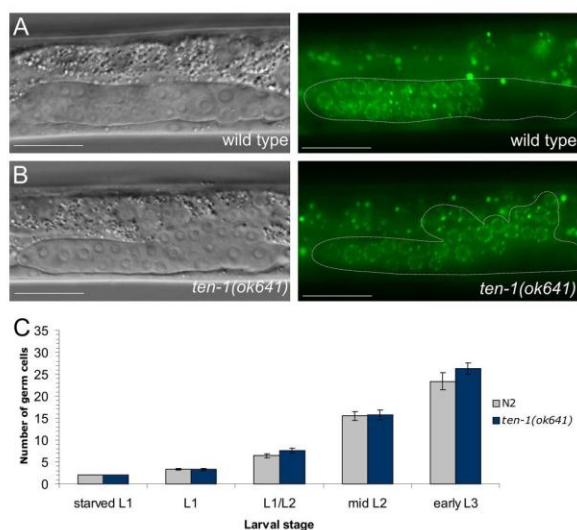


Figure 2. Germ cells are released from the early gonad of *ten-1(ok641)* mutant through the central break. Germ cell number and localization were evaluated using the P-granule marker *pie-1::GFP::PGL-1*. (A) Wild-type L3 gonad. The somatic gonadal primordium forms in the middle of the gonad, and germ cells fill the two gonad arms (only one arm is shown). (B) Ruptured gonadal primordium of a *ten-1(ok641)* L3 larva. Germ cells are released into the body cavity and localize in the vicinity of the developing somatic gonad primordium. (C) Time course of germline development in wild-type animals and *ten-1(ok641)* mutants. There is no germline overproliferation in the early gonads of the *ten-1(ok641)* mutant. Scale bar, 20 μ m.

wild type as well as a large part of *ten-1(ok641)* gonad (Figure 2, A and B) but absent on the dorsal side of the mutant gonad, where the germ cells leaked out into the pseudocoelom. Gonad bursting was not the result of germline overproliferation causing increased pressure on the gonadal basement membrane (BM), because we did not find any difference in the number of germ cells between wild-type and *ten-1* mutants at this stage (Figure 2C).

Gonadal Basement Membrane Is Not Maintained in the *ten-1* Mutant

Bursting of the early gonads in the *ten-1* mutant suggested that mutant worms have defects in BM formation or maintenance. Therefore, we examined the organization of the BMs in the *ten-1(ok641)* worms using a laminin- β *LAM-1::GFP* marker and an anti-collagen IV antibody that label most BMs in worms.

At hatching, wild-type and the majority of *ten-1* mutant gonad primordia were compact and completely surrounded by laminin (Figure 3, A and B). At the L2 stage the laminin layer surrounding the developing gonad of the mutants appeared to get thinner at the dorsal side, but germ cells did not lose contacts and gonads kept their tubular shape, similarly to wild-type (Figure 3, C and D). As the gonadal precursor cells divided, a discontinuity appeared in the *ten-1(ok641)* gonadal BM that could be seen by a lack of laminin as well as of collagen IV LET-2 (Figure 3, C and E). In L3 larvae germ cells were released in the center of the mutant gonad, where there was no laminin-GFP detectable. Gonad disruption appeared always on the dorsal side, whereas gonad arms were normally covered with BM (Figure 3F). In wild-type animals the gonads re-

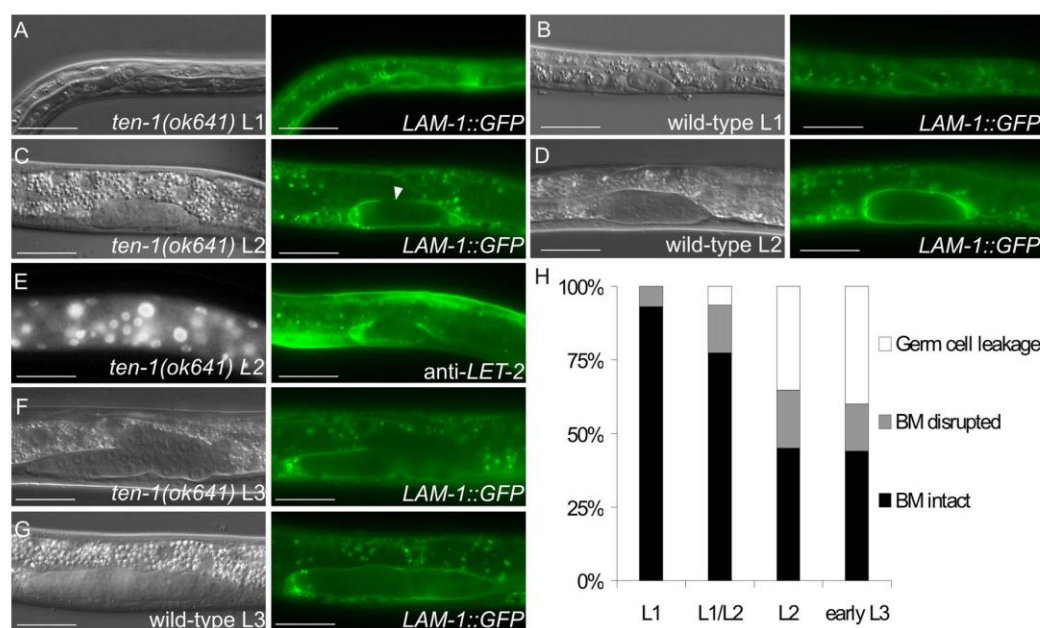


Figure 3. The basement membrane breaks on the dorsal side of the *ten-1(ok641)* gonads. Basement membranes were visualized by the *LAM-1::GFP* marker (A–D and F–G) and the anti-LET-2 immunostaining (E). The *ten-1(ok641)* L1 gonad (A), wild-type L1 (B), and L2 (D) gonads are uniformly covered by laminin. (C) In the *ten-1(ok641)* mutant, the gonadal basement membrane becomes thinner or fails to assemble correctly (arrowhead) at the L2 stage. (E) Lack of gonadal BM on the dorsal side of *ten-1(ok641)* L2 gonad is visualized by collagen IV immunostaining with anti-LET-2. (F) There is no laminin present in the center of the *ten-1(ok641)* L3 gonad. The basement membrane is absent completely, and germ cells are released. (G) The wild-type L3 gonad is entirely covered by laminin. (H) Time-course analysis of gonadal BM integrity in *ten-1(ok641)* worms carrying the *LAM-1::GFP* marker. Scale bar, 20 μ m.

A. Trzebiatowska *et al.*

mained completely ensheathed by a BM (Figure 3G). A time course of the appearance and the penetrance of BM defects in young *ten-1(ok641)* larvae is summarized in Figure 3H.

Furthermore, we compared the BM ultrastructure in wild-type and *ten-1* mutant worms using transmission electron microscopy of thin sections of L3 larvae. Wild-type gonads were completely ensheathed by BM, which appeared as a thin mesh of extracellular material along the plasma membranes (Figure 4, B and B1). In *ten-1(ok641)* worms, gonads had a round shape and were entirely covered by BM in sections localized distally from the break (Figure 4C and C1). However, in the midbody region no BM was present on the dorsal side of the broken gonad and germ cells invaded the intestine (Figure 4, D and D1). In contrast, the BMs on the ventral side of the burst gonad as well as the BMs between the intestine and the hypodermis showed a wild-type ultrastructure (Figure 4, D and D2). Moreover, we did not find any whorls or clumps of extracellular material that might suggest a general defect in BM organization. Such a phenotype was described for some BM mutants such as *epi-1*, *lam-1*, or *dig-1* (Huang *et al.*, 2003; Benard *et al.*, 2006; Kao *et al.*, 2006).

In summary, the gonadal BM in the *ten-1(ok641)* hermaphrodites was properly assembled at hatching but was not maintained later in development. The localized BM deficiency could result from defects in BM assembly, stability, or protein expression.

Gonadal Defects of *ten-1* Mutants Are Similar to Those Found in the Dystroglycan *dgn-1*, Integrin *ina-1*, and Laminin *epi-1* Mutants

Laminins are secreted proteins that play fundamental roles in BM formation and function (Previtali *et al.*, 2003; Miner and Yurchenco, 2004). EPI-1 is one of two laminin α chains found in the *C. elegans* genome. Both *C. elegans* laminin isoforms are broadly distributed among BMs, but the gonadal BM contains the EPI-1 isoform only (Huang *et al.*, 2003). Dystroglycan and integrins, two cell surface receptors interacting with laminin, are required for BM assembly, adhesion, and signal transduction (Bokel and Brown, 2002; Higginson and Winder, 2005). In *C. elegans*, gonadal epithelialization defects were reported for the dystroglycan *dgn-1(cg121)* worms and laminin α chain *epi-1* mutants (Huang *et al.*, 2003; Johnson *et al.*, 2006). Gonads of integrin α chain *ina-1* mutants are oddly sized and show germ cell leakage, but the cause of the defects remains unknown (Baum and Garriga, 1997).

Gonads of *dgn-1* mutants and *epi-1(RNAi)* worms were variably misshapen (Figure 5, C and E), burst during development, and led to worm sterility. Early gonads of *ina-1(gm39)* worms hardly ever burst (Figure 5F) and rather seemed to be swollen in the center. However, at the L4 stage *ina-1* mutant gonads were clearly ruptured, and the germ cells clustered around the developing vulva (Figure 5G), similarly to *ten-1(ok641)* gonads (Figure 5H). Gonads of adult worms carrying the weaker *ina-1* allele, *gm144*, had enlarged arms but we did not observe any germ cell leakage (unpublished data).

We analyzed the organization of the laminin network surrounding the developing gonad in *dgn-1* mutants using the *LAM-1::GFP* marker. Although the DIC pictures of *ten-1* and *dgn-1* mutants appeared similar, *dgn-1(cg121)* hermaphrodite gonads did not have any localized breaks as did the *ten-1(ok641)* gonads. In contrast, the *dgn-1* mutant gonads were generally disorganized, and *LAM-1::GFP* seemed to be more diffuse throughout the gonadal surface in comparison

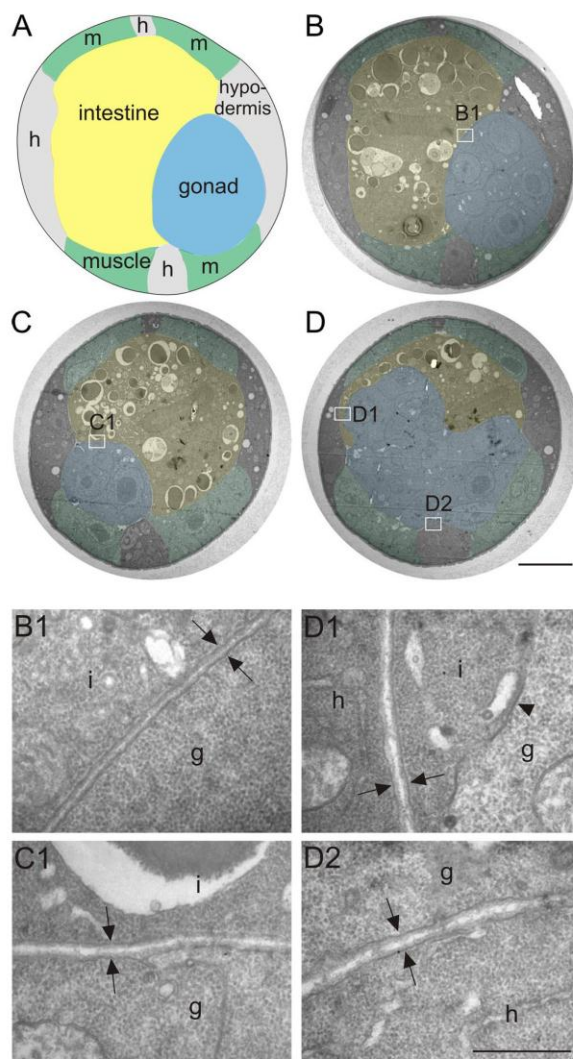


Figure 4. Basement membrane ultrastructure in *ten-1* mutant worms. Schematic cross-section through the midbody of wild-type worm (A). Transmission electron microscopy sections of a wild-type L3 (B) and a *ten-1(ok641)* mutant (C and D). Tissues are labeled as follows: blue, gonad; yellow, intestine; green, muscles; and gray/unlabeled, hypodermis. Enlargements (B1–D2) are marked on the cross-sections (B–D) with white rectangles. Morphology of wild-type BMs at the boundaries between gonad and intestine (B1, arrows). The gonadal and intestinal BM of the *ten-1* mutant appears wild-type in a section 2 μm distant from the central break (C1, arrows). In the midbody region, the mutant gonad breaks on its dorsal side, and there is no BM present between germ cells and intestine (D1, arrowhead). However, BMs between intestine and hypodermis (D1, arrows) or ventral gonad and hypodermal ridge (D2, arrows) have a normal ultrastructure. Scale bar, 5 μm (A–D) and 500 nm (B1–D2).

to *ten-1* mutant gonads (Figure 5D). Nevertheless, gonadal defects described for *dgn-1(cg121)*, *ina-1(gm39)*, and *epi-1(RNAi)* worms resembled the defects that we observed in the *ten-1* mutants (Figure 5B), suggesting that TEN-1 could be involved in gonadal BM maintenance, together with laminin receptors INA-1 and DGN-1.

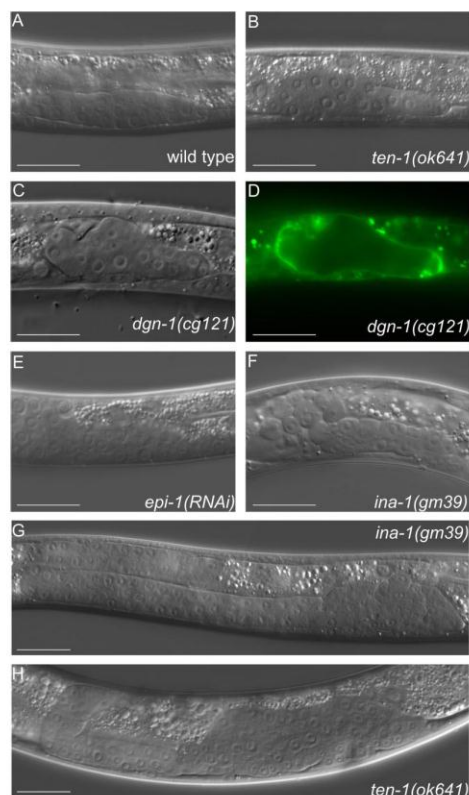


Figure 5. Misshapen gonadal primordia are found in several basement membrane mutants, i.e., dystroglycan *dgn-1*, integrin *ina-1*, and laminin *epi-1(RNAi)* worms. DIC pictures of early gonads in wild type (A), *ten-1(ok641)* (B), *dgn-1(cg121)* (C), and the corresponding *LAM-1::GFP* pattern (D), *epi-1(RNAi)* (E), *ina-1(gm39)* L2 larva (F), *ina-1(gm39)* L4 larva (G), and *ten-1(ok641)* L4 larva (H). Mutant gonads do not form a tube-like structure but grow into a disorganized mass. Scale bar, 20 μ m.

In early gonads TEN-1 was found to be expressed in the somatic gonad founder cells Z1 and Z4 (Drabikowski *et al.*, 2005). Also their descendants, the somatic gonad precursor cells (SGPs) during the L2 stage express TEN-1 (Figure 6, A and B). We found that Z1 and Z4 cells were often displaced from the tips of the early L1 gonads in *ten-1(ok641)* worms (Figure 6C). In almost 20% of the mutants, Z1 and/or Z4 cells interdigitated between germ cell precursors Z2 and Z3, or sometimes one of the SGPs was lost. Because the SGPs are required for the deposition of the gonad BM, the BM defects observed in the *ten-1* mutant worms might be due to the inability of the SGPs to form an intact epithelial layer around the gonad primordium. Interestingly, similar gonad epithelialization defects were reported for *dgn-1* and *epi-1* mutant worms (Johnson *et al.*, 2006).

ten-1 Is Synthetic Lethal with *dgn-1*, *ina-1*, *epi-1*, and *nid-1*

The similar gonadal phenotypes of *ten-1*, *dgn-1*, and *ina-1* mutants and *epi-1(RNAi)* worms suggested that TEN-1 could act in a parallel pathway and have a partly redundant function to dystroglycan and/or integrin receptors. To assess the interaction between *ten-1* and genes encoding various BM components, we constructed double mutant combinations.

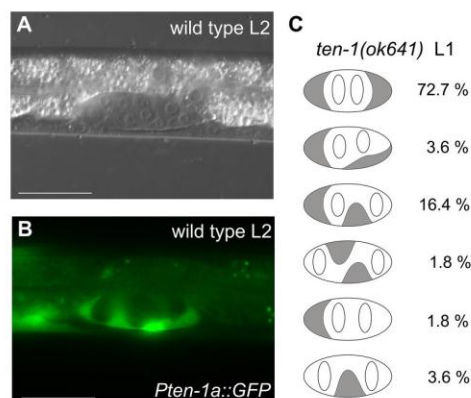


Figure 6. Teneurin is expressed in somatic cells of the early gonads and SGPs are mislocalized in the L1 gonads of *ten-1* mutants. Expression from the upstream promoter of *ten-1* is found in the SGPs of L2 gonads in wild-type worms (A and B). In C we present a schematic representation of the position of the Z1 and Z4 (gray shading) and Z2 and Z3 (white) cells in gonads of *ten-1(ok641)* L1 larvae carrying the *lag-2::gfp* marker (n = 55). We found that Z1 and Z4 cells are often mispositioned, and the percentage of animals showing the observed patterns is indicated to the right. Scale bar, 20 μ m.

In the crosses we used *ten-1(ok641)* and *dgn-1(cg121)* null alleles, the weak *ina-1* hypomorphic allele *gm144*, and an RNAi approach in the case of *epi-1*.

To analyze the genetic interaction network of *ten-1* further, we included additional genes encoding BM proteins, namely nidogen *nid-1*, perlecan *unc-52*, and collagen XVIII *cle-1*. *C. elegans* nidogen deletion does not affect BM assembly (Kang and Kramer, 2000), but *nid-1* mutants show defects in neuromuscular junction organization (Ackley *et al.*, 2003) and axonal tract positioning (Kim and Wadsworth, 2000). Interestingly, the *nid-1(cg119)* null mutant was found to be synthetic lethal with *dgn-1* as a result of pharyngeal defects (J. M. Kramer, personal communication). Mutation *e444* in the perlecan *unc-52* gene causes progressive paralysis in worms as well as gonad disorganization and germ cell release into the body cavity (Gilchrist and Moerman, 1992). Loss-of-function mutation in the collagen *cle-1* gene leads to cell migration and axon guidance defects. Some *cle-1(cg120)* mutant larvae are unable to pump and arrest at the L1 stage with misshapen pharynges (Ackley *et al.*, 2001).

Interestingly, we observed more severe phenotypes in several double mutants than in any single mutant alone (Table 3). Synthetic lethality was found in *ten-1(ok641);dgn-1(cg121)*, *ten-1(ok641);ina-1(gm144)*, *ten-1(ok641);nid-1(cg119)* double mutants, and *ten-1(ok641);epi-1(RNAi)* worms. Lack of dystroglycan or nidogen in the *ten-1* mutant background led to developmental arrest during late embryogenesis or L1 larval stage in almost 100% of worms. Double-mutant larvae were translucent suggesting a feeding defect. Morphological defects found in *epi-1* deficient worms (Figure 7C) were enhanced by *ten-1* deletion. More than 90% of *ten-1(ok641);epi-1(RNAi)* animals arrested during embryogenesis or as early larvae and showed dramatic disorganization of developing tissues (Figure 7E). Moreover, *ten-1;jna-1* mutants showed severe morphological defects not found in any single mutant alone (Figure 7, B and D), and nearly 100% of double mutant worms arrested as disorganized embryos or L1 larvae (Figure 7F).

Table 3. *ten-1* is synthetic lethal with *dgn-1*, *ina-1*, *epi-1*, and *nid-1*

Genotype	Embryonic lethality	Larval arrest	Sterile and/or vulva defects ^a	Fertile adults	n
Wild type	0.9	0	0	99.1	321
<i>Ten-1(ok641)</i>	6.4	32.1	16.7	44.8	346
<i>dgn-1(cg121)</i>	5.4	2.2	92.4	0	92
<i>Ten-1(ok641);dgn-1(cg121)</i>	14.0	84.2	1.8	0	57
<i>Ina-1(gm144)</i>	10.0	30.6	23.5	35.9	170
<i>ten-1(ok641);ina-1(gm144)</i>	12.9	85.7	1.4	0	70
<i>nid-1(cg119)</i>	4.2	7.3	0.3	88.2	765
<i>ten-1(ok641);nid-1(cg119)</i>	34.7	65.2	0	0	88
<i>epi-1(RNAi)</i>	17.1	29.5	53.4	0	442
<i>ten-1(ok641);epi-1 (RNAi)</i>	48.5	44.2	7.3	0	293
<i>cle-1(cg120)</i>	0.7	0.7	1.1	97.5	283
<i>ten-1(ok641);cle-1(cg120)</i>	3.4	24.5	23.1	49.0	147
<i>unc-52(e444)</i>	3.5	1.5	5.6	89.4	198
<i>ten-1(ok641);unc-52(e444)</i>	4.8	21.5	36.5	37.2	293

Percentage of wild-type and mutant worms (single and double mutants) showing the following phenotypes: embryonic lethality, larval arrest, sterility or vulval defects, and wild-type fertile adults.

^a The "Vulva defects" category includes protruding vulva and bursting-at-the-vulva phenotypes.

In contrast, mutations in *unc-52* or *cle-1* did not cause synthetic lethality in the *ten-1* mutant background. These two mutations did not enhance embryonic lethality, larval arrest, or sterility of the *ten-1(ok641)* worms. However, we cannot exclude that *unc-52* and *cle-1* interact genetically with *ten-1* in other processes, such as axon guidance or distal tip cell migration.

Teneurin Functions with Nidogen and Dystroglycan in Pharynx Development

Because larval arrest was significantly increased in several double mutants, we decided to investigate the phenotypes of the starved L1 larvae of *ten-1;dgn-1* and *ten-1;nid-1* double mutants, suspecting that these three proteins could have an important role in pharyngeal morphogenesis. This hypothesis was supported by the fact that the expression of the long TEN-1 isoform rescued the larval arrest phenotype of *ten-1* mutants (Table 1) and *GFP::TEN-1L* was detectable in the developing pharynx (Figure 8, A and B) until adulthood (Figure 8, C and D). As 30% of *ten-1* single mutant worms arrest as L1 translucent larvae, we examined their pharyngeal defects. The wild-type foregut is a short tube, with two bulbs, surrounded by a thick BM (Figure 9, A and B). As viewed by DIC microscopy, *ten-1*-arrested larvae had variably misshapen pharynges, and the outline of the pharynx was often barely visible (Figure 9C). In addition, we examined the pharyngeal BM organization with the *LAM-1::GFP* marker and found that it seemed to be disordered and missing in some parts of the pharynx (Figure 9D).

In contrast to *ten-1* mutant worms, only a low percentage of *dgn-1* and *nid-1* single mutants arrested during larval stages. Pharynges of *dgn-1* larvae showed mostly wild-type appearance (Figure 9E), whereas the few *nid-1* arrested larvae had a bend in the anterior-most part of their foregut (Figure 9F). Another phenotype found at low penetrance in the *nid-1* single mutant was pharynx unattached (Pun), where the pharyngeal epithelium did not connect to the arcade cells of the hypoderm.

Removal of *dgn-1* in the *ten-1* mutant background enhanced the defects found in the *ten-1* single mutant and double mutants of *ten-1;dgn-1* arrested as larvae with their pharynges variably misshapen (Figure 9G). Interestingly,

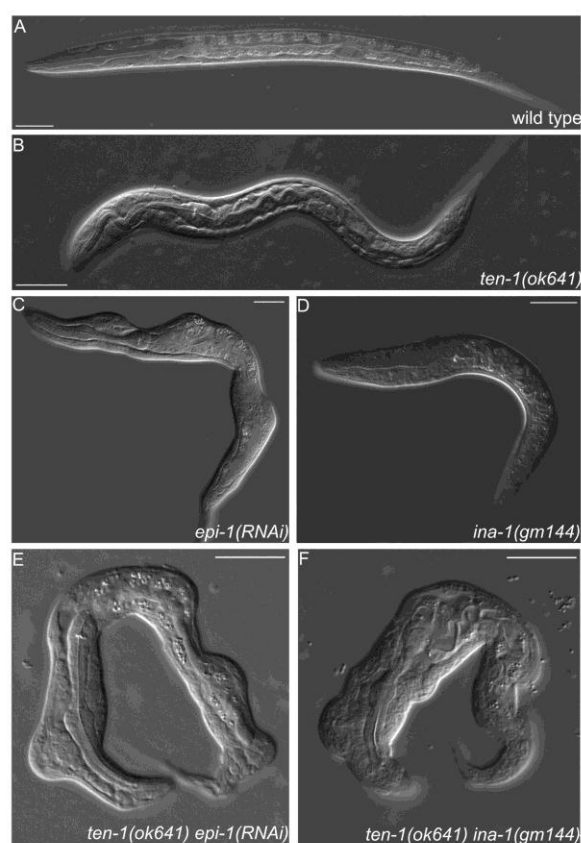


Figure 7. Morphological defects found in *epi-1(RNAi)* worms, *ten-1(ok641); epi-1(RNAi)* animals, and *ten-1; ina-1* double mutants. Wild-type (A) and *ten-1(ok641)* L1 larvae (B). *epi-1*-depleted worms are often misshapen, but defects are relatively mild (C). Arrested larva of *ina-1(gm144)* mutant (D). Morphological defects of *epi-1(RNAi)* worms were enhanced by *ten-1(ok641)* deletion and caused deformation of the entire body in the arrested larvae (E). Similar defects were found in *ten-1(ok641);ina-1(gm144)* double mutants (F). Severity and penetrance of the defects were greatly enhanced in the double mutants compared with single mutants. Scale bar, 20 μ m.

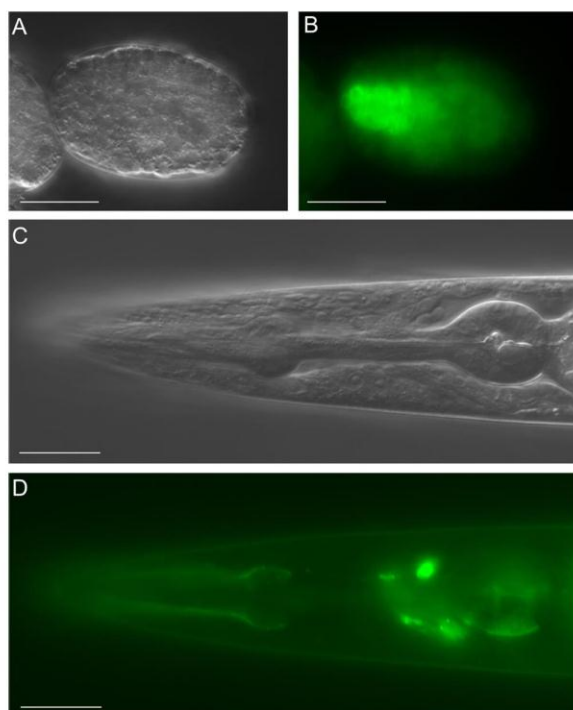


Figure 8. The long TEN-1 isoform is expressed in the developing and adult pharynx. The GFP::TEN-1 transgene (*kdEx121*) is expressed in the developing pharynx of the early embryo (A and B) and outlines the adult pharynx (C and D). Expression of the *kdEx121* is also found in some head neurons (D). Scale bar, 20 μ m.

ten-1;mid-1 double mutants arrested as larvae that were unable to feed because their pharynges were not attached to the lips (Figure 9H).

In summary, our data suggest that *ten-1* and *dgn-1* act redundantly in pharyngeal morphogenesis and/or function. Moreover, both *ten-1* and *dgn-1* caused synthetic lethality in the *nid-1* mutant background, implying an important role for these two receptors in the process of pharyngeal attachment.

DISCUSSION

Function of TEN-1 in Somatic Gonad Precursor Cells

We found that TEN-1 is essential for the maintenance of the BM early in development of the gonads in *C. elegans*. The BM surrounding the gonad was formed properly at hatching but during larval development ruptured at a very specific location on the dorsal side in the middle of the gonad. The *ten-1a* promoter is active in the SGP of L1-L2 larvae and RNAi specific for the TEN-1 long variant is known to cause gonadal disorganization (Drabikowski *et al.*, 2005). Therefore, SGPs may play an important role in extracellular matrix production or BM assembly by expression of specific receptors that organize extracellular matrix proteins provided by adjacent tissue. Such a mechanism has been described for several BM proteins. Graham *et al.* (1997) showed that type IV collagen is assembled on tissues that do not express it themselves, and they postulated that these tissues express receptors that facil-

itate collagen IV assembly. Another example is fibulin-1, which is secreted by the intestine and deposited on the gonadal surface (Muriel *et al.*, 2005). Also in the case of laminin isoforms it was suggested that their differential distribution is at least partly based on differential assembly mediated by cell surface receptors (Huang *et al.*, 2003). TEN-1 could be a novel receptor promoting BM assembly in the gonad. Another possibility is that teneurin is essential for SGPs polarization, adhesion, or migration. We showed that the position of Z1 and Z4 cells is often altered in the early gonads of *ten-1* mutants. This could indicate that TEN-1 plays an important role in SGPs at the early stages of gonad epithelialization and that gonadal BM discontinuity is the consequence of somatic cell mispositioning.

Teneurin Acts Redundantly with BM Receptors Integrin and Dystroglycan

Mutants in the *ten-1*, *ina-1* and *dgn-1* genes share several phenotypic features, including gonad disorganization, protruding vulva, defasciculation of the ventral nerve cord, distal tip cell migration, and axonal guidance defects (Baum and Garriga, 1997; Drabikowski *et al.*, 2005; Johnson *et al.*, 2006; Meighan and Schwarzbauer, 2007). Double mutants between *ten-1*, *ina-1*, and *dgn-1* showed synergistic genetic interaction implying that these three genes act in similar developmental processes and have partly redundant function. However, the mechanism of teneurin signaling remains unclear. Related roles of these receptors in gonad development could not be directly assessed because of functional redundancy in other developmental processes, i.e., pharyngeal or hypodermal morphogenesis.

Although *dgn-1* mutants do not show any obvious pharyngeal defects, arrested larvae of *ten-1;dgn-1* worms were translucent with misshapen pharynges. This suggests that there is compensation between *ten-1* and *dgn-1* in pharynx development and function. Interestingly, lack of the *ten-1* gene in *nid-1* mutant worms had the same effect as the removal of *dgn-1* in the *nid-1* mutant background (J. M. Kramer, personal communication), and both double mutants show a Pun phenotype. Therefore, loss of teneurin or dystroglycan sensitizes the worms strongly to loss of nidogen, which confirms the functional redundancy between *ten-1* and *dgn-1*.

Furthermore, *ten-1;ina-1* mutants were synthetic lethal and arrested as embryos or early larvae, frequently with severe morphological defects. Integrin loss-of-function mutants *ina-1(gm39)* show malformation of the anterior hypoderm, manifesting as a notched-head phenotype (Baum and Garriga, 1997), whereas *ten-1* mutants have low penetrance morphological defects in the posterior body (Drabikowski *et al.*, 2005). Combination of mutations in both genes resulted in worms arrested as L1 larvae with the entire body deformed. Mosaic analysis revealed that INA-1 is important in hypodermis (Baum and Garriga, 1997), and TEN-1 is known to be expressed in hypodermal cells of the developing embryo (Drabikowski *et al.*, 2005). Therefore, mild defects found in single mutants may be due to compensation by activity in a parallel pathway. This strongly suggests that *ina-1* and *ten-1* could act together in several developmental processes, including hypodermal morphogenesis.

In summary, TEN-1, INA-1, and DGN-1 are not required for BM function in general, but they are crucial in particular tissues and organs such as the gonad, pharynx, or hypodermis. The lack of a phenotype in all BMs could also reflect redundancy between these three receptors, where deletion

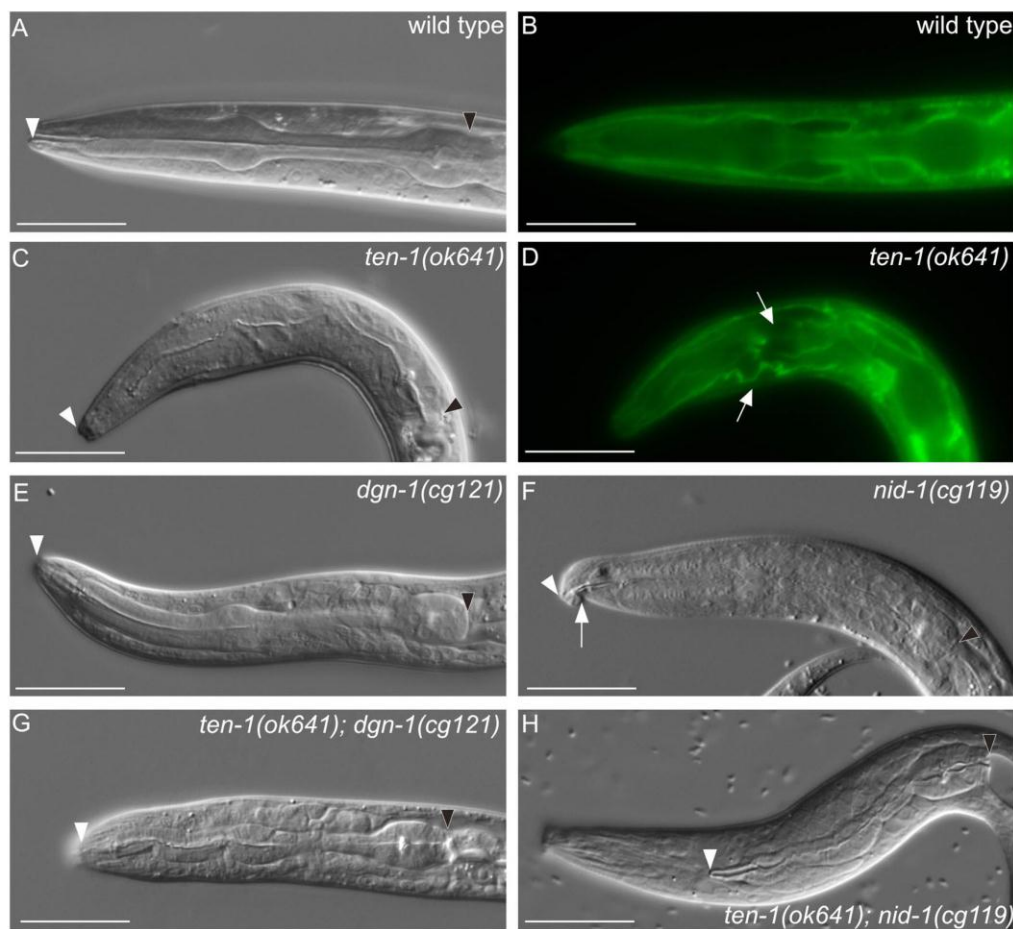
A. Trzebiatowska *et al.*

Figure 9. Pharyngeal defects in *ten-1*, *nid-1*, and *dgn-1* single and double mutants. Pharynx morphology of L1 larva is shown. *LAM-1::GFP* marker labels the pharyngeal basement membrane. Wild-type pharynx is outlined by a sharp DIC boundary visible by DIC microscopy (A). Basement membrane organization in the wild-type larva visualized by *LAM-1::GFP* (B). Arrested larvae of *ten-1(ok641)* mutant have misshapen pharynxes and the pharyngeal outline is invisible on DIC pictures (C). In the *ten-1* mutant, the basement membrane around the pharynx is disorganized or missing in some parts (arrows) (D). The pharynx of the *dgn-1* mutant worms shows no obvious defects (E). Arrested larvae of *nid-1* mutants have sometimes bent pharynxes (arrow) (F) or their pharynxes do not attach to the hypoderm (similar to the double mutant shown in H). Variably misshapen pharynxes were found in the *ten-1;dgn-1* double mutants (G). An unattached pharynx (Pun) phenotype observed in *ten-1;nid-1* double mutants (H). White arrowheads mark the anterior and black arrowheads posterior ends of the pharynxes. Scale bar, 20 μm .

of a single gene can be compensated for by the presence of other receptors.

ten-1 Is Synthetic Lethal with Genes Encoding Two BM Proteins: Laminin and Nidogen

The *ten-1* mutant phenotype resembled in many aspects the phenotypes of *epi-1* as well as the laminin binding receptors *ina-1* and *dgn-1*. Laminin *epi-1* mutants are generally sick and show cell polarization defects, tissue disorganization, and physical disruption of BMs (Huang *et al.*, 2003). Similar phenotypes have been described for laminin β loss-of-function mutants, *lam-1(rh219)* (Kao *et al.*, 2006). Thus, mutations in the laminin genes cause more severe defects than *dgn-1* or *ina-1* single mutants, suggesting that these two receptors might be functionally redundant or that additional laminin receptors exist. Mutation in the *ten-1* gene strongly enhanced the effects of *epi-1* depletion by RNAi, leading to almost

complete lethality of *ten-1(ok641);epi-1(RNAi)* worms. This result suggests that EPI-1 could be a ligand for TEN-1; however, direct interaction between TEN-1 and EPI-1 needs confirmation by further biochemical studies.

C. elegans nidogen is found in most BMs (Kang and Kramer, 2000), but loss of *nid-1* alone causes very mild defects, mainly in the nervous system (Kim and Wadsworth, 2000; Ackley *et al.*, 2003). The defects are, however, dramatically enhanced, if a *nid-1* deletion is combined with a mutation in teneurin, BM receptor *dgn-1*, or axon guidance molecules such as the *sax-3* Robo receptor or the *unc-40* netrin receptor (J. M. Kramer, personal communication). In such sensitized backgrounds, lack of *nid-1* causes a highly penetrant Pun phenotype. It appears that correct attachment of pharyngeal epithelium to arcade cells requires several receptors and guidance molecules as well as nidogen. Currently, NID-1 is considered more as a regulatory molecule

(Kim and Wadsworth, 2000; Hobert and Bulow, 2003) rather than being a purely structural component linking laminin and collagen networks (Fox *et al.*, 1991).

Conservation in Higher Organisms

Our data provide the first indication of a link between TEN-1 and BM function. There is little evidence from previous studies in vertebrates suggesting that teneurins could be BM receptors. However, in retrospect, the finding that induction of filopodia formation in neuroblastoma cells by teneurin-2 depends on the substrate and is more prominent on laminin than on poly-L-lysine (Rubin *et al.*, 1999) may reflect a direct interaction between these proteins. Furthermore, chicken teneurin-2 was found to colocalize with laminin in BMs of the optic cup and the heart endocardium (Tucker *et al.*, 2001).

Teneurin-3 knockout mice show defects in the positioning of specific visual circuits, leading to impaired binocular vision (Leamey *et al.*, 2007). Such a mild phenotype in the single mutant might be due to functional redundancy with other teneurins or, in the context of the present study, with BM receptors like integrins and dystroglycan. Our studies in *C. elegans* could be instructive for further analyses of teneurins, integrins, or dystroglycan function in vertebrates, because they point out redundancy not only between several receptors of the same family but also between structurally distinct receptor families.

ACKNOWLEDGMENTS

We thank Shohei Mitani (Tokyo Women's Medical University School of Medicine, Tokyo, Japan) and the Japanese National BioResource Project for providing the *ten-1(tm651)* strain and the *C. elegans* Gene Knockout Consortium for *ten-1(ok641)* strain; James M. Kramer for the generous gift of antibodies and strains, William Wadsworth and Susan Strome for GFP marker strains; Andrew Fire (Stanford University School of Medicine, Stanford, CA) for GFP expression vectors. We acknowledge Julie Ahringer, Cambridge University Technical Services Limited and Medical Research Council gene service for the RNAi clone. Some strains used in this study were provided by the *Caenorhabditis* Genetics Center (CGC). We thank Richard P. Tucker for critical reading of the manuscript. This work was supported by the Novartis Research Foundation.

REFERENCES

- Ackley, B. D., Crew, J. R., Elamaa, H., Pihlajaniemi, T., Kuo, C. J., and Kramer, J. M. (2001). The NCI/endostatin domain of *Caenorhabditis elegans* type XVIII collagen affects cell migration and axon guidance. *J. Cell Biol.* **152**, 1219–1232.
- Ackley, B. D., Kang, S. H., Crew, J. R., Suh, C., Jin, Y., and Kramer, J. M. (2003). The basement membrane components nidogen and type XVIII collagen regulate organization of neuromuscular junctions in *Caenorhabditis elegans*. *J. Neurosci.* **23**, 3577–3587.
- Bagutti, C., Forro, G., Ferralli, J., Rubin, B., and Chiquet-Ehrismann, R. (2003). The intracellular domain of teneurin-2 has a nuclear function and represses zic-1-mediated transcription. *J. Cell Sci.* **116**, 2957–2966.
- Baum, P. D., and Garriga, G. (1997). Neuronal migrations and axon fasciculation are disrupted in *ina-1* integrin mutants. *Neuron* **19**, 51–62.
- Baumgartner, S., and Chiquet-Ehrismann, R. (1993). Tena, a *Drosophila* gene related to tenascin, shows selective transcript localization. *Mech. Dev.* **40**, 165–176.
- Baumgartner, S., Martin, D., Hagios, C., and Chiquet-Ehrismann, R. (1994). Tenu, a *Drosophila* gene related to tenascin, is a new pair-rule gene. *EMBO J.* **13**, 3728–3740.
- Ben-Zur, T., Feige, E., Motro, B., and Wides, R. (2000). The mammalian Odz gene family: homologs of a *Drosophila* pair-rule gene with expression implying distinct yet overlapping developmental roles. *Dev. Biol.* **217**, 107–120.
- Benard, C. Y., Boyanov, A., Hall, D. H., and Hobert, O. (2006). DIG-1, a novel giant protein, non-autonomously mediates maintenance of nervous system architecture. *Development* **133**, 3329–3340.
- Bokel, C., and Brown, N. H. (2002). Integrins in development: moving on, responding to, and sticking to the extracellular matrix. *Dev. Cell* **3**, 311–321.

- Brenner, S. (1974). The genetics of *Caenorhabditis elegans*. *Genetics* **77**, 71–94.
- Drabikowski, K., Trzebiatowska, A., and Chiquet-Ehrismann, R. (2005). *ten-1*, an essential gene for germ cell development, epidermal morphogenesis, gonad migration, and neuronal pathfinding in *Caenorhabditis elegans*. *Dev. Biol.* **282**, 27–38.
- Fascetti, N., and Baumgartner, S. (2002). Expression of *Drosophila* Ten-a, a dimeric receptor during embryonic development. *Mech. Dev.* **114**, 197–200.
- Finney, M., and Ruvkun, G. (1990). The *unc-86* gene product couples cell lineage and cell identity in *C. elegans*. *Cell* **63**, 895–905.
- Fox, J. W. *et al.* (1991). Recombinant nidogen consists of three globular domains and mediates binding of laminin to collagen type IV. *EMBO J.* **10**, 3137–3146.
- Gilchrist, E. J., and Moerman, D. G. (1992). Mutations in the *sup-38* gene of *Caenorhabditis elegans* suppress muscle-attachment defects in *unc-52* mutants. *Genetics* **132**, 431–442.
- Graham, P. L., Johnson, J. J., Wang, S., Sibley, M. H., Gupta, M. C., and Kramer, J. M. (1997). Type IV collagen is detectable in most, but not all, basement membranes of *Caenorhabditis elegans* and assembles on tissues that do not express it. *J. Cell Biol.* **137**, 1171–1183.
- Higginson, J. R., and Winder, S. J. (2005). Dystroglycan: a multifunctional adaptor protein. *Biochem. Soc. Trans.* **33**, 1254–1255.
- Hobert, O., and Bulow, H. (2003). Development and maintenance of neuronal architecture at the ventral midline of *C. elegans*. *Curr. Opin. Neurobiol.* **13**, 70–78.
- Huang, C. C., Hall, D. H., Hedgecock, E. M., Kao, G., Karantz, V., Vogel, B. E., Hutter, H., Chisholm, A. D., Yurchenco, P. D., and Wadsworth, W. G. (2003). Laminin alpha subunits and their role in *C. elegans* development. *Development* **130**, 3343–3358.
- Johnson, R. P., Kang, S. H., and Kramer, J. M. (2006). *C. elegans* dystroglycan DGN-1 functions in epithelia and neurons, but not muscle, and independently of dystrophin. *Development* **133**, 1911–1921.
- Kamath, R. S., and Ahringer, J. (2003). Genome-wide RNAi screening in *Caenorhabditis elegans*. *Methods* **30**, 313–321.
- Kang, S. H., and Kramer, J. M. (2000). Nidogen is nonessential and not required for normal type IV collagen localization in *Caenorhabditis elegans*. *Mol. Biol. Cell* **11**, 3911–3923.
- Kao, G., Huang, C. C., Hedgecock, E. M., Hall, D. H., and Wadsworth, W. G. (2006). The role of the laminin beta subunit in laminin heterotrimer assembly and basement membrane function and development in *C. elegans*. *Dev. Biol.* **290**, 211–219.
- Kenzelmann, D., Chiquet-Ehrismann, R., Leachman, N. T., Tucker, R. P. (2008). Teneurin-1 is expressed in interconnected regions of the developing brain and is processed in vivo. *BMC Dev. Biol.* **8**, 30
- Kim, S., and Wadsworth, W. G. (2000). Positioning of longitudinal nerves in *C. elegans* by nidogen. *Science* **288**, 150–154.
- Kinel-Tahan, Y., Weiss, H., Dgany, O., Levine, A., and Wides, R. (2007). *Drosophila* odz gene is required for multiple cell types in the compound retina. *Dev. Dyn.* **236**, 2541–2554.
- Leamey, C. A., Glendinning, K. A., Kreiman, G., Kang, N. D., Wang, K. H., Fassler, R., Sawatari, A., Tonegawa, S., and Sur, M. (2008). Differential gene expression between sensory neocortical areas: potential roles for Ten_m3 and Bcl6 in patterning visual and somatosensory pathways. *Cereb. Cortex* **18**, 53–66.
- Leamey, C. A., Merlin, S., Lattouf, P., Sawatari, A., Zhou, X., Demel, N., Glendinning, K. A., Oohashi, T., Sur, M., and Fassler, R. (2007). Ten_m3 regulates eye-specific patterning in the mammalian visual pathway and is required for binocular vision. *PLoS Biol.* **5**, e241.
- Levine, A., Bashan-Ahrend, A., Budai-Hadrian, O., Gartenberg, D., Menasherov, S., and Wides, R. (1994). Odd Oz: a novel *Drosophila* pair rule gene. *Cell* **77**, 587–598.
- Li, H., Bishop, K. M., and O'Leary, D. D. (2006). Potential target genes of EMX2 include Odz/Ten-M and other gene families with implications for cortical patterning. *Mol. Cell. Neurosci.* **33**, 136–149.
- Meighan, C. M., and Schwarzbauer, J. E. (2007). Control of *C. elegans* hermaphrodite gonad size and shape by vab-3/Pax6-mediated regulation of integrin receptors. *Genes Dev.* **21**, 1615–1620.
- Mello, C. C., Kramer, J. M., Stinchcomb, D., and Ambros, V. (1991). Efficient gene transfer in *C. elegans*: extrachromosomal maintenance and integration of transforming sequences. *EMBO J.* **10**, 3959–3970.
- Mieda, M., Kikuchi, Y., Hirate, Y., Aoki, M., and Okamoto, H. (1999). Compartmentalized expression of zebrafish *ten-m3* and *ten-m4*, homologues of the

A. Trzebiatowska *et al.*

Drosophila ten(m) /odd Oz gene, in the central nervous system. *Mech. Dev.* 87, 223–227.

Miner, J. H., and Yurchenco, P. D. (2004). Laminin functions in tissue morphogenesis. *Annu. Rev. Cell Dev. Biol.* 20, 255–284.

Minet, A. D., and Chiquet-Ehrismann, R. (2000). Phylogenetic analysis of teneurin genes and comparison to the rearrangement hot spot elements of *E. coli*. *Gene* 257, 87–97.

Minet, A. D., Rubin, B. P., Tucker, R. P., Baumgartner, S., and Chiquet-Ehrismann, R. (1999). Teneurin-1, a vertebrate homologue of the *Drosophila* pair-rule gene *ten-m*, is a neuronal protein with a novel type of heparin-binding domain. *J. Cell Sci.* 112, 2019–2032.

Muriel, J. M., Dong, C., Hutter, H., and Vogel, B. E. (2005). Fibulin-1C and Fibulin-1D splice variants have distinct functions and assemble in a hemicentin-dependent manner. *Development* 132, 4223–4234.

Ohashi, T., Zhou, X. H., Feng, K., Richter, B., Morgelin, M., Perez, M. T., Su, W. D., Chiquet-Ehrismann, R., Rauch, U., and Fassler, R. (1999). Mouse *ten-m*/Odz is a new family of dimeric type II transmembrane proteins expressed in many tissues. *J. Cell Biol.* 145, 563–577.

Otaki, J. M., and Firestein, S. (1999). Neurestin: putative transmembrane molecule implicated in neuronal development. *Dev. Biol.* 212, 165–181.

Previtali, S. C., Dina, G., Nodari, A., Fasolini, M., Wrabetz, L., Mayer, U., Feltri, M. L., and Quattrini, A. (2003). Schwann cells synthesize $\alpha 7\beta 1$ integrin which is dispensable for peripheral nerve development and myelination. *Mol. Cell. Neurosci.* 23, 210–218.

Rakovitsky, N., Buganim, Y., Swissa, T., Kinel-Tahan, Y., Brenner, S., Cohen, M. A., Levine, A., and Wides, R. (2007). *Drosophila* Ten-a is a maternal pair-rule and patterning gene. *Mech. Dev.* 124, 911–924.

Rubin, B. P., Tucker, R. P., Brown-Luedi, M., Martin, D., and Chiquet-Ehrismann, R. (2002). Teneurin 2 is expressed by the neurons of the thalamofugal visual system in situ and promotes homophilic cell-cell adhesion in vitro. *Development* 129, 4697–4705.

Rubin, B. P., Tucker, R. P., Martin, D., and Chiquet-Ehrismann, R. (1999). Teneurins: a novel family of neuronal cell surface proteins in vertebrates, homologous to the *Drosophila* pair-rule gene product *Ten-m*. *Dev. Biol.* 216, 195–209.

Tucker, R. P., and Chiquet-Ehrismann, R. (2006). Teneurins: a conserved family of transmembrane proteins involved in intercellular signaling during development. *Dev. Biol.* 290, 237–245.

Tucker, R. P., Chiquet-Ehrismann, R., Chevron, M. P., Martin, D., Hall, R. J., and Rubin, B. P. (2001). Teneurin-2 is expressed in tissues that regulate limb and somite pattern formation and is induced in vitro and in situ by FGF8. *Dev. Dyn.* 220, 27–39.

Tucker, R. P., Kenzelmann, D., Trzebiatowska, A., and Chiquet-Ehrismann, R. (2007). Teneurins: transmembrane proteins with fundamental roles in development. *Int. J. Biochem. Cell Biol.* 39, 292–297.

Tucker, R. P., Martin, D., Kos, R., and Chiquet-Ehrismann, R. (2000). The expression of teneurin-4 in the avian embryo. *Mech. Dev.* 98, 187–191.

Zhou, X. H., Brandau, O., Feng, K., Ohashi, T., Ninomiya, Y., Rauch, U., and Fassler, R. (2003). The murine *Ten-m*/Odz genes show distinct but overlapping expression patterns during development and in adult brain. *Gene Expr. Patterns* 3, 397–405.

3.2. Submitted results

C. elegans teneurin, *ten-1*, interacts genetically with the prolyl 4-hydroxylase, *phy-1*, and is important for basement membrane integrity during late elongation of the embryo.

Topf, U. and Chiquet-Ehrismann, R. (2010). *Mol Biol Cell*. *submitted*.

***C. elegans* teneurin, *ten-1*, interacts genetically with the prolyl 4-hydroxylase, *phy-1*, and is important for basement membrane integrity during late elongation of the embryo.**

Ulrike Topf* and Ruth Chiquet-Ehrismann*

*Friedrich Miescher Institute for Biomedical Research, Novartis Research Foundation,
Basel, Switzerland

Running head: *ten-1* genetically interacts with *phy-1*.

Keywords: epidermis, prolyl 4-hydroxylase, collagen IV, odz1

Corresponding author: Ruth Chiquet-Ehrismann
Friedrich Miescher Institute for Biomedical Research
Novartis Research Foundation
Maulbeerstrasse 66
CH-4058 Basel
Switzerland
Tel. + 41 61 697 24 94
Fax + 41 61 697 39 76
e-mail: Ruth.Chiquet@fmi.ch

Abstract

Teneurins are a family of phylogenetically conserved proteins implicated in pattern formation and morphogenesis. The sole ortholog in *Caenorhabditis elegans* named *ten-1* is important for hypodermal cell migration, neuronal migration, pathfinding and fasciculation, gonad development and basement membrane integrity of some tissues. However, the mechanisms of TEN-1 action remain to be elucidated. Using a genome wide RNAi approach we identified *phy-1* as a novel interaction partner of *ten-1*. *phy-1* codes for the catalytical domain of the collagen prolyl 4-hydroxylase. The loss of *phy-1* significantly enhanced the embryonic lethality of *ten-1* null mutants. Double mutant embryos arrest during late elongation with epidermal defects, disruption of basement membranes and rupture of body wall muscles.

In addition, we found that loss of *phy-1* leads to aggregation of collagen IV in body wall muscles in elongated embryos suggesting a function of PHY-1 in modification of basement membrane collagen IV.

We demonstrate that loss of *ten-1* function, together with a reduction of functional basement membrane collagen IV protein, results in instability of the connection between the epidermis, extracellular matrix and muscles during late elongation in *C. elegans* development.

We propose that TEN-1 is important to sustain stability in tissues that are exposed to mechanical stress during *C. elegans* embryogenesis.

Introduction

Morphogenesis, together with cell growth and cellular differentiation, is one of the fundamental processes of development. It governs the biological process of developing the shape of an organism. Many morphogenetic movements involve epithelia. The coordination of morphogenetic movements involve interactions between the extracellular matrix, the cell surface, and the cytoskeleton (Chin-Sang and Chisholm, 2000). The epidermis is the largest organ in *C. elegans*. Its structure defines the shape and the size of the animal. During *C. elegans* embryogenesis an ovoid ball of cells changes into a worm-shaped larva, driven by the migration, fusion, and elongation of epidermal cells (Simske and Hardin, 2001). Disruption of any of these processes leads to arrested embryos. Whereas early embryonic elongation depends on circumferentially oriented actin in the epidermal cells (Priess and Hirsh, 1986), processes beyond the 2-fold stage require proper connections between the epidermis, basement membrane (BM) and the underlying body wall muscles (Francis and Waterston, 1991; Williams and Waterston, 1994). Once elongation is complete, the hypodermal cells secrete the extracellular cuticle to hold the hypodermal cells in their final shape (Priess and Hirsh, 1986).

The teneurins are a family of phylogenetically conserved proteins expressed during pattern formation and morphogenesis. They were discovered in *Drosophila* as *ten-m/odz* and *ten-a* (Baumgartner et al., 1994; Fascetti and Baumgartner, 2002; Levine et al., 1994; Rakovitsky et al., 2007). Since then teneurins were described in zebrafish (Mieda et al., 1999), chicken (Minet et al., 1999; Tucker et al., 2001), mouse (Ben-Zur et al., 2000; Oohashi et al., 1999; Zhou et al., 2003) and *C. elegans* (Drabikowski et al., 2005).

Teneurins encode type II transmembrane proteins with a conserved domain structure. They consist of an intracellular domain containing several conserved proline rich residues, a single transmembrane domain and an extracellular domain, which encompasses the major part of the protein. The extracellular domain consists of eight consecutive epidermal growth factor-like repeats, an extended region of conserved cysteines and a stretch of YD repeats towards the N-terminus. The predicted mass of teneurin monomers is approximately 300 kDa (Feng et al., 2002).

A single gene, named *ten-1*, encodes the sole ortholog of teneurins in *C. elegans*. Gene expression is controlled by two alternative promoters, *ten-1a* and *ten-1b*, resulting into two transcript versions differing in the length of the intracellular domain.

Promoter GFP fusion proteins show distinct expression pattern: the upstream promoter *ten-1a* is predominantly active in mesoderm whereas the downstream promoter *ten-1b* is predominantly active in the ectoderm (Drabikowski et al., 2005). TEN-1 is important for epidermal morphogenesis, gonad migration, neuronal pathfinding and BM integrity of several tissues (Drabikowski et al., 2005; Trzebiatowska et al., 2008). Two deletion alleles of *ten-1* were characterized as genetic null alleles: *ok641* and *tm651* (Trzebiatowska et al., 2008). Both mutants display pleiotropic phenotypes, including embryonic lethality, larval arrest, sterility, protruding vulva or bursting through the vulva. Null mutants exhibit germ cells leaking from the developing gonad into the body cavity because of rupture in the gonadal BM during the second larval stage. Attempts to investigate the function of *ten-1* led to the discovery of genetic interactions of *ten-1* with BM associated genes dystroglycan *dgn-1*, integrin *ina-1*, laminin *epi-1*, and nidogen *nid-1*. These experiments suggested that *ten-1* acts in a parallel pathway with a partly redundant function to dystroglycan and/or integrin receptors (Trzebiatowska et al., 2008).

Several studies on mutations in genes encoding BM molecules illustrate the importance of these components in morphogenesis. In *C. elegans*, a thin BM lines the pseudocoelomic cavity and separates the body wall muscle cells from the hypodermis and nervous system (White et al., 1976). A similar BM surrounds the intestine and gonad, while a thicker BM surrounds the pharynx (Albertson and Thomson, 1976; White, 1988). In *C. elegans*, type IV collagen is expressed by the body wall muscle cells (Graham et al., 1997). Two genes have been identified to encode BM collagen IV, *emb-9* and *let-2*. Before the proteins are secreted to the BM they undergo several steps of modifications in the endoplasmic reticulum. In vertebrates an essential role has been identified for the prolyl 4-hydroxylase (P4H). Proline hydroxylation of procollagen is important for the stable folding of the collagen trimer at physiological temperatures (Fessler and Fessler, 1978). The enzyme P4H consists of an enzymatic subunit and a protein disulfide isomerase subunit. The loss of the enzymatic subunit causes embryonic lethality in the mouse due to loss of BM integrity (Holster et al., 2007). Genes encoding the subunits of the P4H are phylogenetically conserved. Four genes have been identified to encode the enzymatic subunit of the *C. elegans* P4H: *phy-1* (also known as *dpy-18*), *phy-2*, *phy-3* and *phy-4* (Keskiäho et al., 2008; Myllyharju et al., 2002; Riihimaa et al., 2002; Winter and Page, 2000). Epistasis analyses show that *phy-1* in complex with *phy-2* is essential for the survival of the worm. *Phy-1* mutations alone result in a mild dumpy

phenotype whereas worms lacking *phy-2* alone do not show any phenotype indicating that *phy-1* is the most important subunit for the function of P4H at normal physiological conditions. The P4H in *C. elegans* has been implicated in the modification of cuticle collagens but not in the maturation of BM collagen.

In this study, we characterize a novel genetic interaction between *ten-1* and *phy-1* in *C. elegans*. We investigate *ten-1* function during late embryonic elongation in a *phy-1* deletion background. The characterization of the genetic interaction between *ten-1* and *phy-1* indicate a further link between TEN-1 and the extracellular matrix involving BM collagen IV. Furthermore, we contribute new insights into the function of *phy-1* in *C. elegans*.

Results

***ten-1* genetic interaction screen**

To identify new genetic interaction partners of *ten-1*, we performed a genome-wide RNAi screen. Synchronized L1 larvae of wild type and *ten-1(ok641)* mutant strain were fed continuously with RNAi bacteria for five days. Parental animals were analyzed for arrest, lethality and brood size. We also analyzed the F1 progeny for embryonic lethality and larval arrest. We only considered the genes whose knock downs resulted in a different phenotype in wild type versus *ten-1* mutant worms as putative *ten-1* interaction partners. We expected to find genes enhancing or suppressing the *ten-1(ok641)* mutant phenotypes, as well as genes whose knock down in wild type worms would be suppressed by depletion of *ten-1*. Identified genes were grouped according their molecular function (Figure 1 and Table S1). Genes acting in the nervous system or during gonad development were overrepresented in our *ten-1* interaction screen (Table S1). Suppressors and genes suppressed by loss of *ten-1* act most likely in the same pathway as *ten-1*. The potential suppressors seemed to have a positive effect on *ten-1* mutants reaching adulthood but knock down did not suppress a specific *ten-1* phenotype and we decided not to investigate those further. Unfortunately, no mutants for genes being suppressed by loss of *ten-1* were available or they were lethal making the investigation of these interactions more difficult. Thus, we decided to focus on genes acting redundantly to *ten-1*.

Since we already reported a possible link between *ten-1* and the extracellular matrix (Trzebiatowska et al., 2008), we choose to investigate in detail the genetic interaction between *ten-1* and *phy* genes, the latter coding for the catalytic subunits of a collagen modifying enzyme.

Loss of P4H function in *ten-1* null mutant results in embryonic lethality and ovulation defects

The *ten-1* interaction screen identified *phy-3* as an interaction partner of *ten-1*. Knock down of *phy-3* by RNAi in a *ten-1* deletion background resulted in enhanced embryonic and larval lethality, as well as an overall reduced brood size in comparison to empty vector control. Knock down of *phy-3* in a wild-type background did not lead to any obvious effect. *phy-3* belongs to a family of genes coding for catalytic subunits of the collagen modifying enzyme prolyl 4-hydroxylase. Four isoforms have been

identified in the worm: *phy-1*, *phy-2*, *phy-3* and *phy-4*. The mRNA sequences of all genes are very similar. To investigate whether the decrease of *phy-3* mRNA level caused off-target effects, we performed real time PCR analysis during rescreening of this candidate. We found that the RNAi for *phy-3* also affects the expression levels of *phy-1* and *phy-2* (Figure S1). To determine whether a single gene or a combination of them caused the enhancement of the *ten-1* mutant phenotype, we generated double and triple knock-out mutants. We found that only depletion of *phy-1* results in significant increase to 20% of embryonic lethality in a *ten-1* mutant background (Table 1). We also noticed a consistent increase in larval lethality (Table 1). *ten-1 phy-1* mutant animals were dumpy to the same extent as the *phy-1(ok162)* single mutant itself. Depletion of *phy-3* in *ten-1 phy-1* mutant background did not increase any analyzed phenotype (Table 1). We also analyzed the *ten-1 phy-1* double mutant animals for sterility, protruding vulva and bursting through the vulva phenotypes but could not find any differences concerning these phenotypes in comparison with the *ten-1* single mutant (data not shown). We did not generate a *ten-1 phy-1;phy-2* triple mutant because it was previously shown that *phy-1;phy-2* double mutants are embryonic lethal (Friedman et al., 2000). Interestingly, in contrast to *ten-1 phy-1* double mutants, *ten-1;phy-2* and *ten-1;phy-3* double mutants both showed ovulation defects, resulting in smaller and abnormally shaped eggs (data not shown). However, the ovulation defects could not be enhanced in a *ten-1;phy-2;phy-3* triple mutant and ovulation defects did not affect overall brood size (Table 1).

We also performed the double mutant analysis for another allele of *ten-1*, *tm651*, and found a similar increase of embryonic lethality when *phy-1* function is depleted (Table 1). Thus, the genetic interaction between *ten-1* and *phy-1* is true for two independent alleles of *ten-1*.

To show that the phenotype of the *ten-1(ok641) phy-1(ok162)* double mutant is specific for the loss of *phy-1*, we expressed the *phy-1* cDNA under its endogenous promoter in the double mutant. The construct rescued the dumpy phenotype, as well as the increased embryonic and larval lethality (Table 1). Thus, the analysis identified *phy-1* as a novel genetic interaction partner of *ten-1*, specifically affecting embryonic lethality.

Further characterization of the mechanism underlying the genetic interaction was done using the *ten-1(ok641) phy-1(ok162)* double mutant and corresponding single mutants.

***ten-1 phy-1* mutant arrests during late elongation showing morphological defects**

To determine the nature of the embryonic lethality in *ten-1 phy-1* double mutant we analyzed embryos using time-lapse Nomarski microscopy. We found that *ten-1 phy-1* double mutant embryos display defects in epidermal elongation (Figure 2). Wild-type embryos cultured at 20°C begin to elongate by ~350 minutes after first cleavage and complete elongation by ~600 minutes. At the 1.75-fold stage muscle contractions begin and embryos start to twitch. By the twofold stage embryos roll vigorously. Synthesis and deposition of larval cuticle start by ~690 minutes (Figure 2A and movie S1). The embryos hatch by ~800 minutes. *phy-1(ok162)* deletion mutant embryos were indistinguishable from wild type in their embryonic elongation (Figure 2C and movie S3). *ten-1(ok641)* deletion mutant embryos show low embryonic lethality (Drabikowski et al., 2005; Trzebiatowska et al., 2008). Embryonic elongation following epidermal enclosure was found to be mostly normal in the *ten-1(ok641)* deletion mutant (Figure 2B and movie S2). About 20% of the *ten-1 phy-1* double mutant embryos were embryonic lethal due to arrest at various stages of late elongation. Double mutant embryos displayed normal elongation prior to the 2-fold stage. Using time-lapse analysis, we recorded embryos arresting at the 2 or 2.5-fold stage (Figure 2D). Embryos were twitching and occasionally rolling. Nevertheless, movements seemed to be distinct from wild-type movements at the same stage of elongation (movie S4 and S5). The development continued, as indicated by cuticle formation and development of the pharynx. None of the recorded embryos displaying the elongation defects hatched. Quantitative phenotypic analysis of the *ten-1 phy-1* double mutant revealed an increase of worms arresting as early larvae (Table 1). Their phenotypic appearance was mostly undistinguishable from the arrested larvae caused by loss of *ten-1* alone. Embryos that did not hatch showed morphological defects of different severity (Figure 3). Morphology was analyzed approximately 15 hours after the eggs were laid. By this time control animals have all hatched. About 4% of the embryos had visible body shape defects and bulge formations (Figure 3 C). About 2% of the embryos ruptured during elongation (Figure 3D). However, 13% of the double mutant embryos elongated to a 3-fold like stage prior to arrest with constrictions in the epidermis or with other mild morphological defects (Figure 3B). Often a thicker epidermis at the anterior side of the animal was observed. The pharynx appeared bent in the anterior part and misplaced from its central position in comparison to a wild-type embryo at a 3-fold stage (Figure 3B, G). Double mutant

embryos, arresting at the 3-fold stage, showed rolling movements. We never observed that arrested embryos at the 3-fold stage had defects in cuticle formation since embryos kept their shape and never retracted. Double mutants and the *ten-1(ok641)* single mutant embryos showed a similar percentage of embryonic arrest during epidermal enclosure (Figure 3A). Only a minor percentage of *ten-1(ok641)* single mutant embryos showed late elongation defects, and when this occurred, it was accompanied by severe morphological defects and epidermal rupture (Figure 3F).

***ten-1 phy-1* embryos have epidermal defects and ruptured body wall muscles**

Elongation of the embryo reflects the elongation of epidermal cells along the anterior-posterior axis (Priess and Hirsh, 1986). We investigated this process by expressing the *ten-1b* promoter translational fusion to *gfp* as a reporter in *ten-1 phy-1* double mutant animals and all control strains. As previously shown, this promoter GFP fusion protein is expressed in neurons and in epidermal cells, excluding seam cells (Drabikowski et al., 2005). We analyzed randomly picked embryos of various stages during late elongation. We found that already at the 1.5-fold stage epidermal cells of the double mutant embryos were misshapen and mislocalized. Cells fused incorrectly (Figure 4B). Syncytia of epidermal cells of embryos at the 2-fold stage were misplaced (Figure 4D). Ventral epidermal cells still showed cell protrusions similar to migrating cells during ventral enclosure. Three-fold embryos of the double mutant showed protrusion encompassing epidermal cells and neurons (Figure 4F).

Soon after the birth of the major epidermal cells, they start to express and localize the AJM-1 protein, an apical epidermal junction marker. We used AJM-1 fused to GFP to analyze the epidermal cell junctions in arrested *ten-1 phy-1* double mutant embryos and the control strains. A wild type embryo at a 3-fold stage showed localization of AJM-1 only at cell-cell junctions. Seam cells can be distinguished from the main hypodermal syncytia hyp 3 to hyp 7 (Figure 5A). *ten-1(ok641)* single mutant had correct localization of AJM-1, although overall appearance seems mildly disorganized (Figure 5B). AJM-1 localization in *phy-1(ok162)* single mutant was indistinguishable from wild type (Figure S2C). Arrested *ten-1 phy-1* double mutant embryos showed high disorganization of AJM-1 and often mislocalization of AJM-1 at basal, as well as apical position of the epidermis was observed (Figure 5C, D).

During late embryogenesis, body wall muscles have been shown to be important for proper elongation (Hresko et al., 1994). The fact that double mutant embryos arresting around the 2-fold stage have difficulties with twitching and rolling prompted us to examine the structure of the body wall muscles. We visualized the body wall muscle structure of arrested *ten-1 phy-1* embryos expressing a *myo-3p::mcherry* marker (Figure 6). Wild type embryos at a 3-fold stage showed a continuous outline with muscle strands along the body (Figure 6A, B). Arrested double mutant embryos had breaks in the muscle strands or the muscles detached from the epidermis (Figure 6C, D).

***ten-1 phy-1* mutant shows basement membrane defects in arrested embryos**

Body wall muscles and epidermis are separated by a basement membrane. Loss of components connecting body wall muscles, BM and epidermis leads to arrest in elongation and paralysis of the embryo (Bercher et al., 2001; Boshier et al., 2003; Ding et al., 2003; Ding et al., 2008; Gettner et al., 1995; Hapiak et al., 2003; Hresko et al., 1999; Mackinnon et al., 2002; Woo et al., 2004). We investigated whether a loss of *ten-1* in the *phy-1* deletion background has an effect on BM integrity. To visualize basement membranes, we used the LAM-1::GFP reporter. This laminin chain localizes to all basement membranes in *C. elegans* (Kao et al., 2006). We found that arrested *ten-1 phy-1* double mutant embryos showed disrupted basement membranes of the muscle and the epidermis (Figure 7G, H). Frequently, we found disorganized BM surrounding the pharynx (Figure 7C, D). Defects in intestinal BM and gonadal BM could not be observed. None of the defects was found in wild type, *phy-1* or *ten-1* single mutant embryos (Figure S3).

Laminins in *C. elegans* are the first component forming basement membranes (Huang et al., 2003). In addition, collagen IV is essential to stabilize the basement membranes. Loss of collagen IV leads to embryonic lethality due to late elongation arrest and detachment of body wall muscles from the epidermis (Gupta et al., 1997). We stained *phy-1(ok162)* single mutant for EMB-9 and LET-2, the two *C. elegans* collagen IV chains identified (Figure 8, S4). In wild-type worms, collagen IV is expressed in body wall muscles. Embryos at the 2-fold stage have bright clusters of protein in the endoplasmic reticulum surrounding the nuclei of the muscles. Only small part of the protein is already localized to the basement membranes. No obvious differences in localization or amount of protein clusters were found in *phy-1(ok162)*

single mutant at this developmental stage. Three-fold stage wild-type embryos show staining of EMB-9 and LET-2 of basement membranes surrounding the intestine, pharynx, developing gonad and between body wall muscles and epidermis (Figure 8A, S4A). In contrast, we found that *phy-1(ok162)* deletion mutant still showed intracellular aggregations of protein in muscles of 3-fold embryos when stained with anti-collagen IV antibodies (Figure 8D-F). Also the staining of 3-fold embryos did not appear as smooth as in wild type. Sometimes staining appeared to be weaker in some parts of the basement membrane, although we never observed disruption or deformation of basement membranes. Note that we could not observe any general defects with the laminin gfp reporter either (Figure S3).

When we stained the *ten-1 phy-1* double mutant embryos with anti collagen IV antibodies, we observed an enhancement of protein aggregation in embryos that arrested around the 2-, 2.5-fold stage (Figure 8G-I). Nevertheless, a large fraction of the collagen IV was secreted and correctly localized. We observed a weakening of basement membranes at places where actin bundles were ruptured. In addition, a loss of integrity of the pharyngeal BM was observed, but not of the one surrounding the intestine or developing gonad. These findings correlated well with the ones made with the laminin gfp reporter described above.

The results of the immunostaining for collagen IV suggested a role for PHY-1 in muscle cells. To test this hypothesis, we expressed the *phy-1* cDNA specifically in body wall muscles using the *myo-3* promoter. Indeed, we rescued the increased embryonic lethality in *ten-1 phy-1* double mutant but not the dumpy phenotype (Table 1). Thus, our results uncovered a novel role for PHY-1 in body wall muscles during elongation, in addition to its role in the modification of cuticle collagens in the hypodermis.

Discussion

Genetic interaction screen

To further analyze the function of *ten-1* in *C. elegans*, we performed a genetic interaction screen for the *ten-1(ok641)* deletion mutant vs. wild type. Besides previously reported interactions between *ten-1* and integrin *ina-1* (Trzebiatowska et al., 2008) and *ten-1* and the notch receptor *glp-1* (Byrne et al., 2007) we found a variety of novel interactions.

Our screen uncovered candidate genes associated with functions in the nucleus like transcription, DNA repair or chromatin-structure associated proteins. They might become interesting in terms of *ten-1* intracellular domain function in the nucleus. Nuclear accumulation of the teneurin intracellular domains has been observed in several situations both in the worm (Drabikowski et al., 2005) and in vertebrates (Bagutti et al., 2003; Kenzelmann et al., 2008; Nunes et al., 2005).

Our screen also revealed genetic interactions with genes related to the cytoskeleton. In vertebrate cell culture experiments teneurin-2 induced formation of filopodia (Rubin et al., 1999) and filopodia formation requires remodeling of the cytoskeleton. Further analysis of the putative cytoskeleton-related interactors might help to understand how teneurins are connected to the cytoskeleton.

Genes involved in gonad and neuronal development were enriched in our screen. This is in agreement with phenotypes observed in *ten-1* mutants. Nevertheless, the essential function of *ten-1* might be during the development of the embryo. Thus, we decided to investigate further the interaction between *ten-1* and *phy-1*, which significantly enhanced the *ten-1* mutant embryonic lethality.

Loss of *phy-1* function enhances *ten-1* embryonic lethality

In this study we analyzed a novel genetic interaction between *ten-1* and *phy-1*. We found that *phy-1* loss of function significantly increases embryonic lethality of *ten-1* mutant animals. The interaction concerning this phenotype is allele independent. We analyzed double mutant embryos by time-lapse microscopy. *ten-1 phy-1* embryos arrest during late elongation. The loss of *phy-1* enhances the late embryonic defects which are only rarely found in *ten-1* single mutants. *phy-1(ok162)* mutant is indistinguishable from wild-type worms in terms of embryonic and larval lethality. Therefore, the phenotype of the double mutant does not just display an additive

effect but also a mechanistic connection between TEN-1 and PHY-1. Using several gfp fusion markers, we characterized the arrested embryos. We found defects in the migration and fusion of epidermal cells. Defects in early epidermal development during enclosure of the embryo were observed after knock down of *ten-1* by RNAi (Drabikowski et al., 2005). Recent study showed late embryonic defects of *ten-1(ok641)* single mutants (Morck et al., 2010). However, embryos with gross epidermal defects are rarely found in *ten-1(ok641)* single mutant and our analysis shows embryos predominantly arrest during enclosure. Only 0.36 % of *ten-1(ok641)* single mutant animals arrest around the 2-fold stage or rupture during elongation (Figure 3A).

Proper connection between body wall muscles, epidermal cells and the separating BM are crucial for successful late elongation (Zhang and Labouesse, 2010). *ten-1 phy-1* double mutant displayed rupture of body wall muscles and misplacement of epidermal cells during development. These observations suggest a compromised connection between these tissues. The downstream promoter of *ten-1*, *ten-1b*, is strongly active in the dorsal and ventral epidermis in the embryo. The subcellular localization of TEN-1 within the epidermis remains to be determined. Interestingly, mutants defective in the basal components of the epidermal attachment structures like myotactin, *let-805*, or the spectraplakins isoform, *vab-10A*, display similar phenotypes as we found in the *ten-1 phy-1* double mutant (Bosher et al., 2003; Hresko et al., 1999). Additionally, *ten-1* single mutants show low penetrance of embryonic lethality due to late elongation arrest, indicating a redundant role of *ten-1* with other genes during embryonic elongation. Loss of *phy-1* function seems to affect a process that supports proper *ten-1* function.

Does PHY-1 function in modification of basement membrane collagens?

In order to form stable helices, procollagen needs to be post-translationally modified. *phy-1* codes for the enzymatic subunit of *C. elegans* P4H and has been shown to be important for modification of cuticle collagens (Hill et al., 2000). Double mutants between *phy-1* and *phy-2* are embryonic lethal and embryos burst around the time of cuticle secretion (Winter and Page, 2000). Nevertheless, other observations of double mutant embryos elongating only to a 2-fold like stage prior to their explosion suggest an additional role for the enzyme complex (Friedman et al., 2000). Another collagen modifying enzyme, lysyl hydroxylase, *let-268*, was shown to be essential for

collagen IV secretion into the BM (Norman and Moerman, 2000). Loss of lysyl hydroxylation leads to elongation arrested and paralyzed embryos around the 2-fold stage and collagen IV aggregates in the endoplasmic reticulum. Staining *phy-1(ok162)* mutant embryos with anti-collagen IV antibodies also revealed accumulations of protein aggregates around the nuclei of body wall muscle cells in fully elongated embryos. We did not observe similar aggregations in wild-type worms. Nevertheless, collagen IV is still correctly localized to the basement membranes in *phy-1* mutants and we did not observe defects or breaks in basement membranes in these animals. Overall, the *phy-1(ok162)* single mutant did not display any embryonic defect above wild-type background. Modification of collagen IV seems sufficient to allow complete embryonic development and the paralogs of *phy-1* probably compensate for *phy-1* loss-of-function. Expression of PHY-1 in the muscle cells producing the type IV procollagen could not be shown by expression of *phy-1* promoter gfp fusion or immunostainings (Hill et al., 2000; Myllyharju et al., 2002). We were able to rescue the embryonic lethality of *ten-1 phy-1* double mutant by transient overexpression of *phy-1* under the muscle-specific promoter, *myo-3*. This argues for an important function of PHY-1 in the muscle cells.

In summary, our results indicate that in the worm P4H is responsible for the modification of type IV procollagen and this is in agreement with similar results obtained in vertebrates (Holster et al., 2007).

TEN-1 and its role in extracellular matrix assembly/ maintenance

There is increasing evidence that TEN-1 functions in the assembly or maintenance of the extracellular matrix in *C. elegans*. Previously, genetic interactions of *ten-1* with the BM receptors integrin *ina-1* and dystroglycan *dgn-1* were reported. Additionally, loss of *ten-1* function sensitizes animals towards an enhanced phenotype when combined with mutations in the BM components the laminin EPI-1 and the nidogen NID-1 (Trzebiatowska et al., 2008). Recently, a genetic interaction between *ten-1* and perlecan, *unc-52*, was found (Morck et al., 2010).

In this study we found that a compromised BM lacking collagen IV enhances *ten-1* mutant lethality. The morphological appearance of *ten-1 phy-1* double mutant partially resembles defects seen in collagen IV mutants. Collagen IV mutants arrest at the 2-fold or 3-fold stage due to detachment of body wall muscles from the epidermis (Gupta et al., 1997). Accumulations of collagen IV protein in *ten-1 phy-1*

mutant animals appear frequently as two strong spots on the opposite sites of each of the body wall muscle cell nuclei (Figure 8G, I). Similar staining has been reported when *emb-9* mutants were stained for LET-2 protein, indicating that LET-2, the alpha2(IV) chain, is not secreted in the absence of full-length EMB-9, the alpha1(IV) chain (Gupta et al., 1997). We postulate that Collagen IV is insufficiently modified by PHY-1, resulting in intracellular accumulation of protein and subsequent instability of basement membrane. The increased accumulation of collagen IV in *ten-1 phy-1* double mutant in contrast to *phy-1* single mutant led us also speculate whether TEN-1 itself could influence expression or maturation of collagen IV. Improper proportions of EMB-9 and LET-2 might lead to failure of correct assembly of the collagen triple helix and accumulation of protein in the cells that express it. Processing and translocation of TEN-1 intracellular domain to the nucleus has been described previously (Drabikowski et al., 2005), but its function in the nucleus is unclear.

We found defects in the BM surrounding the pharynx and between body wall muscles and epidermal cells. During elongation, these sites are exposed to mechanical forces by muscle contraction. Fibrous organelles, the structural homologs of vertebrate hemidesmosomes, provide mechanical stability with the onset of muscle contraction during elongation. However, whether collagen IV affects fibrous organelle formation is not clear. In addition, receptors responsible for collagen IV binding are not yet defined in *C. elegans*. It remains to be discovered whether TEN-1 provides guidance for assembly or is a receptor of collagen IV in *C. elegans*.

In summary, our results provide evidence that TEN-1 has a role in BM formation or stabilization required for mechanical stability during the process of late elongation in *C. elegans*. It is also possible that Ten-1 could represent a cellular collagen IV receptor.

Conservation in higher organisms

Our data provide evidence that TEN-1 links epidermal cells via BM proteins, like collagen IV, to muscle structures. In *Drosophila*, the Ten-a protein localizes to muscle attachment structures during embryogenesis (Fascetti and Baumgartner, 2002). Muscle attachment in *Drosophila* depends on PS integrin (Prokop et al., 1998). Loss of integrin leads to detachment of epidermal and muscle cells from the ECM. Nevertheless, in the absence of PS integrin, the connection between microtubules

and the epidermis is retained suggesting involvement of additional receptors (Brown, 2000).

In chicken, teneurin-2 co-localizes with laminin in the optic cup and ventricular endocardium (Tucker et al., 2001). A recent study investigating the expression of teneurin-4 in the avian embryo describes co-localization of teneurin-4 with laminin in the BM surrounding the endoderm, as well as nests of cells in the mesenchyme (Kenzelmann Broz et al., 2010). Thus, teneurins might be important for the organization and/or stabilization of basement membranes in vertebrates, too. Recently, another report described a co-expression of the mouse teneurin isoform, Odz3, with collagen I and II in distinct regions of the fibrous layer and in the proliferating layer of mandibular condylar cartilage (Murakami et al., 2010).

The co-expression and co-localization of teneurins with collagens and basement membranes on the one hand and the action of TEN-1 in conjunction with PHY-1 on the other hand point to a function of TEN-1 in morphogenesis, as established by the proper deposition of collagenous extracellular matrices and adequate attachment of the cells to these extracellular matrices.

Materials and Methods

General Methods and *C. elegans* strains

C. elegans strains were cultured at 20°C as described in (Brenner, 1974). Wild type refers to the *C. elegans* variety Bristol strain N2. Furthermore, the following strains were used: JK2729 [*phy-1(ok162)*], JK2757 [*phy-2(ok177)*], TP7 [*phy-3(ok199)*], RU90 [*ten-1(ok641)*], RU98 [*ten-1(tm651)*]. Strains were at least 4 times outcrossed prior analysis. The following GFP marker strains were used: RU9 [*kdEx31(ten-1b::gfp)*], IM253 [*urEx131(lam-1::gfp)*], SU93 [(*ajm-1::gfp; rol-6*); *him-5*], GW397 [*gwls28(myo-3p::mCherry; unc-119+)*; *gwls39*] (Meister et al.). Double and triple mutant worms were maintained as RU171 [*ten-1(ok641) phy-1(ok162)*], RU197 [*ten-1(tm-651) phy-1(ok162)*], RU179 [*ten-1(ok641); phy-2(ok177)*], RU168 [*ten-1(ok641); phy-3(ok199)*], RU177 [*ten-1(ok641) phy-1(ok162); phy-3(ok199)*], RU182 [*ten-1(ok641); phy-2(ok177); phy-3(ok199)*], RU181 [*phy-2(ok177); phy-3(ok199)*] strains.

Constructs and Plasmids

The *phy-1* rescue construct under the endogenous *phy-1* promoter was generated according to the following: *phy-1* 3'UTR was amplified from wild-type genomic DNA using 5'GTATCCAACAAATGGATCCACG3' and 5'TAGCAGCCGACACTAAACAG3'. The ORF of *phy-1* was amplified from cDNA and fused to its 3'UTR by PCR using 5'AGAAATATACCGGTAATCCTTGAC3' and 5'TATGGCGCCTAATTTATCACGG CAAAGAAAAAGGCAG3'. The resulting PCR fragment was cloned into pPD117.01 (A. Fire) into *AgeI* and *NarI* sites. Three kilobases of the *phy-1* 5'UTR was amplified by PCR using 5'TTTGCATGCTCAACTCTAGCAAATGGCAC3' and 5'GGATTACCGGTATATTTCTTTTCAG3'. The PCR fragment was cloned into *SphI* and *AgeI* sites.

To generate the body wall muscle specific rescue construct under the *myo-3* promoter, *phy-1* cDNA was amplified by PCR using 5'TTTCTAGAATGCGCCTGGCACTCCTTGAC3' and 5'TTACCGGTAGGGTCTCCCAGACGTC3'. The PCR fragment was cloned in pPD136.64 (A. Fire) into *XbaI* and *AgeI* sites.

Transgenic animals

Transgenic animals were generated by microinjection of DNA into the distal arms of gonads as described (Mello et al., 1991). *phy-1* under its own promoter was injected into N2 at 5 ng/μl plus 10 ng/μl of *unc-122::gfp* injection marker (made by P. Sengupta) and 85 ng/μl plasmid p3T (MoBiTe). Injection of the full rescue construct resulted in 3 independent lines, one of which is RU192 [kdEx132(*Pphy-1::phy-1::phy-1_3'UTR*)]. The tissue specific rescue construct was injected into N2 worms at a concentration of 5 ng/μl plus 95 ng/μl plasmid p3T (MoBiTe). For these tissue specific rescue, only one line could be obtained named RU191 [kdEx131(*Pmyo-3::phy-1::gfp*)]. All plasmids have been linearized with *AhdI* or *FspI* prior to injection. For rescue of the *ten-1 phy-1* double mutant, hermaphrodites were crossed with transgenic males carrying the extrachromosomal arrays. For summary of results see Table 1.

RNA interference screen

The screen was performed on RNAi plates in a 24-well format. RNAi clones were obtained from ORFeome feeding library. *gfp-1* RNAi was used from the Ahringer library (Kamath and Ahringer, 2003) RNAi bacteria were grown in a 96-well liquid format. Bacteria were induced with 1 mM final concentration of IPTG on the plates. Worms were treated with NaOCL to release eggs. Eggs were allowed to hatch on plates seeded with HT115(DE3) bacteria. L1 larvae were collected and 10 worms per well were distributed on RNAi plates containing ampicillin (100μg/ml) and tetracyclin (12.5μg/ml) using the Copas Biosorter (UnionBiometrica). Worms were grown for 5 days at 20 °C. Positive clones were sequenced for the correct open reading frame and rescreened in duplicate.

Phenotypic analysis

L4 hermaphrodites were placed on separate plates and allowed to lay eggs. The mother was transferred to new plates twice a day. Animals were analyzed for brood size and the progeny for embryonic lethality and larval lethality.

For time-lapse microscopy embryos were placed on 2 % agarose pad in egg buffer (Shakes and Epstein, 1995). Recording was performed for 4 to 6 h at 20°C in multiple focal planes using Nomarski optics Images were acquired with Z1

microscope (Zeiss) and Axio-Cam MRM camera (Zeiss). Movies were assembled using the ImageJ software.

Immunofluorescence staining

The protocol for staining of embryos was adapted from Graham et al. Samples were blocked with 10% normal goat serum (NGS) (Invitrogen) in phosphate-buffered saline (PBS) containing 0.5% TWEEN-20 (PBS-T). Primary antibodies against EMB-9 (NW1910, gift of J. M. Kramer), LET-2 (NW68, gift of J. M. Kramer) and actin (MAB 1501 from Chemicon) were added in PBS-T-NGS over night at 4°C. Embryos were washed with PBS-T and incubated with fluorescein-conjugated goat anti-rabbit (Alexa 488 from Invitrogen) or goat anti-mouse (Alexa 543 from Invitrogen) secondary antibody. Embryos were washed in PBS-T, containing Hoechst, followed by PBS alone.

Microscopy

Confocal images were acquired with Zeiss Axiovert 200M equipped with LSM510. Optical sections were collected at 0.7 μm intervals and combined using the maximum projection function. For publication, confocal images were annotated using ImageJ. For confocal imaging of embryos expressing gfp reporters, embryos of the appropriate ages were collected in egg buffer (Shakes and Epstein, 1995). The embryos were treated with NaOCL (1:10 diluted in water) for approximately 2 min. The embryos were washed in egg buffer, treated with chitinase (2.5U in egg buffer) for approximately 3 min and washed again in egg buffer only. Embryos were transferred to a 2 % agarose pad containing 10 mM sodium azide. Images of immobilized embryos were acquired immediately after treatment.

Acknowledgement

We thank James M. Kramer for the generous gift of antibodies and Andrew Fire for GFP expression vectors. We are grateful to Jacqueline Ferralli for technical assistance. We thank Joy Alcedo for critical comments on the manuscript.

Some nematode strains used in this work were provided by the Caenorhabditis Genetics Center funded by the NIH National center for Research Resources (NCRR). This work was supported by the Novartis Research Foundation.

References

- Albertson, D. G. and Thomson, J. N. (1976). The pharynx of *Caenorhabditis elegans*. *Philos Trans R Soc Lond B Biol Sci* 275, 299-325.
- Bagutti, C., Forro, G., Ferralli, J., Rubin, B. and Chiquet-Ehrismann, R. (2003). The intracellular domain of teneurin-2 has a nuclear function and represses zic-1-mediated transcription. *J Cell Sci* 116, 2957-66.
- Baumgartner, S., Martin, D., Hagios, C. and Chiquet-Ehrismann, R. (1994). Tenm, a *Drosophila* gene related to tenascin, is a new pair-rule gene. *Embo J* 13, 3728-40.
- Ben-Zur, T., Feige, E., Motro, B. and Wides, R. (2000). The mammalian Odz gene family: homologs of a *Drosophila* pair-rule gene with expression implying distinct yet overlapping developmental roles. *Dev Biol* 217, 107-20.
- Bosher, J. M., Hahn, B. S., Legouis, R., Sookhareea, S., Weimer, R. M., Gansmuller, A., Chisholm, A. D., Rose, A. M., Bessereau, J. L. and Labouesse, M. (2003). The *Caenorhabditis elegans* vab-10 spectraplakins isoforms protect the epidermis against internal and external forces. *J Cell Biol* 161, 757-68.
- Brown, N. H. (2000). Cell-cell adhesion via the ECM: integrin genetics in fly and worm. *Matrix Biol* 19, 191-201.
- Byrne, A. B., Weirauch, M. T., Wong, V., Koeva, M., Dixon, S. J., Stuart, J. M. and Roy, P. J. (2007). A global analysis of genetic interactions in *Caenorhabditis elegans*. *J Biol* 6, 8.
- Chin-Sang, I. D. and Chisholm, A. D. (2000). Form of the worm: genetics of epidermal morphogenesis in *C. elegans*. *Trends Genet* 16, 544-51.
- Drabikowski, K., Trzebiatowska, A. and Chiquet-Ehrismann, R. (2005). *ten-1*, an essential gene for germ cell development, epidermal morphogenesis, gonad migration, and neuronal pathfinding in *Caenorhabditis elegans*. *Dev Biol* 282, 27-38.
- Fascetti, N. and Baumgartner, S. (2002). Expression of *Drosophila* Ten-a, a dimeric receptor during embryonic development. *Mech Dev* 114, 197-200.
- Feng, K., Zhou, X. H., Oohashi, T., Morgelin, M., Lustig, A., Hirakawa, S., Ninomiya, Y., Engel, J., Rauch, U. and Fassler, R. (2002). All four members of the Ten-m/Odz family of transmembrane proteins form dimers. *J Biol Chem* 277, 26128-35.
- Fessler, J. H. and Fessler, L. I. (1978). Biosynthesis of procollagen. *Annu Rev Biochem* 47, 129-62.
- Francis, R. and Waterston, R. H. (1991). Muscle cell attachment in *Caenorhabditis elegans*. *J Cell Biol* 114, 465-79.

- Friedman, L., Higgin, J. J., Moulder, G., Barstead, R., Raines, R. T. and Kimble, J. (2000). Prolyl 4-hydroxylase is required for viability and morphogenesis in *Caenorhabditis elegans*. *Proc Natl Acad Sci U S A* 97, 4736-41.
- Graham, P. L., Johnson, J. J., Wang, S., Sibley, M. H., Gupta, M. C. and Kramer, J. M. (1997). Type IV collagen is detectable in most, but not all, basement membranes of *Caenorhabditis elegans* and assembles on tissues that do not express it. *J Cell Biol* 137, 1171-83.
- Gupta, M. C., Graham, P. L. and Kramer, J. M. (1997). Characterization of alpha1(IV) collagen mutations in *Caenorhabditis elegans* and the effects of alpha1 and alpha2(IV) mutations on type IV collagen distribution. *J Cell Biol* 137, 1185-96.
- Hill, K. L., Harfe, B. D., Dobbins, C. A. and L'Hernault, S. W. (2000). dpy-18 encodes an alpha-subunit of prolyl-4-hydroxylase in *caenorhabditis elegans*. *Genetics* 155, 1139-48.
- Holster, T., Pakkanen, O., Soininen, R., Sormunen, R., Nokelainen, M., Kivirikko, K. I. and Myllyharju, J. (2007). Loss of assembly of the main basement membrane collagen, type IV, but not fibril-forming collagens and embryonic death in collagen prolyl 4-hydroxylase I null mice. *J Biol Chem* 282, 2512-9.
- Hresko, M. C., Schriefer, L. A., Shrimankar, P. and Waterston, R. H. (1999). Myotactin, a novel hypodermal protein involved in muscle-cell adhesion in *Caenorhabditis elegans*. *J Cell Biol* 146, 659-72.
- Hresko, M. C., Williams, B. D. and Waterston, R. H. (1994). Assembly of body wall muscle and muscle cell attachment structures in *Caenorhabditis elegans*. *J Cell Biol* 124, 491-506.
- Huang, C. C., Hall, D. H., Hedgecock, E. M., Kao, G., Karantza, V., Vogel, B. E., Hutter, H., Chisholm, A. D., Yurchenco, P. D. and Wadsworth, W. G. (2003). Laminin alpha subunits and their role in *C. elegans* development. *Development* 130, 3343-58.
- Kamath, R. S. and Ahringer, J. (2003). Genome-wide RNAi screening in *Caenorhabditis elegans*. *Methods* 30, 313-21.
- Kao, G., Huang, C. C., Hedgecock, E. M., Hall, D. H. and Wadsworth, W. G. (2006). The role of the laminin beta subunit in laminin heterotrimer assembly and basement membrane function and development in *C. elegans*. *Dev Biol* 290, 211-9.
- Kenzelmann Broz, D., Tucker, R. P., Leachman, N. T. and Chiquet-Ehrismann, R. (2010). The expression of teneurin-4 in the avian embryo: potential roles in patterning in the limb and nervous system. *Int.J.Dev.Biol.* in press.

- Kenzelmann, D., Chiquet-Ehrismann, R., Leachman, N. T. and Tucker, R. P. (2008). Teneurin-1 is expressed in interconnected regions of the developing brain and is processed in vivo. *BMC Dev Biol* 8, 30.
- Keskiaho, K., Kukkola, L., Page, A. P., Winter, A. D., Vuoristo, J., Sormunen, R., Nissi, R., Riihimaa, P. and Myllyharju, J. (2008). Characterization of a novel *Caenorhabditis elegans* prolyl 4-hydroxylase with a unique substrate specificity and restricted expression in the pharynx and excretory duct. *J Biol Chem* 283, 10679-89.
- Levine, A., Bashan-Ahrend, A., Budai-Hadrian, O., Gartenberg, D., Menasherow, S. and Wides, R. (1994). Odd Oz: a novel *Drosophila* pair rule gene. *Cell* 77, 587-98.
- Meister, P., Towbin, B. D., Pike, B. L., Ponti, A. and Gasser, S. M. The spatial dynamics of tissue-specific promoters during *C. elegans* development. *Genes Dev* 24, 766-82.
- Mello, C. C., Kramer, J. M., Stinchcomb, D. and Ambros, V. (1991). Efficient gene transfer in *C.elegans*: extrachromosomal maintenance and integration of transforming sequences. *Embo J* 10, 3959-70.
- Mieda, M., Kikuchi, Y., Hirate, Y., Aoki, M. and Okamoto, H. (1999). Compartmentalized expression of zebrafish ten-m3 and ten-m4, homologues of the *Drosophila* ten(m)/odd Oz gene, in the central nervous system. *Mech Dev* 87, 223-7.
- Minet, A. D., Rubin, B. P., Tucker, R. P., Baumgartner, S. and Chiquet-Ehrismann, R. (1999). Teneurin-1, a vertebrate homologue of the *Drosophila* pair-rule gene ten-m, is a neuronal protein with a novel type of heparin-binding domain. *J Cell Sci* 112 (Pt 12), 2019-32.
- Morck, C., Vivekanand, V., Jafari, G. and Pilon, M. (2010). *C. elegans* ten-1 is synthetic lethal with mutations in cytoskeleton regulators, and enhances many axon guidance defective mutants. *BMC Dev Biol* 10, 55.
- Murakami, T., Fukunaga, T., Takeshita, N., Hiratsuka, K., Abiko, Y., Yamashiro, T. and Takano-Yamamoto, T. (2010). Expression of Ten-m/Odz3 in the fibrous layer of mandibular condylar cartilage during postnatal growth in mice. *J Anat*.
- Myllyharju, J., Kukkola, L., Winter, A. D. and Page, A. P. (2002). The exoskeleton collagens in *Caenorhabditis elegans* are modified by prolyl 4-hydroxylases with unique combinations of subunits. *J Biol Chem* 277, 29187-96.
- Norman, K. R. and Moerman, D. G. (2000). The let-268 locus of *Caenorhabditis elegans* encodes a procollagen lysyl hydroxylase that is essential for type IV collagen secretion. *Dev Biol* 227, 690-705.

- Nunes, S. M., Ferralli, J., Choi, K., Brown-Luedi, M., Minet, A. D. and Chiquet-Ehrismann, R. (2005). The intracellular domain of teneurin-1 interacts with MBD1 and CAP/ponsin resulting in subcellular codistribution and translocation to the nuclear matrix. *Exp Cell Res* 305, 122-32.
- Oohashi, T., Zhou, X. H., Feng, K., Richter, B., Morgelin, M., Perez, M. T., Su, W. D., Chiquet-Ehrismann, R., Rauch, U. and Fassler, R. (1999). Mouse ten-m/Odz is a new family of dimeric type II transmembrane proteins expressed in many tissues. *J Cell Biol* 145, 563-77.
- Priess, J. R. and Hirsh, D. I. (1986). *Caenorhabditis elegans* morphogenesis: the role of the cytoskeleton in elongation of the embryo. *Dev Biol* 117, 156-73.
- Prokop, A., Martin-Bermudo, M. D., Bate, M. and Brown, N. H. (1998). Absence of PS integrins or laminin A affects extracellular adhesion, but not intracellular assembly, of hemiadherens and neuromuscular junctions in *Drosophila* embryos. *Dev Biol* 196, 58-76.
- Rakovitsky, N., Buganim, Y., Swissa, T., Kinel-Tahan, Y., Brenner, S., Cohen, M. A., Levine, A. and Wides, R. (2007). *Drosophila* Ten-a is a maternal pair-rule and patterning gene. *Mech Dev* 124, 911-24.
- Riihimaa, P., Nissi, R., Page, A. P., Winter, A. D., Keskiaho, K., Kivirikko, K. I. and Myllyharju, J. (2002). Egg shell collagen formation in *Caenorhabditis elegans* involves a novel prolyl 4-hydroxylase expressed in spermatheca and embryos and possessing many unique properties. *J Biol Chem* 277, 18238-43.
- Rubin, B. P., Tucker, R. P., Martin, D. and Chiquet-Ehrismann, R. (1999). Teneurins: a novel family of neuronal cell surface proteins in vertebrates, homologous to the *Drosophila* pair-rule gene product Ten-m. *Dev Biol* 216, 195-209.
- Shakes, D. C. and Epstein, H. F. (1995). *Caenorhabditis elegans*: Modern Biological Analysis of an Organism: Academic Press, Inc.
- Simske, J. S. and Hardin, J. (2001). Getting into shape: epidermal morphogenesis in *Caenorhabditis elegans* embryos. *Bioessays* 23, 12-23.
- Trzebiatowska, A., Topf, U., Sauder, U., Drabikowski, K. and Chiquet-Ehrismann, R. (2008). *Caenorhabditis elegans* teneurin, *ten-1*, is required for gonadal and pharyngeal basement membrane integrity and acts redundantly with integrin *ina-1* and dystroglycan *dgn-1*. *Mol Biol Cell* 19, 3898-908.
- Tucker, R. P., Chiquet-Ehrismann, R., Chevron, M. P., Martin, D., Hall, R. J. and Rubin, B. P. (2001). Teneurin-2 is expressed in tissues that regulate limb and somite pattern formation and is induced in vitro and in situ by FGF8. *Dev Dyn* 220, 27-39.

- White, J. G. (1988). The anatomy. In "The Nematode *Caenorhabditis elegans*". NY: Cold Spring Harbor Laboratory Press, Cold Spring Harbor.
- White, J. G., Southgate, E., Thomson, J. N. and Brenner, S. (1976). The structure of the ventral nerve cord of *Caenorhabditis elegans*. *Philos Trans R Soc Lond B Biol Sci* 275, 327-48.
- Williams, B. D. and Waterston, R. H. (1994). Genes critical for muscle development and function in *Caenorhabditis elegans* identified through lethal mutations. *J Cell Biol* 124, 475-90.
- Winter, A. D. and Page, A. P. (2000). Prolyl 4-hydroxylase is an essential procollagen-modifying enzyme required for exoskeleton formation and the maintenance of body shape in the nematode *Caenorhabditis elegans*. *Mol Cell Biol* 20, 4084-93.
- Zhang, H. and Labouesse, M. (2010). The making of hemidesmosome structures in vivo. *Dev Dyn* 239, 1465-76.
- Zhou, X. H., Brandau, O., Feng, K., Oohashi, T., Ninomiya, Y., Rauch, U. and Fassler, R. (2003). The murine Ten-m/Odz genes show distinct but overlapping expression patterns during development and in adult brain. *Gene Expr Patterns* 3, 397-405.

Table 1. Embryonic lethality and larval arrest phenotype of *ten-1* with genes coding for prolyl 4-hydroxylase

Worm strain	Genotype	n	Total laid eggs (mean ± SEM)	Embryonic lethality (%) (mean ± SEM)	Larval arrest (%) (mean ± SEM)
N2	WT	26	269 ± 11.4	0.5 ± 0.1	0.3 ± 0.1
RU90	<i>ten-1(ok641)</i>	16	249 ± 18.3	3.8 ± 1.9**	30.0 ± 1.4
RU98	<i>ten-1(tm651)</i>	18	227 ± 17.0	3.9 ± 0.4**	21.3 ± 0.9
RU170	<i>phy-1(ok162)</i>	13	254 ± 10.6	1.0 ± 0.2	0.3 ± 0.1
RU178	<i>phy-2(ok172)</i>	7	279 ± 12.3	0.2 ± 0.1	0.2 ± 0.1
RU148	<i>phy-3(ok199)</i>	30	263 ± 7.8	1.3 ± 0.2	0.8 ± 0.2
RU171	<i>ten-1(ok641) phy-1(ok162)</i>	15	160 ± 11.6	20.2 ± 2.0***	40.9 ± 2.1
RU197	<i>ten-1(tm651) phy-1(ok162)</i>	20	264 ± 12.7	17.2 ± 0.8***	35.1 ± 1.5
RU179	<i>ten-1(ok641); phy-2(ok172)</i>	17	248 ± 12.1	6.1 ± 1.4	33.5 ± 1.2
RU168	<i>ten-1(ok641); phy-3(ok199)</i>	29	217 ± 8.9	4.8 ± 0.5	37.5 ± 1.0
RU177	<i>ten-1(ok641) phy-1(ok162); phy-3(ok199)</i>	6	224 ± 25.6	15.7 ± 2.2	41.7 ± 2.2
RU182	<i>ten-1(ok641); phy-2(ok172); phy-3(ok199)</i>	13	284 ± 11.6	2.5 ± 0.3	33.5 ± 1.5
RU181	<i>phy-2(ok172); phy-3(ok199)</i>	6	304 ± 21.5	0.1 ± 0.1	0.4 ± 0.2
RU191	kdEx131(<i>myo-3p::phy-1::gfp</i>)	5	234 ± 12.7	0.2 ± 0.2	0
RU195	<i>ten-1(ok641) phy-1(ok162); kdEx131</i>	13	163 ± 7.7	5.4 ± 0.7	34.3 ± 2.9
RU194	kdEx132(<i>phy-1p::phy-1; unc-122::gfp</i>)	7	260 ± 20.2	1.3 ± 0.6	1.5 ± 0.3
RU196	<i>ten-1(ok641) phy-1(ok166); kdEx132</i>	21	168 ± 8.6	4.5 ± 0.5	25.7 ± 2.2

Percentage of wild type, mutant worms and rescue lines of *ten-1(ok641) phy-1(ok162)* double mutant analysed for embryonic lethality and larval arrest. n, number of animals that have been tested for brood size.

** ($p < 0.003$) in comparison to embryonic lethality of N2

*** ($p < 10^{-7}$) in comparison to embryonic lethality of RU90 or RU98 respectively

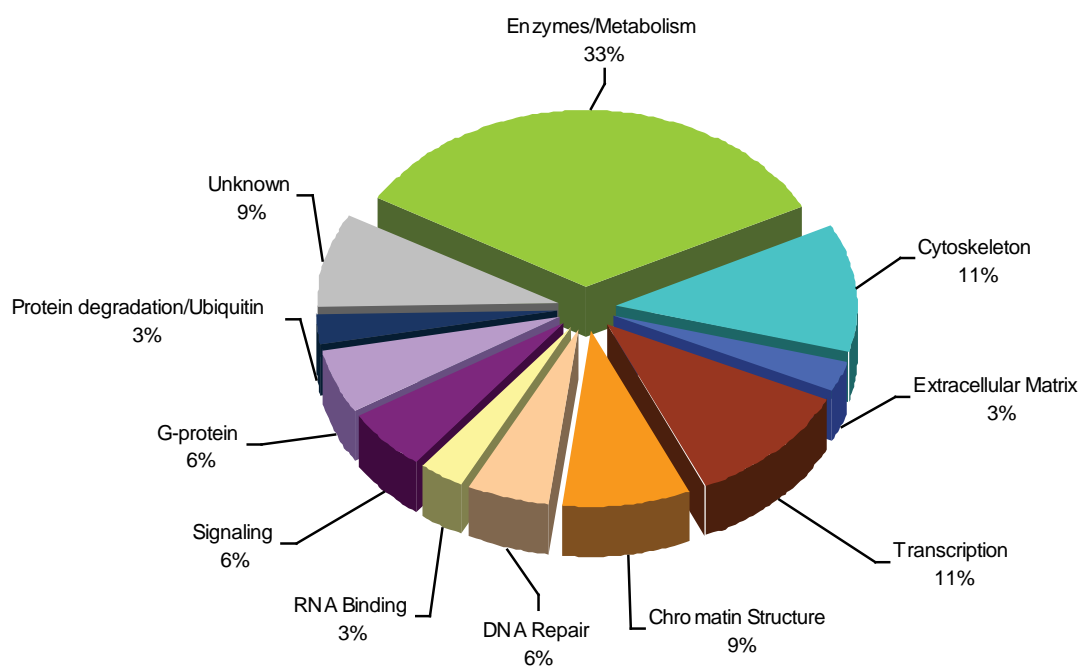


Figure 1. *ten-1* putative genetic interaction partners. The identified interaction partners are arranged in functional groups according to their relative abundance. *ten-1* interacts predominantly with genes involved in metabolism, cytoskeleton and transcription. The entire list of candidates is presented in Table S1.

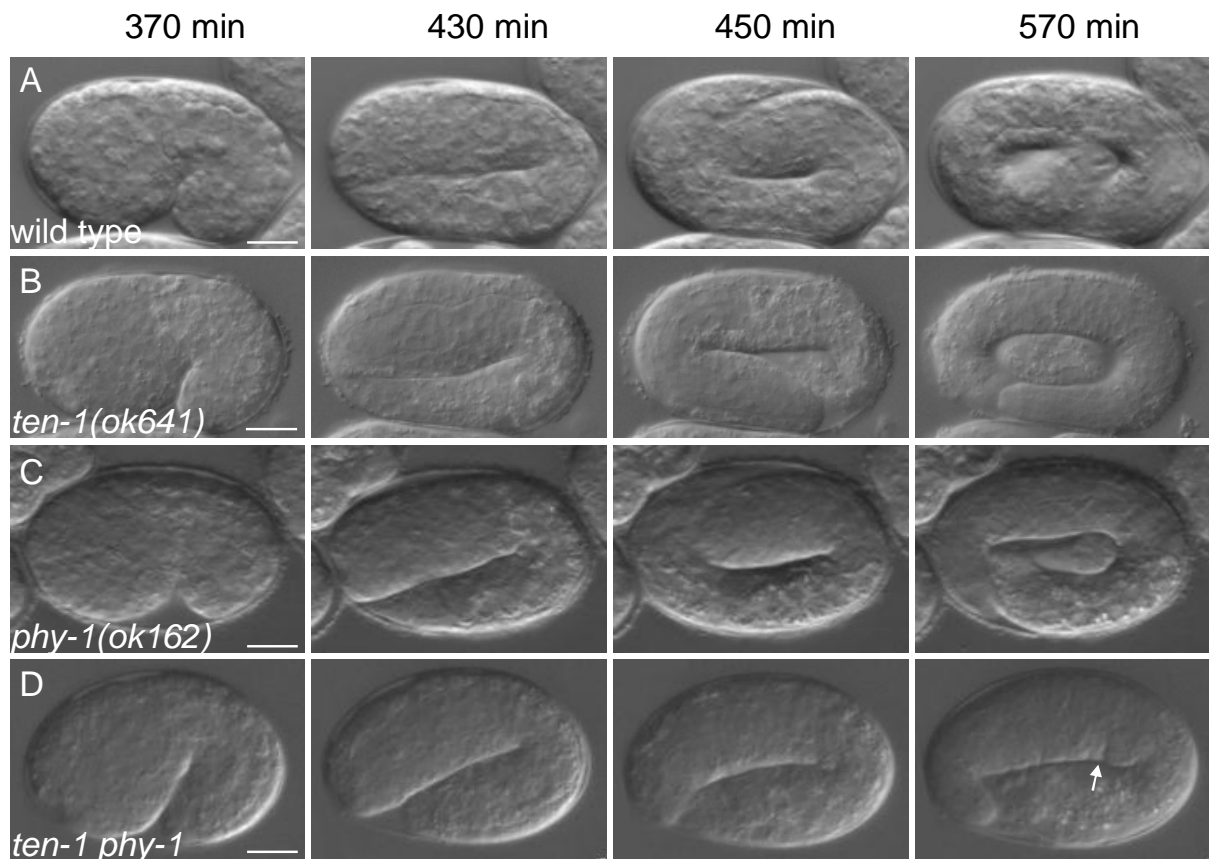


Figure 2. *ten-1 phy-1* double mutant embryos arrest late in elongation. Nomarski images of representative embryos undergoing elongation of (A) wild type, (B) *ten-1(ok641)*, (C) *phy-1(ok162)* and (D) *ten-1 phy-1* double mutant are shown at indicated time points. Elongation and morphology of both single mutants are comparable to the wild-type embryo. Double mutant stops elongation at 2-fold or 2.5-fold stage. Embryo looks swollen and develops constrictions in the epidermis (arrow). Scale bar 10 μ m.

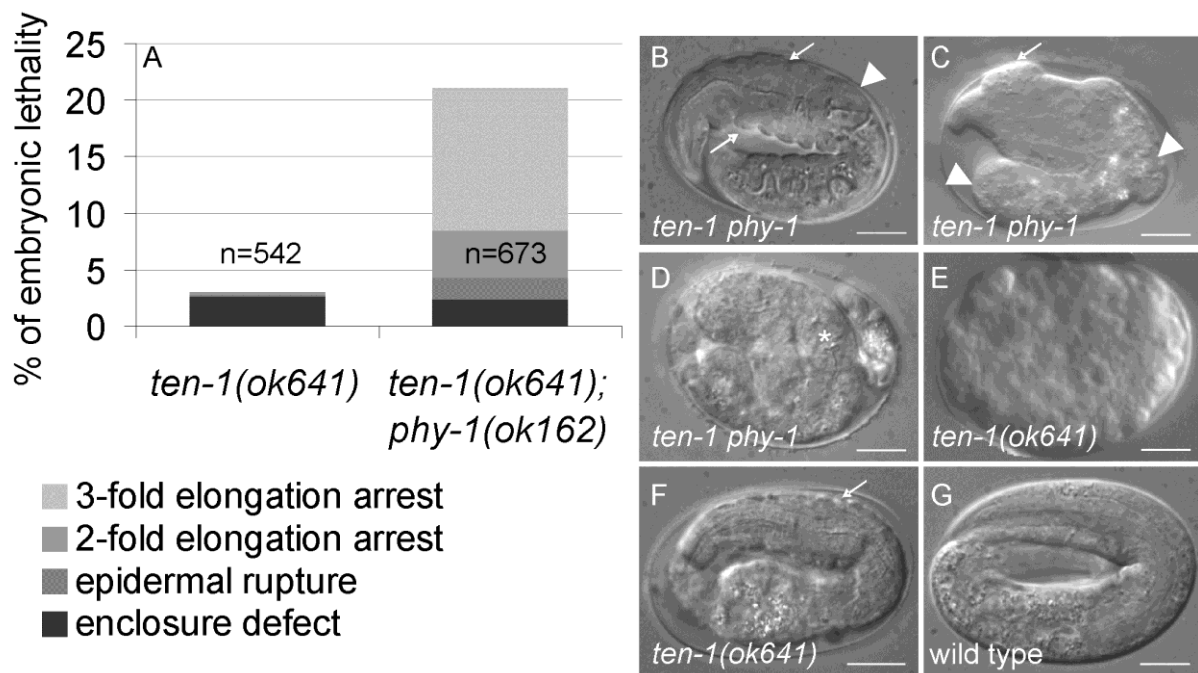


Figure 3. Loss of *phy-1* function in *ten-1* mutant background enhances embryonic lethality and morphological defects of late embryos. (A) Distribution of embryonic lethal phenotypes of *ten-1(ok641)* and *ten-1(ok641) phy-1(ok162)*. The graph represents a summary of three independent experiments of each strain. N is the number of all embryos analyzed. (B-F) Representative images of arrested embryos with most common morphological defects. (B) Approximately 13 % of the double mutant embryos arrest at a 3-fold stage showing constrictions in the epidermis (arrows) and misplacement of the pharynx from its central position (arrowhead). (C) Approximately 6 % of the double mutant embryos arrest before the 3-fold stage. These embryos develop anterior blisters (arrow) and strong deformation of the posterior part (arrowhead). (D) Some embryos rupture during elongation (the asterisk marks the developed pharynx). (E) *ten-1(ok641)* single mutant arrest mainly during embryonic enclosure. Equivalent arrested embryos can be found in the double mutant (data not shown). (F) Occasionally, *ten-1* single mutants arrest during embryonic elongation showing constrictions (arrow) and deformation of the epidermis. (G) A 3-fold wild-type embryo does not show any of the described phenotypes. Scale bar 10 μ m.

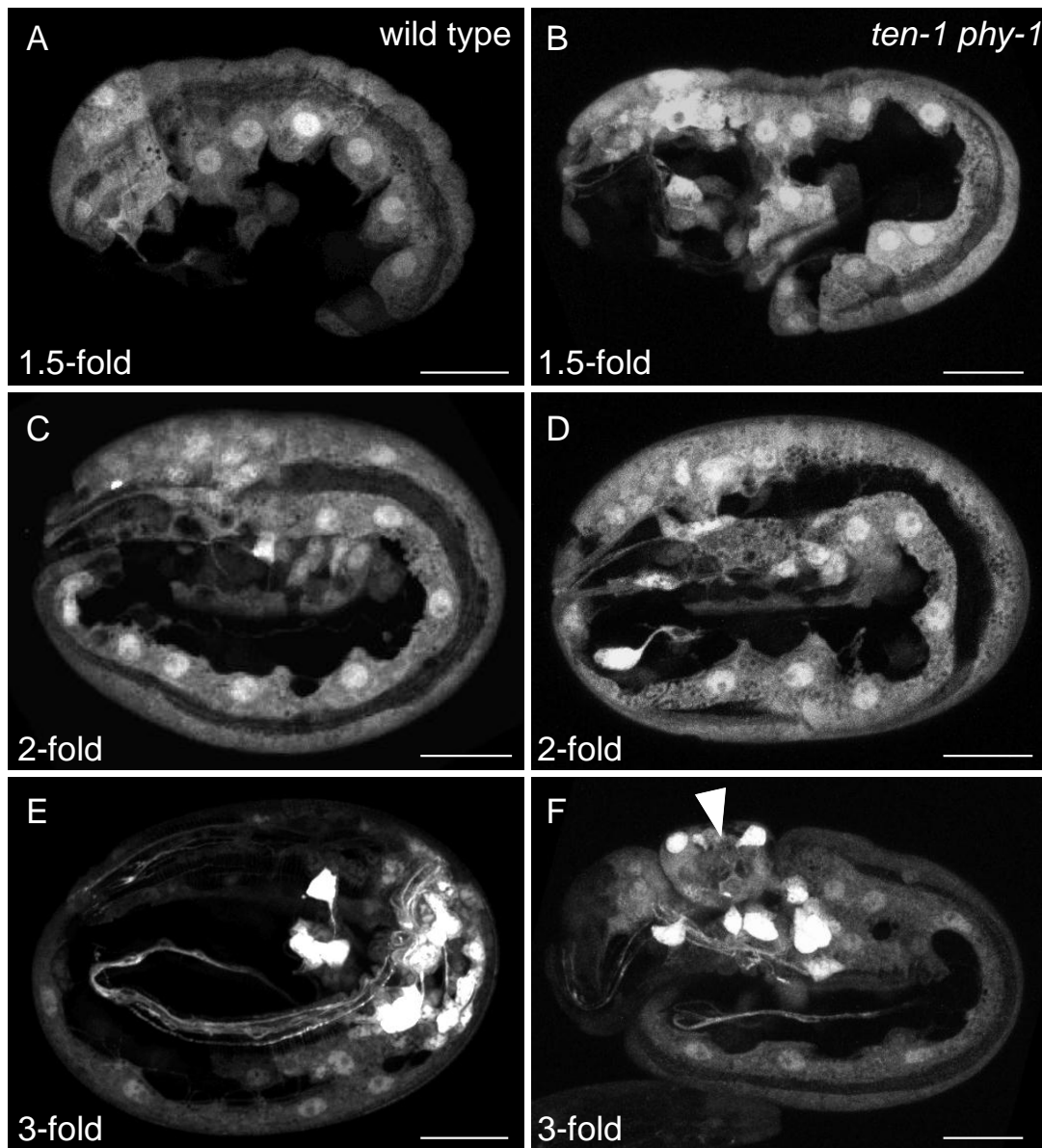


Figure 4. *ten-1 phy-1* embryos display defects during epidermal development. Expression of *gfp* under the *ten-1b* promoter in the epidermis and neurons in wild type (A, C, E) and *ten-1 phy-1* double mutant embryos (B, D, F) at indicated stages of embryonic elongation. Confocal images of the lateral view of the embryos are shown. (B) Hypodermal cells are misshaped and delayed in migration in 1.5-fold double mutant embryos. (D) Embryos in 2-fold stage show misplacement of epidermal cells. Cells are not correctly or incompletely fused. (F) 3-fold embryo with bulge in the anterior part containing epidermal cells and neurons (arrowhead). Corresponding images of 3-fold embryos of *ten-1(ok641)* and *phy-1(ok162)* single mutants were indistinguishable from wild type and are presented in Figure S2. Scale bar represents 10 μm .

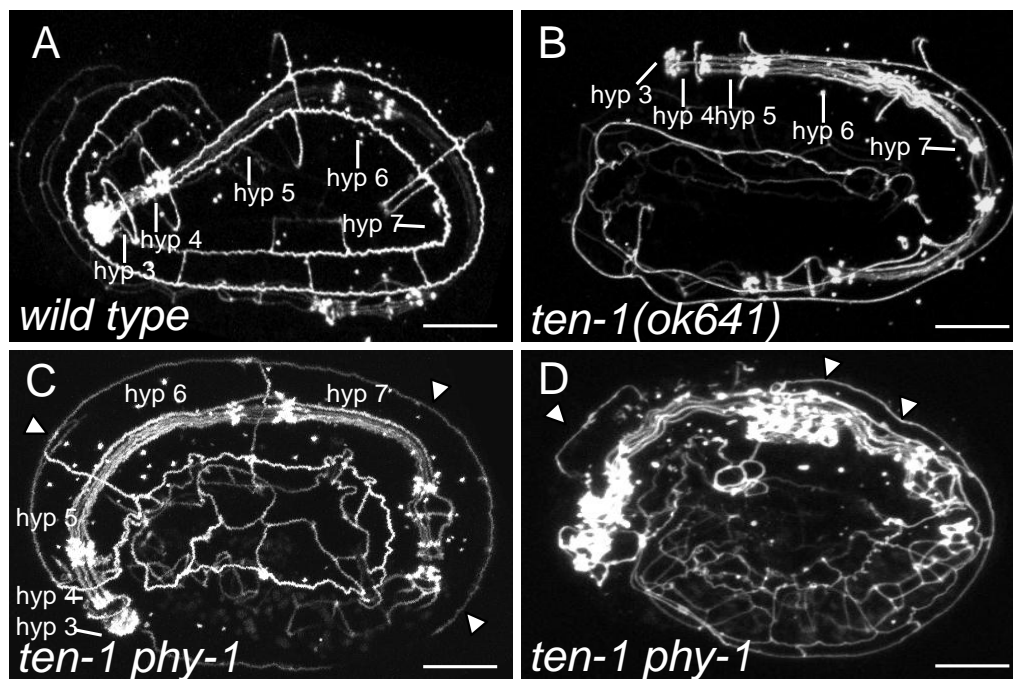


Figure 5. *ten-1 phy-1* embryos show mislocalization of epidermal junction marker AJM-1. Confocal images of embryos expressing apical epidermal junction marker AJM-1 fused to GFP. (A) 3-fold wild type embryo showing syncytia of fused hypodermal cells as indicated. (B) 3-fold embryo of *ten-1(ok641)* single mutant. Hypodermal cells are fused comparable to wild type. Note the minor disorganization of the lateral epidermal cells. (C, D) Arrested *ten-1 phy-1* embryos showing major disorganization of epidermal cell junctions. Mislocalization of AJM-1 on the apical side of dorsal epidermal cells is indicated by arrowheads. (D) Note the defects of the pharyngeal cells. Corresponding image of a 3-fold embryo of *phy-1(ok162)* single mutant is undistinguishable from wild type and is presented in Figure S2. Scale bar 10 μ m.

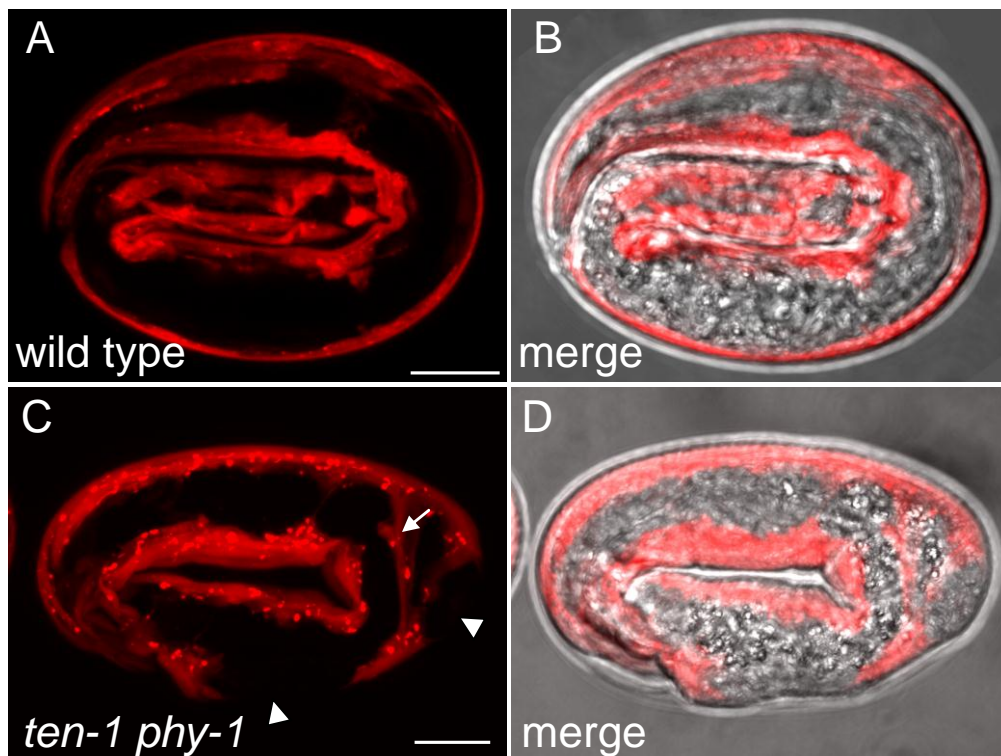


Figure 6. Arrested *ten-1 phy-1* embryos show severe defects in body wall muscles. (A, C) Confocal images of embryos expressing mCherry under the muscle specific *myo-3* promoter and (C, D) the corresponding DIC image. (A, B) Wild type embryos at 3-fold stage show continuous strands of body wall muscles from the head to the tail. (C, D) Double mutant embryo arrested at the 2.5-fold stage. Muscle strands are broken (arrowhead) and detached from the epidermal cells (arrow). Scale bar 10 μm .

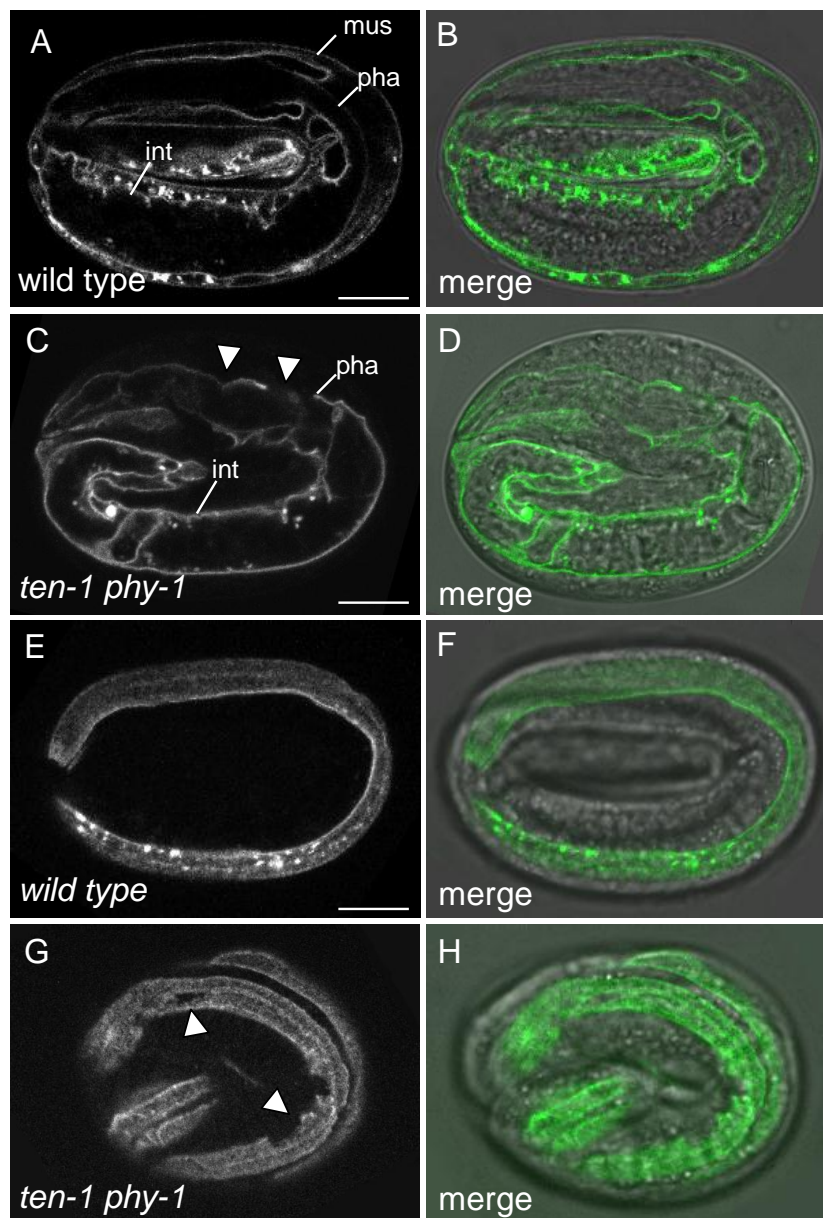


Figure 7. Basement membrane integrity is affected in arrested *ten-1 phy-1* mutant embryos. Localization of LAM-1 fused to GFP in a single focal plane (left panel), and merged with corresponding DIC image (right panel). (A,B) Laminin is localized to BM of the pharynx (pha), intestine (int) and developing gonad (not in focus) of 3-fold wild-type embryo. (C,D) Disruption and disorganization of pharyngeal BM in arrested *ten-1 phy-1* embryo. Laminin is generally correctly localized. (E,F) Localization of laminin to BM between the hypodermis and body wall muscles in a 3-fold wild type embryo. One muscle strand is in focus. (G,H) BM between body wall muscles and hypodermis shows breaks in double mutant embryos (arrowheads). Corresponding images of 3-fold embryos of *ten-1(ok641)* and *phy-1(ok162)* single mutants are presented in Figure S3. Scale bar 10 μ m.

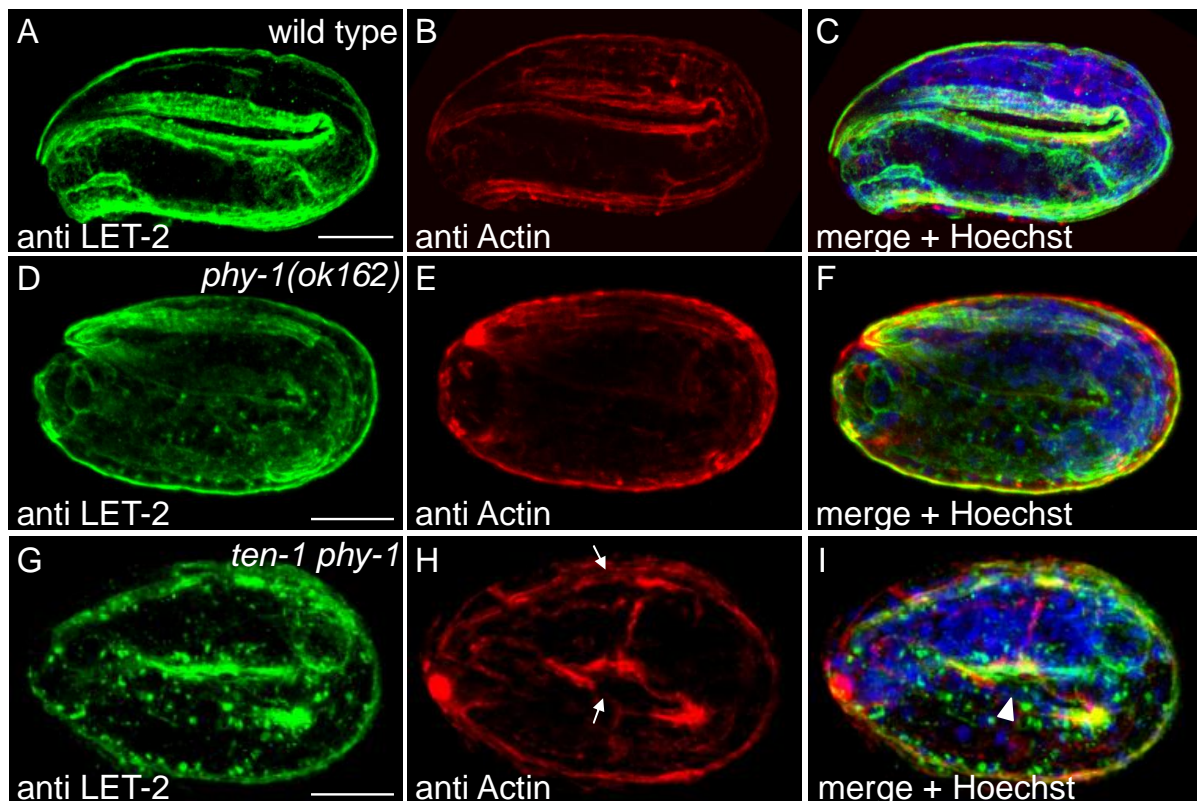


Figure 8. Loss of *phy-1* function causes aggregation of collagen IV in body wall muscles. Immunostaining with antibodies against LET-2 (green) and actin (red). DNA is stained with Hoechst dye (blue). (B, E, H) Longitudinal actin bundles correspond to position of body wall muscles. (A, C) LET-2 is nearly completely secreted into basement membranes in wild type embryo at the 3-fold stage. Focus is on BM separating muscles from epidermal cells. Aggregations of LET-2 in muscles cannot be detected. (D, F) *phy-1(ok162)* single mutant at 3-fold stage show frequently intracellular aggregations of LET-2. Spots are close to muscle nuclei. (G, I) In arrested *ten-1;phy-1* double mutant embryos, cluster formation of LET-2 protein is enhanced. (H) Actin bundles appear disorganized and rupture at some places (arrow). Similar results were obtained with anti EMB-9 and are represented in Fig S4. Scale bar 10 μ m.

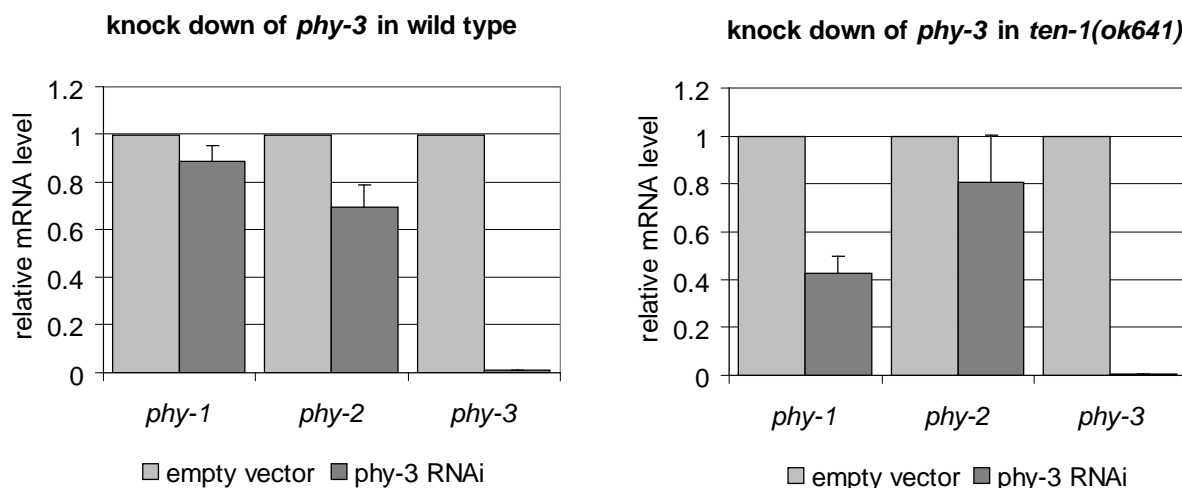


Figure S1. *phy-3* RNA interference reduces mRNA levels of *phy-1* and *phy-2*.

Results are the summary of 3 independent biological replicates. Eggs of gravid hermaphrodites of wild type and RU90 [*ten-1(ok641)*] strain were released by NaOCL treatment. Eggs were allowed to hatch on RNA interference plates seeded with *phy-3* RNAi bacteria. Worms were grown until young adulthood and collected in distilled water. Total RNA was isolated using Trizol (Invitrogen). cDNA was synthesized using ThermoScript™ RT-PCR system with random hexamer primers (Invitrogen), according to the manufacture's protocol. A concentration of 10ng of cDNA was used for each sample for quantitative real time PCR using Platinum® SYBR® Green reaction (Invitrogen). Analysis was done using $\Delta\Delta\text{ct}$ method. Results were normalized to *ama-1* mRNA levels.

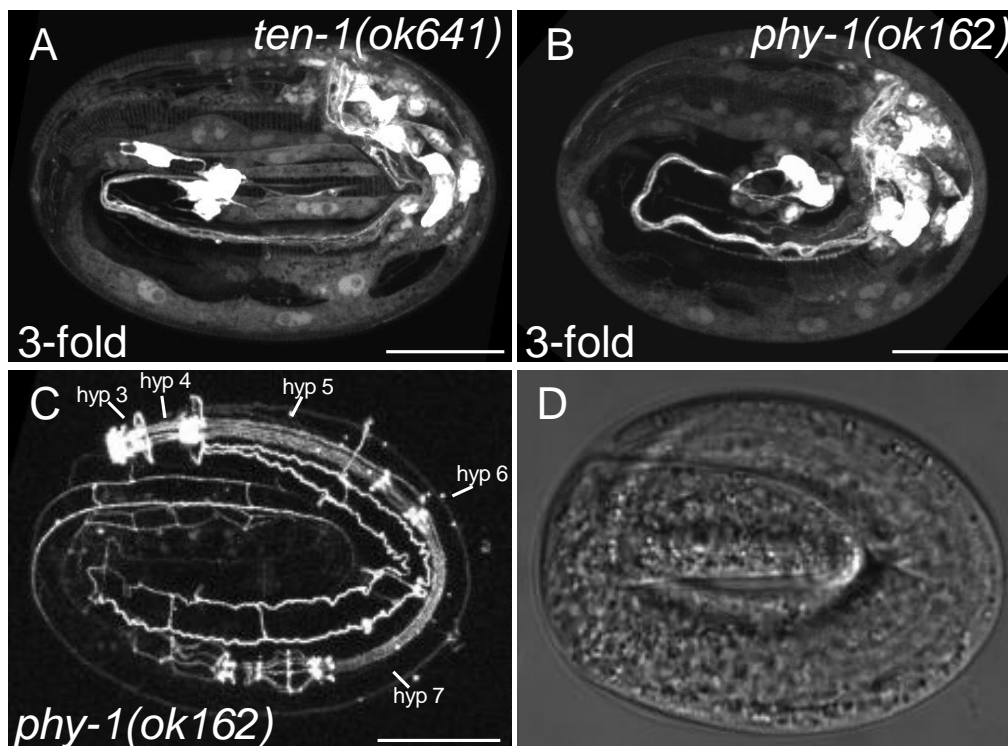


Figure S2. Analysis of epidermal development in *ten-1(ok641)* and *phy-1(ok162)* single mutants. (A, B) Confocal images of 3-fold embryos expressing *Pten-1b::gfp* fusion in *ten-1(ok641)* and *phy-1(ok162)*. Both single mutants did not show defects in the migration, fusion and positioning of epidermal cells by this stage of elongation. (C, D) Expression of *ajm-1::gfp* marker in 3-fold *phy-1(ok162)* single mutant and the corresponding DIC image. AJM-1 is correctly localized at epidermal cell junctions. Scale bar 10 μm .

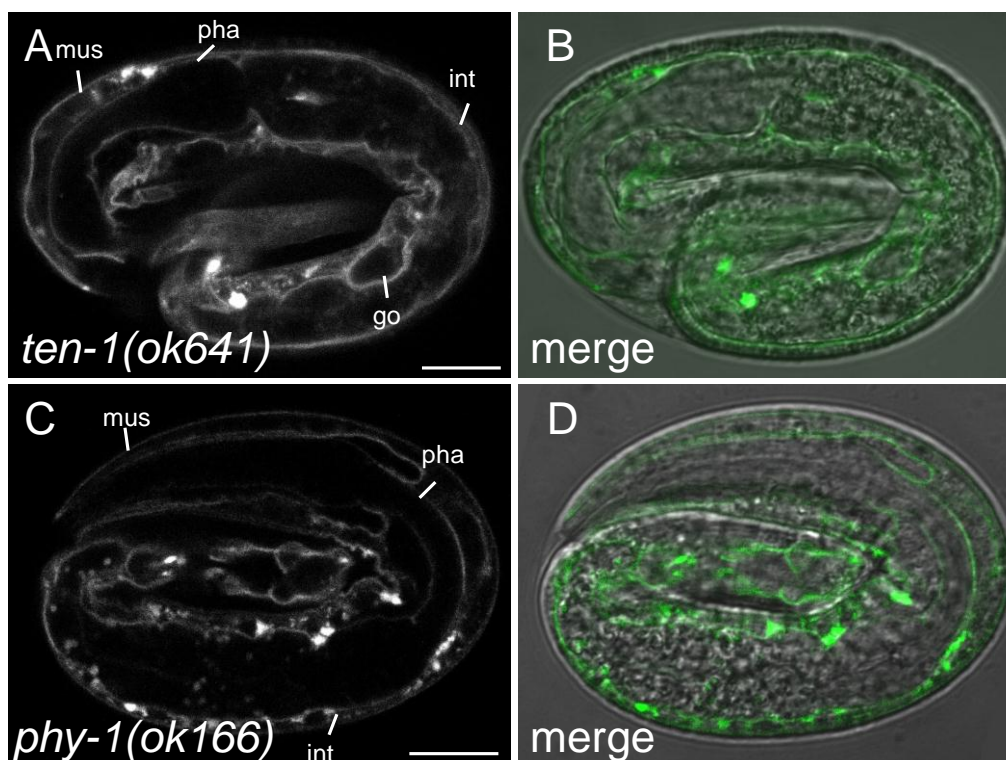


Figure S3. Analysis of basement membrane integrity in *ten-1(ok641)* and *phy-1(ok166)* single mutants. (A, C) Confocal images of single focal plane of *lam-1::gfp* marker in 3-fold stage worms and (B, D) merged with DIC images. Both single mutant did not show defects in BM surrounding the pharynx (pha), intestine (int), gonad (go) and BM underlying the epidermis (mus). Scale bar 10 μ m.

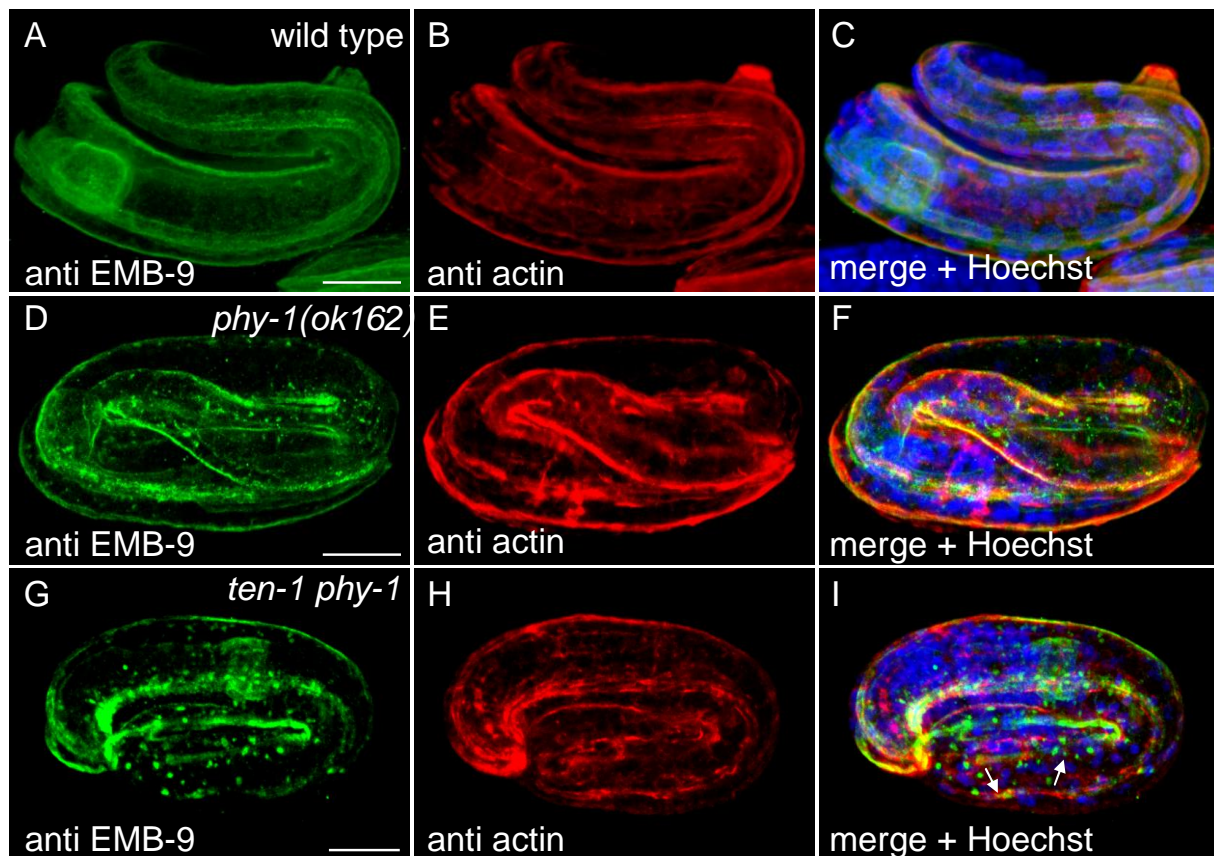


Figure S4. Immunostaining with EMB-9 antibody of wild type, *phy-1(ok162)* and *ten-1 phy-1* double mutant. Immunostaining with antibodies against EMB-2 (green) and actin (red). DNA is stained with Hoechst dye (blue). (B, E, H) Longitudinal actin bundles correspond to position of body wall muscles. (A, C) EMB-9 was localized to basement membranes in 3-fold stage wild-type embryo. (D, F) In *phy-1(ok162)* single mutant at a comparable developmental stage, a cluster of EMB-9 protein was visible close to the muscle nuclei. (G, I) Aggregation of EMB-9 was observed in 2.5-fold arrested embryo of *ten-1 phy-1* double mutant. In the posterior part of the embryo, clusters of protein appear bright, whereas the secreted protein between the muscle and epidermis seem to vanish (arrow). Scale bar 10 μ m.

Table S1. Putative interaction partners of *ten-1*

Enhancers (part I)								
Swiss-Prot Accession No.	cosmid	Gene	protein	Molecular function	biological process	expression	cellular component	Human Ortholog
P52275	C36E8.5	<i>tbb-2</i>	Beta-2-tubulin	Cytoskeleton	microtubule-based movement, spindle organization	gonad	cytoskeleton	tubulin beta
Q18503	C36H8.1		Major sperm protein	Cytoskeleton	sperm motility	spermatheca		
Q9XWV3	Y37D8A.1	<i>arx-5</i>	actin-related protein	Cytoskeleton	Arp2/3 complex subunit		cytoskeleton	actin related protein 2/3 complex, subunit 3
Q19325	F10G7.4	<i>scc-1</i>	Yeast scc (Mitotic condensin subunit) homolog protein	DNA Repair	cohesion protein	germline	nucleus	RAD21 homolog
Q21554	M18.5	<i>ddb-1</i>	DNA damage-binding protein	DNA Repair	component of an E3 ubiquitin-protein ligase which promotes histone ubiquitination in response to UV irradiation	hypodermis, spermatheca	cytoplasm, nucleus	damage-specific DNA binding protein 1
Q20223	F40F4.3	<i>lbp-1</i>	Fatty acid-binding protein homolog 1	Enzymes/Metabolism	lipid binding	intestine, epidermis, neurons, reproductive system	extracellular	fatty acid binding protein 4
A4F310	F38A1.4	<i>clec-167</i>	C-type lectin	Enzymes/Metabolism	sugar binding			Gamma-glutamyltranspeptidase 1
O18256	Y7A9A.1		Gamma-glutamyltransferase	Enzymes/Metabolism				
Q10576	Y47D3B.10	<i>phy-1</i>	Prolyl 4-hydroxylase subunit alpha-1	Enzymes/Metabolism	procollagen modification	hypodermis, neurons, vulva	endoplasmatic reticulum	prolyl 4-hydroxylase, alpha polypeptide I
O44452	C04C3.2	<i>lgc-9</i>	Ligand-Gated ion Channel	Enzymes/Metabolism	ion transport		integral to membrane	Neuronal acetylcholine receptor subunit alpha-3

Table S1. Putative interaction partners of *ten-1*

Enhancers (part II)								
Swiss-Prot Accession No.	cosmid	gene	Protein	Molecular function	biological process	expression	cellular component	Human Ortholog
Q18434	C34D1.3	<i>odr-3</i>	Odorant response abnormal protein 3	G-protein	sensory transduction	neurons	cilium	GNAT3
Q9N2Z7	Y65B4BR.4	<i>wwp-1</i>	Ww domain protein	Protein degradation/ Ubiquitin	E3 ubiquitin ligase	intestine, pharynx, neurons, muscles	intracellular	ubiquitin-protein ligase WWP1
P13508	F02A9.6	<i>glp-1</i>	Notch receptor	Signaling		germline	integral to membrane	NOTCH
Q03600	F54G8.3	<i>ina-1</i>	integrin alpha	Signaling	laminin binding	ubiquitous	integral to membrane	Integrin alpha
O62208	F32H2.1	<i>gei-11</i>	GEX interacting protein	Transcription	Myb DNA-binding		nucleus	SNAPC4
Q22355	T08H4.3	<i>ast-1</i>	ETS-box transcription factor	Transcription		neurons	nucleus	Friend leukemia integration 1 transcription factor
Q22024	R53.3	<i>egl-43</i>	zinc finger protein	Transcription		gonad, neuron	nucleus	PRDM16
Q21755	R05G6.4		Nitric oxide synthase-interacting protein	Unknown	inducing nitric oxide synthase translocation to actin cytoskeleton and inhibiting its enzymatic activity	unknown	cytoplasm, nucleus	nitric oxide synthase interacting protein

Suppressors								
Swiss-Prot Accession No.	cosmid	gene	Protein	Molecular function	biological process	expression	cellular component	Human Ortholog
O61750	F37F2.3	<i>gst-25</i>	Glutathione s-transferase	Enzymes/Metabolism	amino acid metabolism			Glutathione S-transferase
P91248	F11G11.10	<i>col-17</i>	Collagen	Extracellular Matrix	cuticle synthesis	hypodermis	extracellular	
Q9TZQ3	ZK381.4	<i>pgl-1</i>	P granule protein	RNA Binding		germline	cytoplasm	
Q93345	C36B1.11		Unknown	Unknown				

Table S1. Putative interaction partners of *ten-1*

Suppressed by <i>ten-1</i>								
Swiss-Prot Accession No.	cosmid	gene	Protein	Molecular function	biological process	expression	cellular component	Human Ortholog
Q95XW8	Y55B1BR.3		CHROMO domain protein	Chromatin Structure	chromatin assembly or disassembly		nucleus	
Q9U3W	C01B10.5	<i>hil-7</i>	Histone	Chromatin Structure		germline	nucleus	Histon H1.5
Q23472	ZK381.1	<i>him-3</i>	Meiotic chromosome core protein	Chromatin Structure	formation of the synaptonemal complex during meiosis	germline	nucleus	HORMA domain-containing protein 1
Q09476	C28H8.6	<i>pxl-1</i>	Paxillin	Cytoskeleton	adapter protein			paxillin
A5JYX5	T02E1.5	<i>dhs-3</i>	dehydrogenases	Enzymes/Metabolism		mitochondrial	integral to membrane	Epidermal retinol dehydrogenase 2
Q8IAA9	Y39A3CL.5	<i>clp-4</i>	Calpain family protein	Enzymes/Metabolism	proteolysis		intracellular	Calpain-3
Q09527	E02H1.6		adenylate kinase	Enzymes/Metabolism	ATP binding	ubiquitous	nucleus	TAF9
Q95Q62	C46H11.4	<i>lfe-2</i>	inositol trisphosphate 3-kinase	Enzymes/Metabolism		intestine, pharynx, spermatheca		Inositol-trisphosphate 3-kinase A
Q9Y0I6	T21C12.1	<i>unc-49</i>	GABA receptor	Enzymes/Metabolism	ion transport	muscles	integral to membrane	Glycine receptor subunit alpha-3
Q27473	C28A5.3	<i>nex-3</i>	Annexin	Enzymes/Metabolism	phospholipid binding		intracellular	Annexin 5
P34443	F54C8.5	<i>rheb-1</i>	GTPase	G-protein			intracellular	RHEB
P46500	F23F12.4	<i>sdz-15</i>	F-box protein	Signaling				
Q19826	F26F4.11	<i>rpb-8</i>	RNA polymerase II	Transcription		ubiquitous	nucleus	polymerase (RNA) II
Q17751	C06G3.3		unknown	Unknown				

Table S2. Primers used for genotyping and quantitative RT-PCR

gene	sequence 5' → 3'
<i>phy-1(ok162)_for</i>	GAAGAAGCTGTCGGAGGAGTA
<i>phy-1(ok162)_rev</i>	ACGGCTAGTGGGTTGAATCTC
<i>phy-1(ok162)_wt_for</i>	CGAATACCTGGCGTTTGCACTG
<i>phy-2(ok177)_for</i>	GATCTATCGTACCTTAAGCTGG
<i>phy-2(ok177)_rev</i>	ATAGTGCGCATTTCGGTTTCA
<i>phy-2(ok177)_wt_for</i>	GAACATGCCACGTACCGTATCTC
<i>phy-3(ok199)_for</i>	CCACCACAACAACACTGACGTAGTG
<i>phy-3(ok199)_rev</i>	CGATGTCCC GAAATCTGACG
<i>phy-3(ok199)_wt_rev</i>	CGTTGATTGTAGGCACGGATCC
<i>ten-1(ok641)_1</i>	TGACACTGACGGAAGATGCCG
<i>ten-1(ok641)_3</i>	CAAACAGTTCCGTCTCCAGCC
<i>ten-1(ok641)_wt</i>	TCAGTTGACCATGAGCTGAGC
<i>phy-1_5_qPCR</i>	GAGGCCAAGTCTACAATTCTG
<i>phy-1_3_qPCR</i>	CTTTCGTAGTCTGAGGATTC
<i>phy-2_5_qPCR</i>	CATCTTGGAAGTCTGTATTC
<i>phy-2_3_qPCR</i>	TTCTCCTGAACTTCCTCCTCC
<i>phy-3_5_qPCR</i>	CAAGTATTGGTTCCACAGTTC
<i>phy-3_3_qPCR</i>	GAATCTGTTTGAGAGACGG
<i>ama-1_5_qPCR</i>	CACAATGATCTACGATCTGTGC
<i>ama-1_3_qPCR</i>	CTTCCATTCTGCGTTGATGTCG

3.3. Unpublished Results

3.3.1. High throughput screen for genes genetically interacting with *ten-1*

To gain insight into the function of *ten-1*, I performed a genome wide RNAi screen comparing the effect of gene knock-down in wild type worms versus the *ten-1(ok641)* deletion mutant. I found genes enhancing and suppressing the *ten-1* phenotype but also genes with an RNAi phenotype which was suppressed by loss of *ten-1* function. A list of all candidates including their known function, expression and vertebrate homologs is presented in my submitted paper. In addition, my thesis contains the list of genes including the observed phenotypes in the appendix (Table 6). The genes obtained are potential interacting candidates that need to be further confirmed by double mutant analysis. I confirmed the genetic interaction of *ten-1* with *phy-1*, a gene coding for the catalytic subunit of the collagen modifying enzyme. Furthermore I analysed the mechanism underlying the genetic interaction. The results are presented in the submitted manuscript “*C. elegans* teneurin, *ten-1*, interacts genetically with the prolyl 4-hydroxylase, *phy-1*, and is important for basement membrane integrity during late elongation of the embryo”.

Furthermore, I was interested in the interaction between *ten-1* and *pxl-1*. *pxl-1* was recently found to be the true ortholog of the vertebrate paxillin (A. Warner and D. Moerman, personal communication). In the RNAi screen I found that the phenotype caused by *pxl-1* knock-down in wild type was suppressed by loss of *ten-1* function. The *ten-1* mutant phenotype itself seemed not to be altered in comparison to the empty vector control. The only known knock-out mutant, *pxl-1(ok1483)*, is 100% lethal in early larval development. Such a strong mutant allele is not suitable for double mutant analysis and all my attempts to create such a double mutant with *ten-1* were not successful. I repeated the knock-down experiment with *pxl-1* in a more quantitative way. To enhance the RNAi effect I performed the experiment in an RNAi sensitized background using the *rrf-3(pk1417)* mutant (Simmer et al., 2002). The brood size of worms in all conditions was comparable. I analysed the F1 progeny for embryonic and larval lethality. Embryonic lethality was not enhanced by knock-down of *pxl-1* over the control background. The larval lethality or arrest was about 25%, that is app. 20% enhanced compared to the control situation. The *ten-1(ok641)* mutant allele was crossed into the *rrf-3(pk1417)* mutant. There was a remarkable increase in the embryonic lethality comparable to the control. I do not have an

explanation for this effect but Drabikowski, et al. found that knock-down of *ten-1* by RNAi in the *rrf-3* mutant background results in high embryonic lethality, much higher than observed in the *ten-1* knock-out mutants. Whether there is a true effect on the *ten-1* mutant phenotype by loss of *rrf-3* need to be investigated. Nevertheless, the knock-down of *pxl-1* in the *rrf-3;ten-1* mutant did not increase the larval lethality comparable to the knock-down of *pxl-1* in the *rrf-3* mutant. Thus, the reduction of *pxl-1* does not further increase the *ten-1* mutant phenotype concerning larval lethality or arrest. I conclude, that therefore *ten-1* might act upstream of *pxl-1* (figure 9).

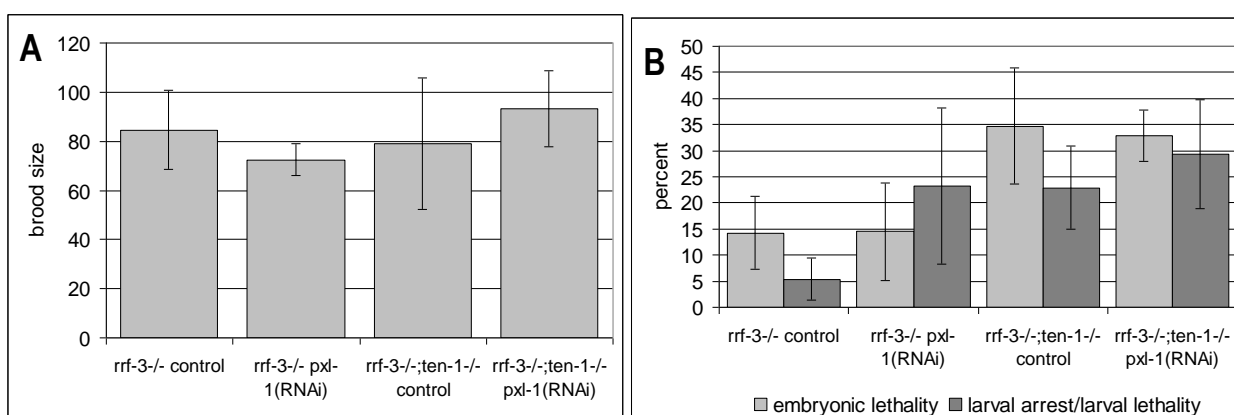


Figure 9. Knock-down of *pxl-1* in *ten-1* mutant background. (A) The brood size is comparable in all experimental conditions. (B) Analysis of embryonic lethality and larval lethality/arrest. Reduction of functional *pxl-1* does not increase the larval defects in *ten-1* mutant background. Knock-down of *pxl-1* has neither an effect on embryonic lethality in the *rrf-3*^{-/-} background or in combination with the *ten-1* mutant.

Another gene, I was interested in, was *wwp-1*. *wwp-1* codes for a E3 ubiquitin ligase and has orthologs in yeast, *Drosophila* and man. WWP-1 is responsible for the proteolysis of the intracellular domain of the Notch homolog LIN-12 and is necessary for protection of germ cells against ionizing radiation or camptothecin, as well as for normal acetylcholine neurotransmission. WWP-1 is widely expressed in the nervous system, in the pharynx, vulva muscles, body wall muscles, intestine, rectal gland cells and rectal epithelium. Figure 10 shows the result of the RNAi screen. Knock-down of *wwp-1* in wild type worms causes partial embryonic lethality. Knock-down of *wwp-1* in *ten-1* mutant background enhances the phenotype drastically. The brood

size is very low and all embryos were dead. A deletion mutant for *wwp-1* is available, *wwp-1(ok1102)*. My attempts to create a double mutant with *ten-1(ok641)* were not successful. I was not able to isolate a homozygote mutant for both mutations. I concluded that a double mutant is embryonic lethal.

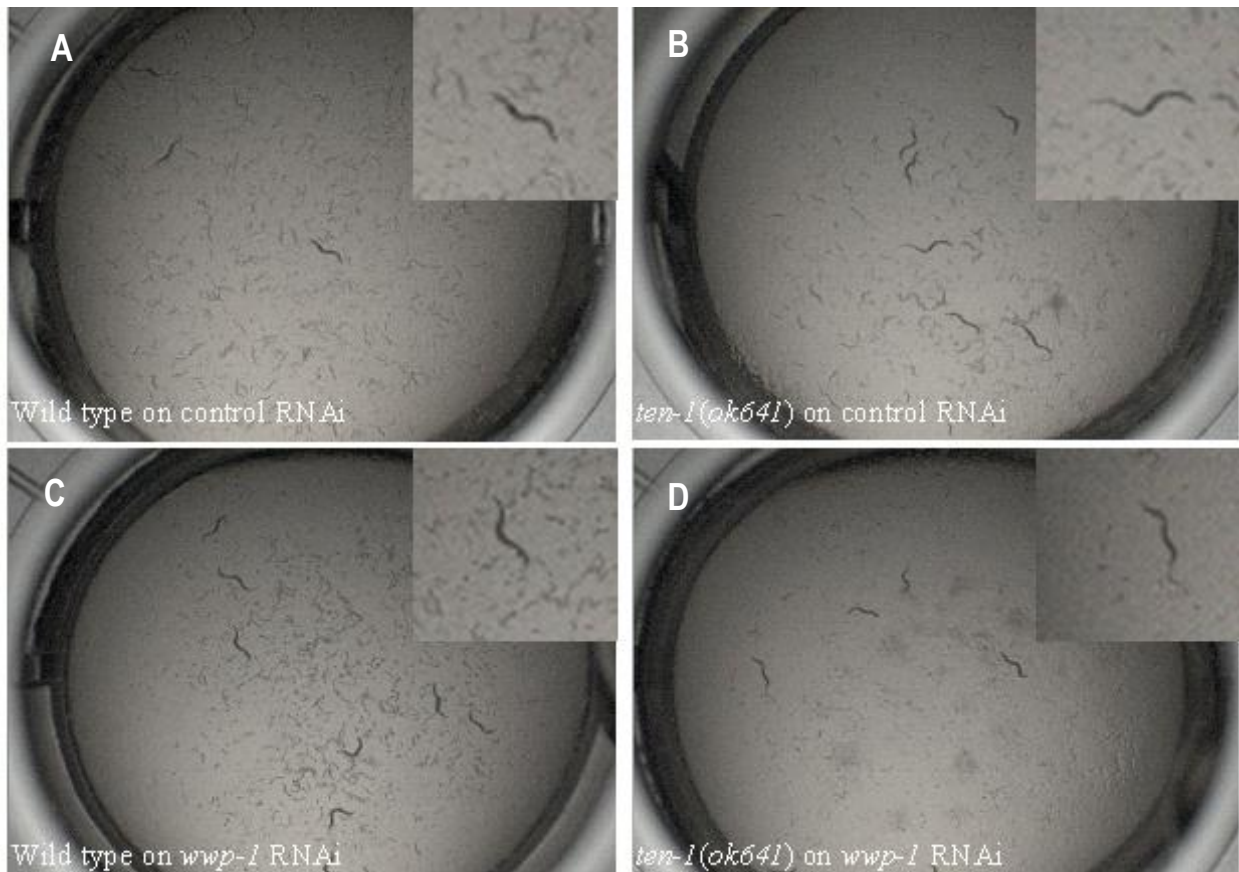


Figure 10. Knock-down of *wwp-1* in *ten-1* mutant enhances *ten-1* mutant phenotype. Worms were fed continuously for five days with RNAi bacteria. (A) Wild type worms and (B) *ten-1(ok641)* worms on control RNAi (empty vector). (C) Knock-down of *wwp-1* in wild type worms causes partial embryonic lethality. (D) Knock-down of *wwp-1* in *ten-1* mutant background causes severe reduction in brood size and complete embryonic lethality.

3.3.2. Knock-down of *phy-2* in *phy-1* loss of function mutant increases collagen IV aggregation in muscle cells

My experiments suggest that *phy-1*, as the catalytic subunit of the enzyme prolyl 4-hydroxylase, has a role in modification of basement membrane collagen IV (see submitted manuscript). Since the double mutant between *phy-1* and *phy-2* is embryonic lethal, I investigated whether the loss of *phy-2* increases the basement membrane defect in these dead embryos. I used RNA interference to knock-down *phy-2* in *phy-1(ok162)* null mutant background. *Phy-1(ok162)* mutant animals at the L4 stage were fed with *phy-2* RNAi bacteria or control RNAi bacteria containing an empty vector for three days. The entire population containing adult worms, larvae and embryos was harvested and prepared for staining as described in “Materials and Methods”. The efficiency of the knock-down was verified by quantitative PCR (qPCR). Total RNA was isolated from the entire sample harvested after RNAi treatment and prepared for analysis as described in “Materials and Methods”. The qPCR result reflects an average of *phy-2* knock-down and is probably more pronounced in the dead embryos and dead larvae (Figure 11). *phy-1(ok162)* embryos fed with control bacteria display the phenotype described in the submitted publication. Three-fold embryos show spots of protein aggregates around the muscle nuclei but most of the collagen IV is secreted to the basement membrane (Figure 12 A, G). In contrast, *phy-1(ok162)* worms treated with *phy-2* RNAi show more frequent protein aggregations. In some embryos no secretion of collagen IV into the basement membrane was visible when stained with anti EMB-9, collagen IV alpha chain (Figure 12 D, F).

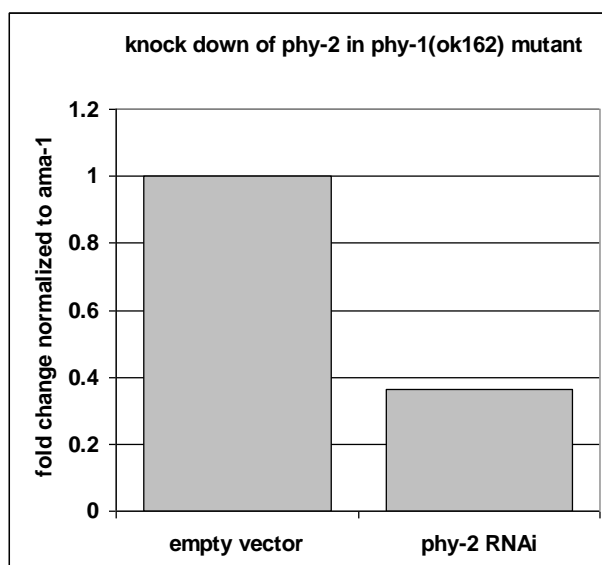


Figure 11. Fold change reflecting the knock-down of *phy-2* in *phy-1(ok162)* null mutants versus treatment with a control RNAi.

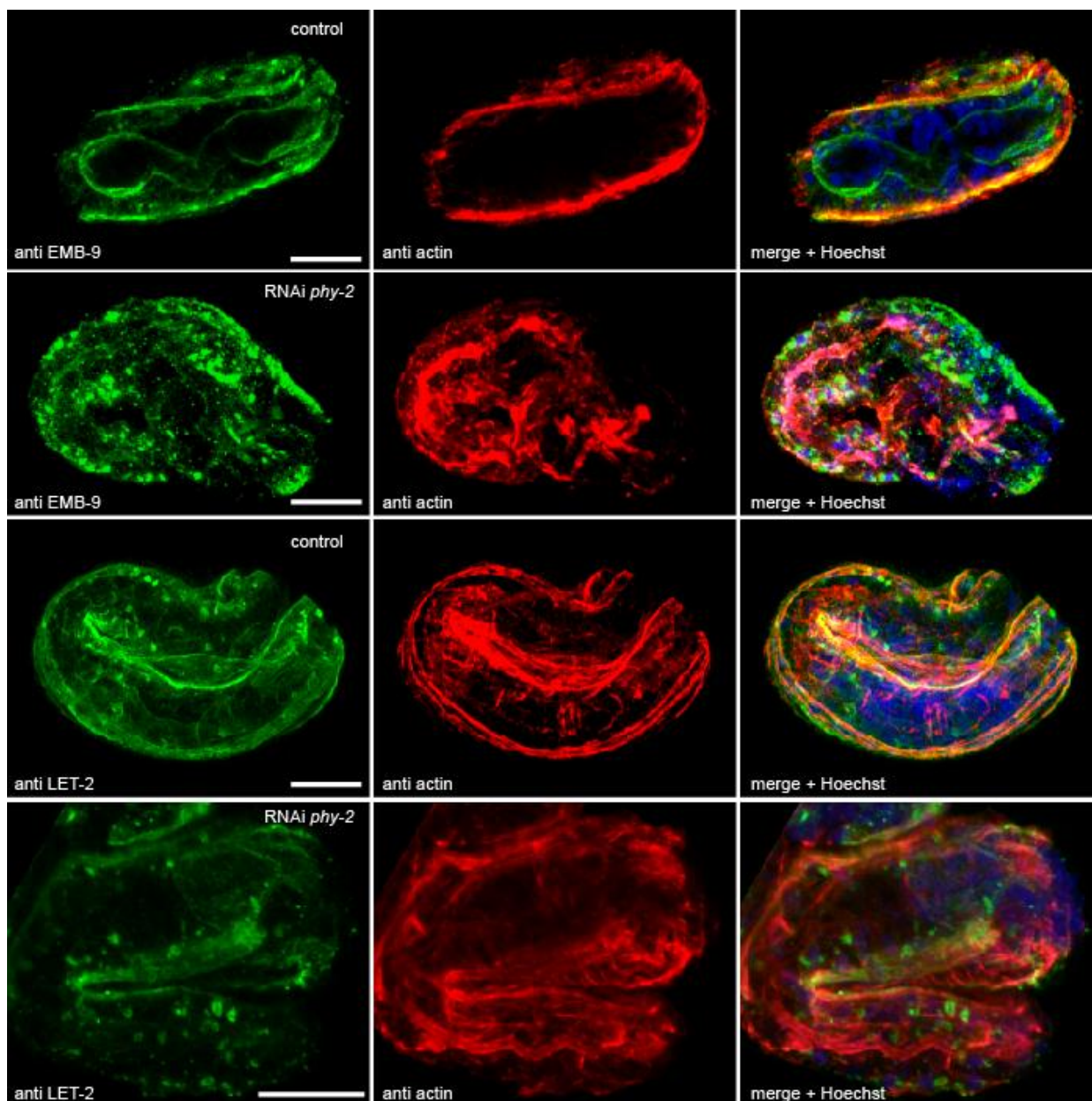


Figure 12. Knock-down of *phy-2* increases protein aggregation of collagen IV in *phy-1(ok162)* mutant embryos. Embryos were stained with anti EMB-9 or anti LET-2 (green), anti actin (red) and DNA was labelled with Hoechst dye (blue). All embryos shown are at a three-fold stage. Actin staining reflects the position of the body wall muscles and massive disorganization of double mutant embryos. Scale bar, 10 μ m.

3.3.3. Micro array analyses of *ten-1* mutants versus wild type

To gain insight into how the *ten-1* mutants differ from wild type worms I did genome profiling. I choose to compare synchronized worms from the first larval stage. Later stages would be less homogeneous in comparison to wild type worms since *ten-1* mutant animals show slower growth and arrested L1 worms. Interestingly, I found that the *ten-1(ok641)* mutant is very similar to wild type worms at this stage. In contrast, the *ten-1(tm651)* mutant is very different from wild type worms and the *ten-1(ok641)* mutant on the gene level. For the analysis a cut-off for genes that changed ≥ 1.5 fold and with a p-value of ≤ 0.05 in comparison with wild type was applied. Figure 13 gives a summary of the number of genes that were increased or decreased in comparison to wild type and which genes the *ten-1* mutants had in common in both gene lists. In general 780 genes were changed in the *ten-1(tm651)* in comparison to wild type whereas only 54 genes were changed in the *ten-1(ok641)*.

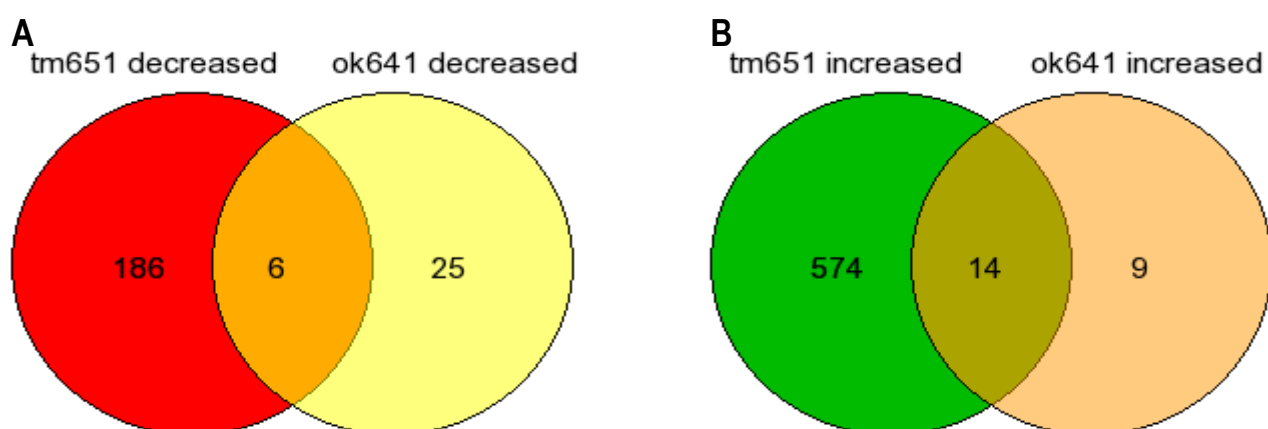


Figure 13. Venn diagram of genes being decreased or increased in the *ten-1* deletion mutants in comparison to wild type regulated genes. The number in the overlapping part indicates the genes commonly regulated in both mutants (A) Genes that are decreased. (B) Genes that are increased. Diagrams were generated using following tool: <http://www.bioinformatics.org/gvenn/>

Table 1 shows a list of the genes that are commonly expressed in both *ten-1* mutants. Most of the genes appear to be uncharacterized in *C. elegans*. Among the genes being increased in both *ten-1* mutants are a cluster of nuclear hormone receptors which also have a homolog in vertebrates. An interesting gene is *zwl-1*, which codes for a subunit of the Rod/Zwilch/Zw10 (RZZ) complex. The RZZ complex is important during chromosome segregation. Loss of function of *zwl-1* is embryonic

lethal. However, the fold change was for *ten-1(tm651)* 2.2 and for *ten-1(ok641)* 1.7. The fold changes need validation by quantitative PCR. Another gene C18H7.1, is poorly characterized in *C. elegans*. Although, its human homolog collagen VI $\alpha 3$ is described to be ubiquitously expressed and localizes to basement membranes surrounding muscle cells. Mutations in the gene cause a variety of muscular dystrophies. The gene is slightly up-regulated in *ten-1* mutants [*ten-1(tm651)* 1.7 fold; *ten-1(ok641)* 1.6 fold].

gln-6 was one of the genes with the most decreased expression value. [*ten-1(tm651)* 7.2; *ten-1(ok641)* 6.7]. The gene is not well characterized in *C. elegans*. It is expressed in the mid germline and its loss of function results in embryonic lethality. *Tiar-2* codes for an RNA-binding protein and is a component of stress granules. Stress granules store untranslated RNA. For the human homolog *tiar* together with *tia-1* was shown to link stress induced phosphorylation of eIF-2 α to the assembly of mammalian stress granules (Kedersha et al., 1999).

Figure 14 shows a heat map comparing expression values of genes that are differently expressed in *ten-1(tm651)* versus *ten-1(ok641)* and compares these genes with the expression value of the same genes in wild type condition. The result showed that the gene expression pattern of *ten-1(ok641)* is more similar to wild type than the expression profile of the *ten-1(tm651)* mutant. Genes in the *ten-1(tm651)* mutant are predominantly up-regulated. In terms of my findings that loss of *ten-1* together with a compromised basement membrane leads to mechanical instability between epidermis and muscles in the *C. elegans* embryos I was interested whether genes known to provide this stability and basement membrane components were changed in their expression. Indeed, I found that the basement membrane components *let-2*, *emb-9* and *unc-52* are down-regulated. In addition, the single plektin homolog, *vab-10* and the ubiquitin ligase *eel-1*, regulating the protein abundance of myotactin, LET-805, are down-regulated. Interestingly, the genes coding for the intermediate filaments, *ifb-1* and *ifa-2*, connecting VAB-10 protein in the epidermis are up-regulated. A summary of the genes with their fold change is presented in figure 15.

Sequence name	Gene name	description	Vertebrate homolog
Decreased in <i>ten-1</i> mutant background			
C28D4.3	<i>gln-6</i>	GLutamiNe synthetase	GLUL
F55B11.6		unknown	unknown
K05C4.9		ZYG-11-like proteins	ZYG11B
T05F1.4		unknown	unknown
Y46G5A.13	<i>tiar-2</i>	Apoptosis-promoting RNA-binding protein TIA-1/TIAR	TIA1
Y73B6A.3		unknown	unknown
Increased in <i>ten-1</i> mutant background			
C14C6.2		Secreted surface protein	unknown
C14C6.5		unknown	unknown
C18H7.1		von Willebrand factor and related coagulation proteins	COL6A3
F31F4.12	<i>nhr-180</i>	Nuclear Hormone Receptor family	NR113
F47B8.2		unknown	unknown
F48G7.11	<i>nhr-190</i>	Nuclear Hormone Receptor family	HNF4A
F48G7.4		unknown	unknown
F54D5.4		unknown	unknown
H25P19.1		unknown	unknown
R11G11.2	<i>nhr-58</i>	Nuclear Hormone Receptor family	PPARG
T01G6.2	<i>nhr-131</i>	Nuclear Hormone Receptor family	NR113
Y39G10AR.2	<i>zwl-1</i>	ZWiLch (<i>Drosophila</i>) homolog	ZWILCH-201
Y58A7A.5		unknown	unknown
ZK488.2	<i>nhr-90</i>	Nuclear Hormone Receptor family	HNF4A

Table 1. Genes which are up- or downregulated in *ten-1(tm651)* and *ten-1(ok641)*

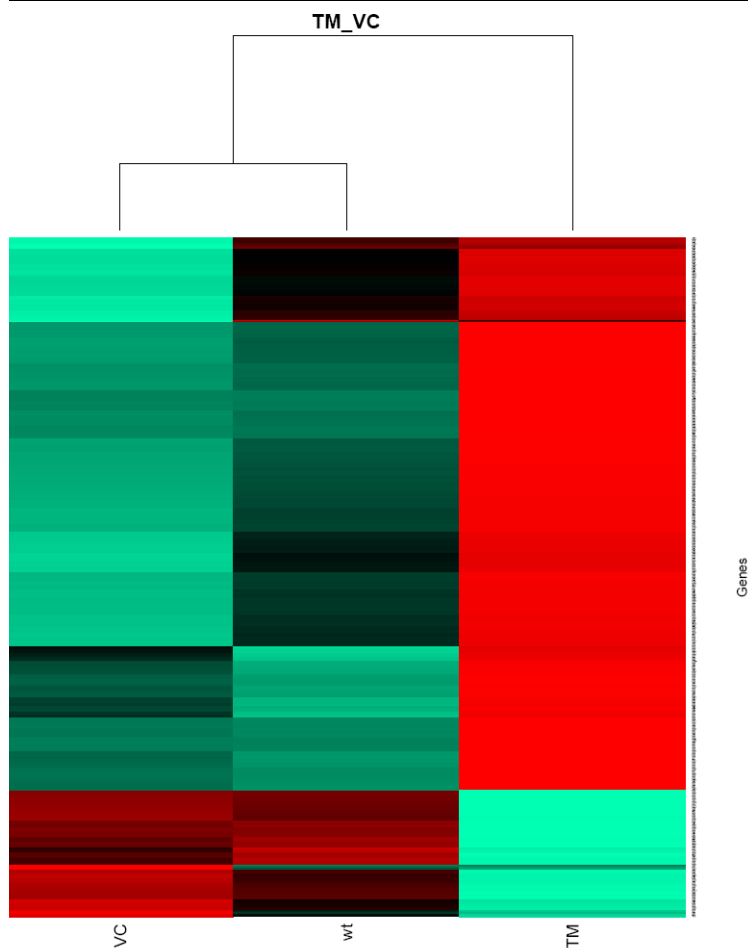


Figure 14. Heat map comparing expression values of genes in the *ten-1* deletion mutants. Genes in green are lower expressed than genes in red. The heat map represents a summary of three biological replicates per condition. The *ten-1(ok641)* mutant has a similar expression to wild type whereas gene expression in the *ten-1(tm651)* mutant is very different from *ten-1(ok641)* and wild type. Genes are predominantly increased in the *ten-1(tm651)* mutant. VC, *ten-1(ok641)*; wt, wild type; TM, *ten-1(tm651)*.

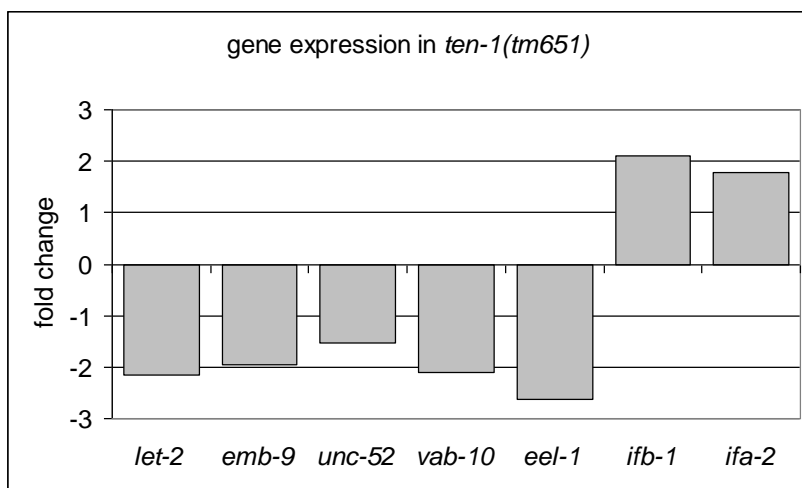


Figure 15. Gene expression in *ten-1(tm651)* obtained from expression profiling. The basement membrane collagens *let-2* and *emb-9* and the perlecan homolog *unc-52* are downregulated. The plakin homolog *vab-10* and the ubiquitin-ligase *eel-1* regulating myotactin are downregulated, too. The two subunits of the intermediate filaments *ifb-1* and *ifa-2* are upregulated.

To investigate whether the down regulation of genes coding for basement membrane proteins is caused by the loss of *ten-1* function, I made use of an integrated worm strain overexpressing the intracellular domain of *ten-1* under an inducible heat shock promoter (unpublished worm strain of K. Drabikowski). Mixed stage population of wild type and worms overexpressing the ICD were heat shocked and samples for isolation of RNA were taken 1.5h, 3h, 4.5h and 6h after heat shock. At the same time points non heat shocked worms were harvested. Upon heat shock stimulation many genes are down regulated in wild type background. This also seems to be the case for the *C. elegans* collagen IV genes. Quantitative RT-PCR results were normalized to the housekeeping gene *ama-1* and corrected for the reduction of mRNA level caused by the heat shock reaction in wild type background (Figure 16). Indeed, expression of at least *emb-9* and *let-2* depends on the activity of the *ten-1* ICD. Whether this is a direct or indirect effect remains to be elucidated.

3.3.4. Generation and characterisation of antibodies against the intracellular domain specific for TEN-1L

An especially interesting role is predicted for the intracellular domain of teneurins. The ICD can be cleaved off from the protein and translocates to the nucleus. Its function in the nucleus is unknown.

To investigate the role of the intracellular domain of *ten-1* in *C. elegans* I expressed and purified the part of the intracellular domain specific for the TEN-1L in bacteria. For construct preparation and purification procedures see “Materials and Methods”. This is the first time the intracellular domain could be purified due to the use of special ArcticExpress™ (DE3)RIL bacteria that can be induced at low temperatures and contain special chaperones helping the protein to fold. Purification from standard bacteria and cell culture led to insoluble protein only.

The purified protein was used to raise antibodies in rabbits and in mice. All antibodies recognize the ICD when overexpressed in worms. The polyclonal antibody cross-reacts also with a bacterial protein with a size of 25 kDa. The detection of endogenous protein was not successful in this experiment (Figure 17).

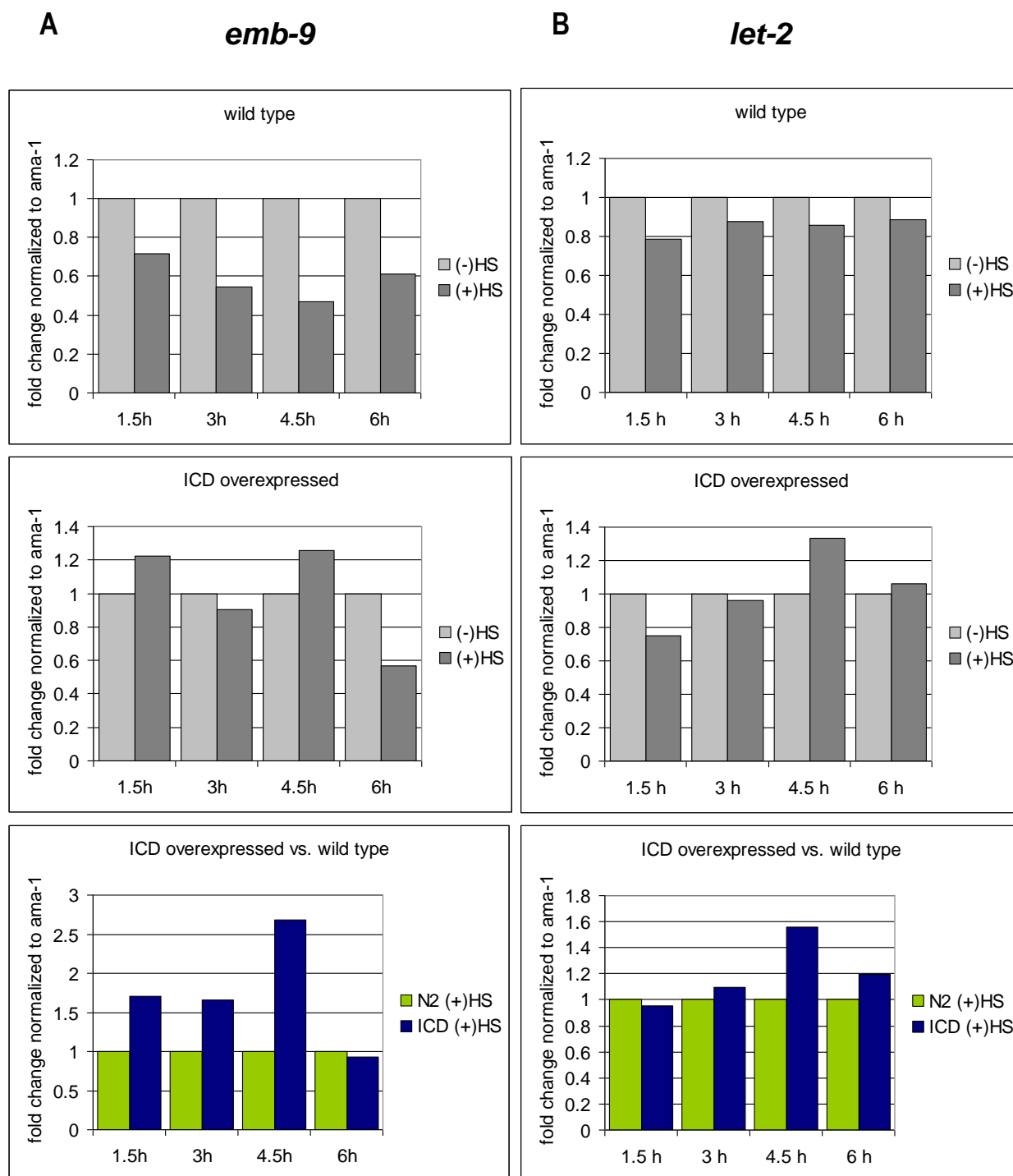


Figure 16. Overexpression of *ten-1* ICD increases the expression of *emb-9* and *let-2*. (A) Fold change of *emb-9* normalized to *ama-1*. (B) Fold change of *let-2* normalized to *ama-1*. First panel shows fold change in wild type worms upon heat shock. Second panel shows fold change in worms overexpressing *ten-1* ICD upon heat shock. Third panel shows fold change depending on overexpression of ICD and corrected for changes in gene expression upon heat shock in wild type worms. HS, heat shock.

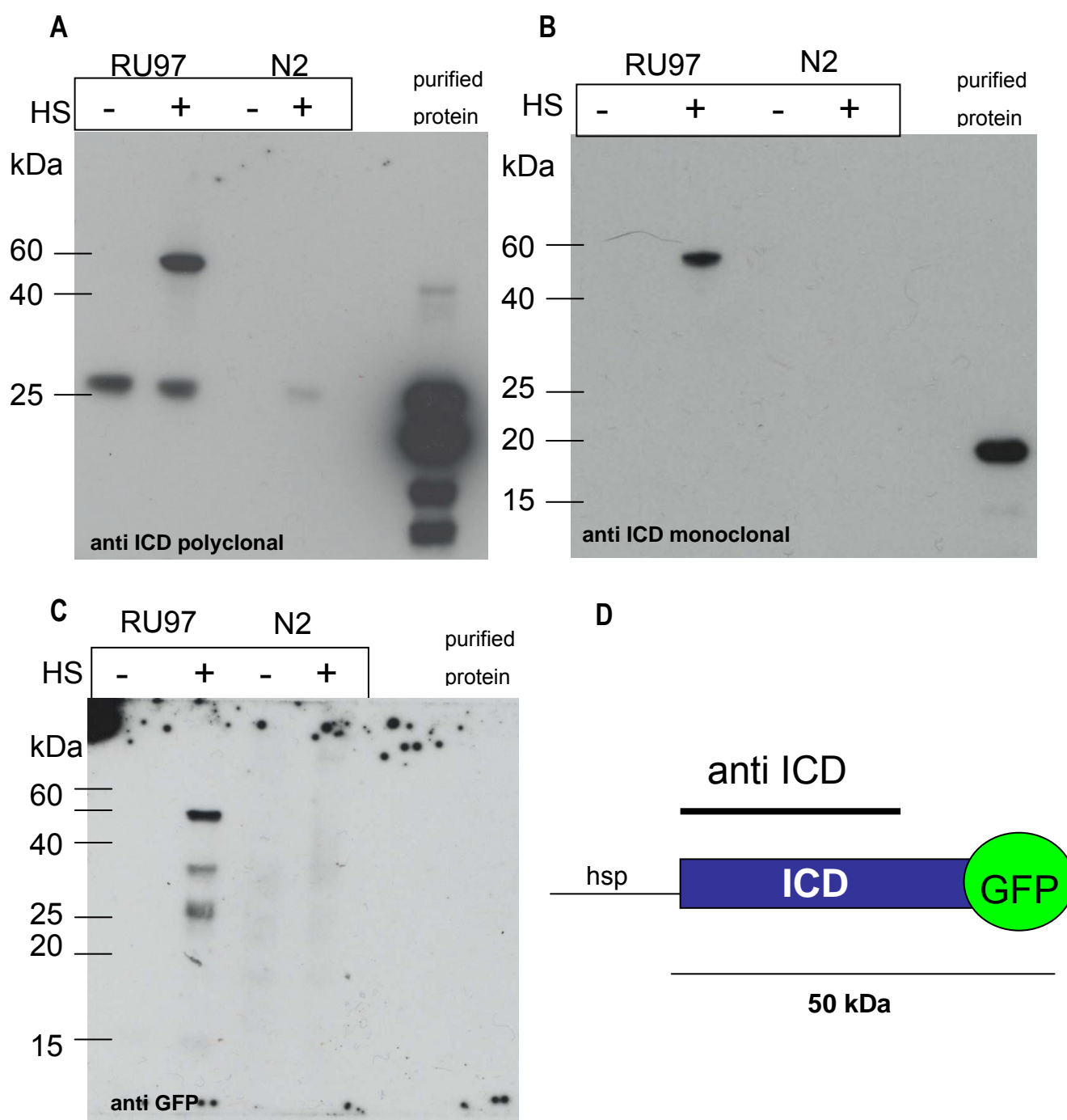


Figure 17. Polyclonal and monoclonal antibodies recognize overexpressed TEN-1 ICD. Worms of RU97[kdEx41(hsp::ICDfull::gfp; rol-6)] and N2 (wild type) were synchronized and developed to late L3 stage. Half of the population of each line was heat shocked (HS) at 33°C for 30 min. Worms were allowed to recover on bacterial plates. All samples were harvested after 6 hours of the heat shock. As control purified protein was used. (A) Western blot using polyclonal antibody against ICD. (B) Western blot using monoclonal antibody against ICD. (C) Western blot anti GFP. (D) Schema of the construct overexpressed in the worm. The molecular weight of the fusion protein is predicted to be app. 50 kDa.

Four clones of the monoclonal antibodies were obtained from the immunization of the mice. Using these antibodies I studied whether the ICD can be cleaved from the rest of the protein by a predicted furin cleavage site after the transmembrane domain. I used worms overexpressing the ICD up to the start of the EGF repeats fused to GFP. Indeed, using an anti GFP antibody I never could detect a full length protein. The experiment confirms unpublished results of K. Drabikowski. Interestingly, the different monoclonal antibodies detected similar band patterns on the Western blot. The mAb94E detected the most prominent bands with a molecular weight of approximately 40 kDa corresponding to the cleaved ICD and approximately 15 kDa which could represent a truncated fragment of the ICD. A band with the molecular weight of approximately 80 kDa could correspond to the full length protein made from the transgene (Figure 18).

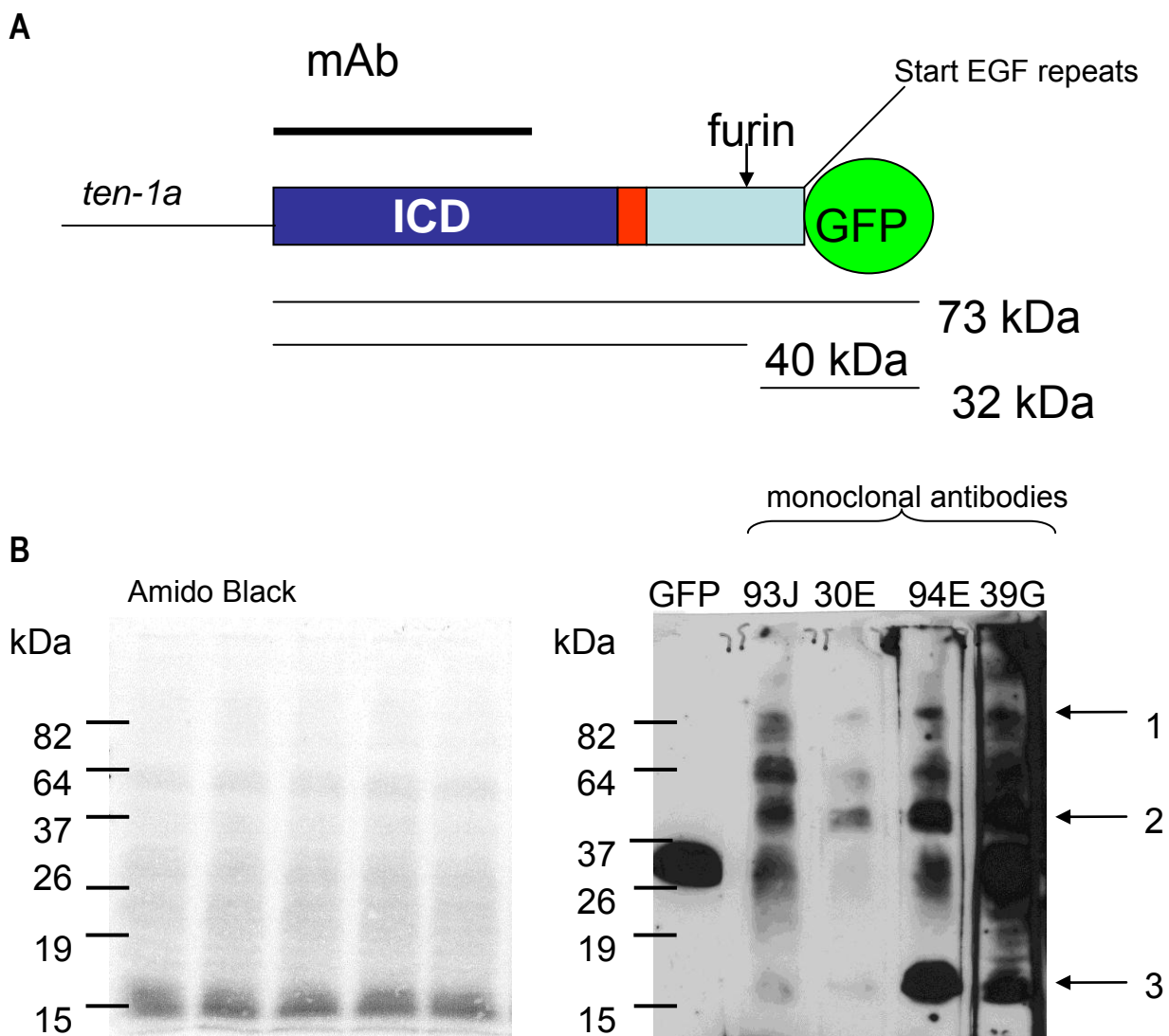


Figure 18. Processing of the TEN-1 intracellular domain. (A) Scheme of construct overexpressed in wild type worms. Resulting worm line was called RU14[kdEx32(*ten-1a*::full_ICD_TM_furin::gfp)]. ICD (blue), transmembrane domain (red), extracellular part including the furin cleavage site up to the start of the EGF repeats (light blue), GFP (green). The part of the ICD detected by the monoclonal antibodies is indicated (mAb). Predicted molecular weight of processed and unprocessed protein is described. (B) Wormlysate of RU14. Amido Black staining serving as loading control (left). Western Blot anti GFP and the monoclonal antibodies as indicated. Arrows indicated full-length and processed protein: (1) full-length protein (2) processing at the furin cleavage site, (3) truncated part of the ICD (right).

To investigate whether the result of the overexpressed protein can be reproduced at endogenous level I used worm lysate of wild type worms. Indeed, I could reproduce the bands with a molecular weight of about 40 kDa and the truncated protein about 18 kDa. The two bands could be competed by pre-incubation of the antibody with the antigen (Figure 19).

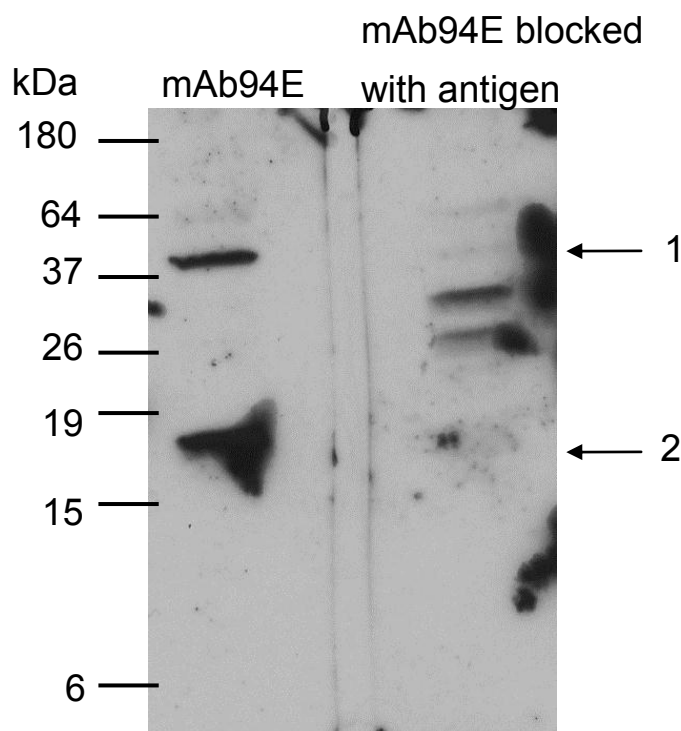


Figure 19. TEN-1 ICD is processed in vivo. Western blot anti ICD using monoclonal antibody clone 94E. Resulting bands are competed by blocking of the antibody with the antigen. (1) Cleavage corresponds to the predicted furin cleavage site. (2) Truncated version of the ICD.

Finally, I studied expression and localization of endogenous TEN-1 by immunostaining using the monoclonal antibody. Expression was often found around the pharynx (Figure 19 A) and in early embryos (Figure 20 B-D). In the embryos TEN-1 was localized in the nucleus and on the cell cortex. Multiple cell stage embryos showed rarely TEN-1 localization in the nucleus.

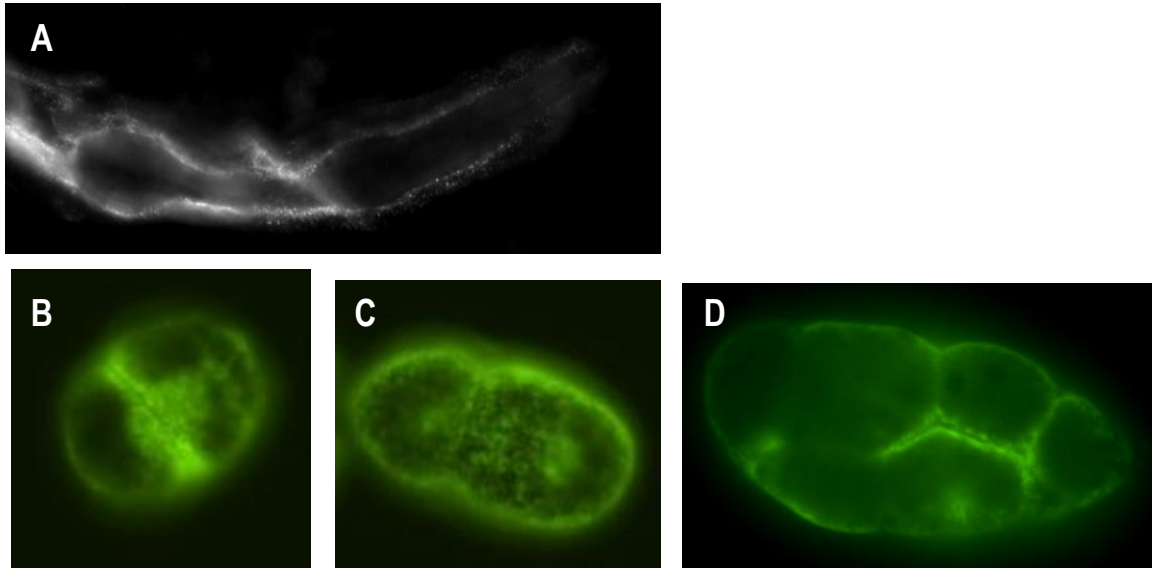


Figure 20. Immunostaining anti TEN-1 ICD. (A) TEN-1 localizes around the pharynx. (B) One-cell stage embryo starting to divide shows staining of the nucleus and the cortex. Staining at the cell boundary seems enhanced. (C) Two-cell stage embryos with TEN-1 localized in the nuclei and at the cell cortex. (D) Multiple cell stage embryo with TEN-1 localization at the cell cortex.

4. DISCUSSION

In my thesis I investigated the function of *ten-1* in *C. elegans* using an RNAi approach to identify novel interaction partners of *ten-1*. I characterized the genetic interaction of *ten-1* and *phy-1*. I found that loss of *ten-1* in combination with a compromised basement membrane, due to reduction of functional collagen IV, results in embryonic lethality (Topf and Chiquet-Ehrismann, submitted). Furthermore, I investigated the maturation and function of the ICD of TEN-1 (unpublished).

4.1. P4H functions in secretion of collagen IV from the muscles into the basement membrane

The prolyl 4-hydroxylase is an essential enzyme during post-translational modification of pro-collagen. The enzyme consists of an alpha domain with catalytic activity and a beta domain which is a protein disulfide isomerase. Both domains are conserved in *C. elegans*. A knock-out mouse lacking the alpha domain is embryonic lethal due to insufficient modification of collagen IV and subsequent instability of the basement membrane. The *C. elegans* P4H is implicated in modification of the cuticle collagens. Under physiological conditions a heterodimer of PHY-1 and PHY-2 forms the catalytic domain of the tetramer enzyme complex. Only the double knock-out results in embryonic lethality. Worms burst after elongation of the epidermis because of an instable cuticle. I investigated the role *phy-1* and *phy-2* in basement membrane stability studying the secretion of collagen IV in the basement membrane during embryogenesis. I found that the loss of *phy-1* function alone leads to aggregation of collagen IV in muscle cells, the tissue of its production. However, this does not significantly influence the development of the embryo (Topf and Chiquet-Ehrismann, submitted). When combined with the knock-down of *phy-2*, aggregation of collagen IV was more frequent and basement membrane appeared weaker than in control animals. I concluded that *phy-1* and *phy-2* must have a function in muscle cells influencing the secretion of collagen IV. Further biochemical analysis is necessary to determine whether it is a reduction of proline hydroxylation of pro-collagen resulting in blockage of protein secretion.

Furthermore, the expression of *phy-1* and *phy-2* needs to be investigated in more detail. Expression and modification of collagen IV takes place in body wall muscle

cells. Expression of *phy-1* or *phy-2* in muscle cells was not shown yet. The *phy-1* promoter is strongly active in the epidermis, the hypodermal cells of the vulva and some unidentified neurons in the head and tail (Hill et al., 2000). Expression of PHY-1 in the epidermis was confirmed by immunostaining (Myllyharju et al., 2002). A *phy-2* promoter *gfp* fusion is expressed in the epidermis and the spermatheca (Shen et al., 2005). Additional tissues expressing *phy-1* or *phy-2* might have been missed by these approaches due to low expression levels of the protein. Used reporter constructs missing regulatory elements or were silenced due to high overexpression of the transgene. Single copy integration of a reporter-gene reflects the endogenous expression better than a multicopy extrachromosomal expression and could be used as additional approach (Frokjaer-Jensen et al., 2008).

In summary, my results show that the important function of the prolyl 4-hydroxylase for basement membranes is also conserved in *C. elegans*.

4.2. Identification of interaction partners of *ten-1* by RNA interference

Using a genome wide RNAi approach I discovered novel interaction partners of *ten-1*. The RNAi screen was already discussed in my submitted manuscript "*C. elegans* teneurin, *ten-1*, interacts genetically with the prolyl 4-hydroxylase, *phy-1*, and is important for basement membrane integrity during late elongation of the embryo". In addition, the manuscript described the interaction of *ten-1* and *phy-1* in detail. Thus, I will focus here on other candidates discovered in the screen and how the interactions could be studied in respect to a conserved function with teneurin.

Preliminary experiments showed that *ten-1* might act upstream of the paxillin homolog *pxl-1*. The *pxl-1* knock-out mutant is lethal at the first larval stage. It was not possible to create a *ten-1;pxl-1* double mutant and confirm the interaction. In addition, there is no published information about expression and localization of *pxl-1*. Interestingly, the micro array data show that *pxl-1* is upregulated (1.8 fold in comparison to wild type) in the *ten-1(tm651)* deletion mutant. In contrast to *C. elegans*, the vertebrate paxillin is intensively studied. Paxillin is a well-established component of focal adhesions, dynamic structures connecting the extracellular matrix to the cytoskeleton. Recently, a physical and functional interaction between paxillin and CAP/ponsin was identified in cell culture (Zhang et al., 2006). CAP/ponsin is an

adaptor protein belonging to the SoHo family and is involved in the regulation of diverse cellular processes like glucose transport, transcriptional activation and ubiquitination (Kioka et al., 2002). Teneurin-1 was found to interact with CAP/ponsin, too. Ponsin binds with its third SH3 domain to the teneurin-1 polyproline-rich stretch of the ICD. Overexpression of teneurin-1 recruits ponsin to the cell membrane (Nunes et al., 2005). Paxillin was found to bind predominantly to the second SH3 domain of ponsin (Gehmlich et al., 2007; Zhang et al., 2006). Overexpression of ponsin induces paxillin, but also actin and vincullin aggregation at cell-ECM adhesion. A gene similar to ponsin can also be found in the *C. elegans* genome, but has not been characterized yet. Studying an interaction between teneurin and paxillin in cell culture could be more promising. Thus, one can imagine that teneurin senses changes in the extracellular environment which triggers the recruitment of these adaptor proteins leading to a signal cascade that influences for example cell migration or remodelling of ECM.

Another group confirmed the interaction of ponsin and paxillin but investigated its role in muscle cells. There the interaction triggers the maturation of focal adhesions to pre-costameres (Gehmlich et al., 2007). Unpublished results in *C. elegans* demonstrate that PXL-1 localizes strongly to dense bodies and adhesion plaques of the muscles. A general role for TEN-1 in muscle cells has not been established but TEN-1 is expressed in some posterior muscles and strongly in the vulva muscles. Knock-down of *ten-1* by RNAi results in detachment of vulva muscles from the body wall and the vulva (Drabikowski et al., 2005). Interestingly, overexpression of truncated versions of TEN-1 missing most of the extracellular domain results in a similar phenotype (unpublished data). Thus it is not unlikely that TEN-1 has broader function in muscle attachment. In addition, the *Drosophila* teneurin protein, Ten-a, localizes to muscle attachment structures during embryogenesis (Fascetti and Baumgartner, 2002). Thus, a function of teneurin in muscle structures could be conserved.

WWP-1 is an E3-ubiquitin ligase which is conserved in vertebrates (Huang et al., 2000). I found that knock-down of *wwp-1* in *ten-1(ok641)* mutant background enhances the *ten-1* mutant phenotype. According to genetic analysis *ten-1(ok641)* is a genetic null mutant (Trzebiatowska et al., 2008). However, it is still possible that

mutant TEN-1 protein is expressed. If this is the case according to the genetic analysis, it should not be functional and thus a regulation of protein turn-over by WWP-1 should not have an effect on the *ten-1* mutant phenotype. Nevertheless, such an experiment could be performed using wild type worms over-expressing the TEN-1 ICD under a heat shock promoter in worms with knock-down of *wwp-1*. Performing a time course experiment and western blotting using the monoclonal antibody against the ICD should answer the question whether WWP-1 influences TEN-1 protein turn over.

Alternatively, *wwp-1* might act in parallel to *ten-1* and influences the turn-over of other target proteins having redundant function to *ten-1*. For example, the ICD of LIN-12, a Notch homolog, is known to be regulated by WWP-1 (Shaye and Greenwald, 2005). WWP-1 ubiquitin ligase activity was found to be essential for longevity, too. Over-expression of WWP-1 extends lifespan, whereas a loss of function mutant completely represses longevity in dietary restricted animals (Carrano et al., 2009). Thus, WWP-1 functions to ubiquitinate substrates that regulate dietary restriction induced longevity. The substrates are unknown but might act in parallel to *ten-1*.

A potential oncogenic role for WWP1 has been suggested by genetic and functional analyses in human cancers. Gene amplification has been detected in approximately 40% of prostate and breast primary tumors (Chen et al., 2007a; Chen et al., 2007b). p53 acts as a substrate of WWP-1 and ubiquitination promotes nuclear export of p53 and therefore inactivation of p53 dependent transcription (Bernassola et al., 2008). Teneurin-4 was found to be strongly overexpressed in brain tumors on transcriptional and protein level. Also teneurin-4 was misregulated in ovary cancer, leukaemia and prostate cancer (D. Kenzelmann Broz, unpublished results). Whether teneurins or the regulation of teneurins is important for cancer development is unclear. Studying the potential interaction between *wwp1* and teneurins in cell culture might give more insights.

4.3. Micro array analysis of *ten-1* deletion mutants

To find molecular differences between the *ten-1* deletion mutants and wild type animals I performed micro array analysis of these strains. I used synchronized L1 worms. Later stages are not suitable for this analysis since *ten-1* mutant animals exhibit a minor developmental delay and the percentage of arrested L1 worms significantly influence the result. To my surprise the result showed that the deletion mutants are significantly different from each other on a transcriptional level. The *ten-1(ok641)* mutant is very similar to wild type animals and showed only a difference in 54 genes compared to wild type. In the *ten-1(tm651)* mutant 780 genes showed different expression levels in comparison to the wild type. The result was unexpected, since both mutants are very similar on a phenotypic level and are considered as genetic null mutants (Trzebiatowska et al., 2008). Considering the theoretically possible gene products, the *ok641* allele (which is an in frame deletion) would give rise to a protein just lacking only the last three EGF-repeats. There is evidence that the EGF-repeats are important for the function of TEN-1, since just the loss of the C-terminal extracellular part after the EGF-repeats results in a much milder phenotype (Morck et al., 2010). The EGF-repeats facilitate dimerization of the protein, which could be impaired in the *ten-1(ok641)* mutant. If dimerization is necessary for recognition of a ligand which triggers the processing of TEN-1, this process would be impaired and release of the ICD would occur at very low and uncontrolled levels. In contrast, the *tm651* allele could give rise to a soluble ICD which would be larger than the wild type TEN-1 ICD due to additional 38 amino acids encoded downstream of the deleted DNA until a stop codon is reached. Since the ICD carries the nuclear localization signal, such a gene product would exist independent of protein dimerization and activation of proteolysis by a ligand. The ICD could have a function in the nucleus similar to its wild type equivalent but would not function in the correct cellular context resulting in up or down-regulation of genes at the wrong time. The micro array could reflect this constitutive signalling.

Further investigations are essential to solve the discrepancy between the phenotypic data and the gene-profiling.

In summary, investigating the hits of the micro array resulting from the *ten-1(tm651)* mutant could give crucial information about the function of the TEN-1 ICD in the

nucleus. The hits need to be validated by quantitative RT-PCR and genes of interest studied in the correct cellular and developmental context.

Closer observation of selected genes changed in the *ten-1(tm651)* mutant revealed that the genes coding for basement membrane proteins, EMB-9, LET-2 and UNC-52 as well as the plakin homolog VAB-10 were down-regulated. All of these proteins are essential during epidermal elongation and contribute to proper connection between epidermis, muscles and separating basement membrane. UNC-52 and VAB-10 are essential for the formation of hemidesmosome-like structures in *C. elegans*. Interestingly, intermediate filaments which are also essential for these structures are up-regulated which could reflect a reaction of the animal to compensate for the reduced levels of the other proteins. I found that loss of *ten-1* in combination with a compromised basement membrane results in elongation defects due to loss of proper connections between epidermis, basement membrane and underlying muscles (Topf and Chiquet-Ehrismann, submitted). It is possible that TEN-1 could have a structural role in the basement membrane, but considering the micro array data also a regulatory function is likely. I could show that the over-expression of TEN-1 ICD resulted in up-regulation of *emb-9* and *let-2* on transcription level. If this result could be confirmed in cell culture in vertebrate teneurins it could define the first true conserved function of teneurins.

4.4. Insights into mechanism of action of TEN-1

Teneurins are transmembrane proteins. They contain a large extracellular part with conserved domain structure. The structure of the protein, the presence of EGF-like repeats and translocation of the ICD to the nucleus, suggests a similar mode of action as the Notch receptor. Whether Teneurins serve as a receptor and bind a ligand(s) is unclear. I showed that loss of function of *ten-1* in combination with a compromised basement membrane due to loss of functional collagen IV protein leads to embryonic lethality (Topf and Chiquet-Ehrismann, submitted). Finding a genetic interaction between collagen IV genes and *ten-1* is difficult since loss of function of collagen IV genes is lethal itself. Additionally, investigations in *C. elegans* showed that genetic interactions of *ten-1* with genes coding for basement membrane proteins are crucial for the development of the nematode. Trzebiatowska et al. showed that

ten-1 loss of function in combination with knock-down of laminin *epi-1* and nidogen *nid-1* is synthetic lethal. A protein-protein interaction between any of these components could not have been shown so far. To screen for ligands on a protein level, expression and purification of the extracellular domain would be necessary. Although I tried several approaches expressing the protein in cell culture I was not successful with the *C. elegans* protein. Neither the extracellular domain, nor truncated versions were secreted from the cells and the protein accumulated in the Golgi/ endoplasmic reticulum.

Previous unpublished data of the lab did not show differences in adherence of isolated *C. elegans* cells adhering to laminin versus a control protein. Nevertheless, it would be interesting to investigate whether cells isolated from the *ten-1* deletion mutants would adhere differently than wild type cells using other experimental conditions. Culturing isolated *C. elegans* cells on different substrates might influence translocation of the ICD to the nucleus in a substrate dependent manner. This experiment would answer the question whether the proteolysis of TEN-1 is ligand dependent and which ligand stimulates the processing.

Using the new antibody against the TEN-1 ICD unique for the long version of TEN-1 I could confirm the result of Drabikowski et al. (2005) that TEN-1 localizes to the cell membrane and the nucleus. Furthermore, the immunostainings demonstrate that TEN-1 is already expressed in one-cell stage embryos. This led me to speculate that TEN-1 has a function already very early during embryogenesis. Accessibility of the antigen in the worm or masking of antigen by fixation of the material greatly limited the results of the immunostaining. Staining of isolated *C. elegans* blastomeres might be an alternative to gain insights into the localization of TEN-1 in differentiated cells like neurons, muscle cells or epidermal cells.

Using a biochemical approach I could show that the endogenous ICD is cleaved off in at least two steps: (1) processing at or close to a predicted furin cleavage site downstream of the transmembrane domain, (2) processing at the cytosolic part. Whether processing within the transmembrane domain occurs, could not be assessed. Using the antibody against the ICD I could not detect a full length protein. Western blot analysis resulted in multiple and not reproducible bands. This might be due to heavy post-translational modifications or additional processing events. In addition, modification and processing could also be altered in different developmental

stages of the worm. Different experimental conditions might be necessary to extract a transmembrane protein for western blot analysis.

Nevertheless, the antibodies I developed are a good tool to characterize the *ten-1* deletion mutants on a protein level. Semi-quantitative PCR results showed that in both mutants *ten-1* mRNA is produced to the same extent than in wild type animals and it was not degraded (A. Trzebiatowska, unpublished results).

In summary, I could confirm that TEN-1 is processed and the ICD can be found in the nucleus. Whether a ligand triggers the proteolyses is unclear, but several genetic interactions with basement membrane genes and the fact that also chicken teneurin-2 co-localizes with laminin on some basement membrane (Tucker et al., 2001) makes it likely that extracellular matrix molecules might be candidates for a binding partner of teneurins.

In summary, my thesis provides the basis of deciphering the genetic interaction network of *ten-1* in *C. elegans*. Many interaction partners I found are conserved in vertebrates pointing to conserved functions of teneurins.

5. MATERIALS AND METHODS

5.1. High-throughput screen for genes interacting with *ten-1*

Approximately 12,000 genes of the *C. elegans* orfem RNAi feeding library (OpenBiosystems) were tested for interaction with *ten-1*. RNAi bacteria were grown in 96-well format in LB medium containing 100 µg/ml ampicillin and 12.5 µg/ml tetracycline for app. 12 h at 37°C with 100 rpm. The OD₅₉₅ was measured using a spectrophotometer (Biorad®). Bacteria were plated on ENGM 24-well plates containing 100 µg/ml ampicillin, 12.5 µg/ml tetracycline and 1 mM IPTG (RNAi plates). Plates with bacteria were dried for at least 12 h at RT. Worms grown on egg plates were washed off with M9 and cleaned by sucrose floatation. Cleaned worms were treated with NaOCl to release eggs of hermaphrodites. The embryos were allowed to hatch over night at 20°C on NGM plates seeded with HT115 bacteria. Synchronized L1 worms were washed off with M9 and extensively cleaned. 10 L1 worms were sorted in each well of the prepared 24-well plate with RNAi bacteria using the Copas BioSorter (Biometrica). Worms were grown for 5 days at 20°C. Phenotype of P₀ and F₁ progeny was recorded by observation using Leica binocular microscope. Specificity of RNAi for the candidate gene was checked by isolation of plasmid DNA from HT115(DE3) bacteria using standard methods (MiniPrep Kit, Quiagen). Insert was sequenced using M13F primer. The sequence was blasted against worm genome sequence. Potential candidates were twice re-screened. For re-screening isolated and validated DNA of the candidate clone was retransformed into chemically competent HT115(DE3) bacteria. A single colony was inoculated over night at 37°C in 3 ml of LB medium containing 100 µg/ml ampicillin, 12.5 µg/ml tetracycline. 50 µl of the over night culture was diluted in 2 ml LB medium containing 100 µg/ml ampicillin, 12.5 µg/ml tetracycline and incubated at 37°C with 250 rpm for 2 h. The bacteria were harvested for 10 min at 3000 rpm. The pellet of bacteria was resuspended in 200 µl LB medium containing 100 µg/ml ampicillin, 12.5 µg/ml tetracycline. The bacteria were plated on RNAi plates in 24-well format. Further procedure was identical to initial screen (see above).

5.2. Generation of chemically competent HT115(DE3) bacteria

An overnight culture of LB containing 12.5 µg/ml tetracycline (LB+Tet) was inoculated at 37°C. A 1:100 dilution was grown in LB+Tet until OD₅₉₅=0.4. The bacteria were harvested for 10 min at 3000 rpm at 4°C. The pellet was resuspended in half of the original volume cold, sterile 50 mM CaCl₂. The suspension was incubated on ice for 30 min and spun as before. The cells were resuspended in 1/10 of the original volume CaCl₂. Resuspended cells were aliquoted and stored at -80°C. 50 µl of bacteria were used for plasmid transformation.

5.3. Generation of chemically competent ArcticExpress™(DE3)RIL bacteria

Buffer 1:	30 mM KOAc	Buffer 2:	10 mM Mops, pH 7.0
	50 mM MnCl ₂		75 mM CaCl ₂
	100 mM RbCl ₂		10 mM RbCl ₂
	10 mM CaCl ₂		15% glycerol
	15% glycerol		
	pH 5.8		

An overnight culture of 2xYT media containing 75 µg/ml streptomycin, 20 µg/ml gentamycin and 12.5 µg/ml tetracycline was inoculated. A 1:100 dilution was grown in LB containing 75 µg/ml streptomycin, 20 µg/ml gentamycin and 12,5 µg/ml tetracycline until OD₅₉₅=0.94. The cells were harvested 3 min at 3000 rpm at 4°C. The pellet was washed in buffer 1 and spun again as before. The pellet was resuspended in buffer 2, aliquoted and stored at -80°C. 50 µl of bacteria were used for plasmid transformation.

5.4. Cloning of *ten-1* ICD

cDNA was amplified by PCR to obtain a 550 bp long fragment of *ten-1* unique to the long version of the ICD using the primer *Ten-1L_EagI_3'* and *Ten-1L_NcoI_5'*. The PCR was performed using pfu polymerase (Promega) resulting in blunt end PCR product. The fragment was cloned in p3T (MoBiTec) vector digested with restriction enzyme EcoRV (NEB) for blue-white selection. The insert was digested with EagI

and NcoI and subcloned into pet28b+ (Novagen). Integrity of insert was validated by restriction digest and sequencing reaction.

5.5. Expression of TEN-1 ICD in ArcticExpress™ (DE3)RIL bacteria

Bacteria were freshly transformed with appropriate plasmid. A single colony was inoculated in LB containing 20 µg/ml gentamycin and 25 µg/ml kanamycin (resistance on plasmid) overnight at 37°C, 220-250 rpm. A 1:50 dilution of the overnight culture was added to LB containing 75 µg/ml streptomycin, 20 µg/ml gentamycin, 12,5 µg/ml tetracycline and 25 µg/ml kanamycin and grow for 3 hours at 30°C, 220-250 rpm. The culture was transferred to an incubator at 11°C and equilibrated for approximately 10 min. The bacteria were induced with 1 mM final concentration of IPTG for 24 hours.

5.6. Purification of TEN-1 ICD

lysis buffer: 100 mM NaH₂PO₄
 500 mM NaCl
 20 mM imidazole
 pH 8.0

washing buffer: 100 mM NaH₂PO₄
 500 mM NaCl
 50 mM imidazole
 pH 8.0

elution buffer: 100 mM NaH₂PO₄
 500 mM NaCl
 300 mM imidazole
 pH 6.9

Preparation of the lysate:

Induced bacteria were harvested. The pellet was washed once in lysis buffer. The washed pellet was resuspended 1/100 of the original volume in lysis buffer. Proteinase inhibitor (Roche) and lysozyme to a final concentration of 1 mg/ml was added. The suspension was incubated on ice for 30 min. The lysate was sonicated, centrifuged for 30 min, 5300 g at 4°C, filtered and degassed.

Preparation of the Ni-column:

A small column was filled with 2 ml of Ni sepharose beads (Clontech). Beads were allowed to settle down. The column was washed with 2 ml of ddH₂O and with lysis buffer. The column was equilibrated with lysis buffer using 1 volume of the bacterial lysate.

Purification:

The lysate was loaded on the column using a peristaltic pump with a speed of 1 ml/min. The column was washed with 1 volume of lysis buffer and 1 volume of washing buffer. The protein was eluted in several fractions.

Dialysis of purified protein:

Appropriate elution fractions were pooled and dialysed in PBS containing 150 mM NaCl as followed: in 500 ml for 3 hours, in 1000 ml overnight and final in 500 ml for 3 hours. A cellulose membrane with a cut-off of 12-14 kDa was used.

5.7. Protein techniques**5.7.1. Protein extraction from worms**

Worms were harvested and intensively cleaned with M9, sucrose flotation and ddH₂O. Small sample volumes (one 10 cm dish) were frozen in 100 µl ddH₂O at -80°C. SDS-loading buffer was added to the frozen sample. Large sample volumes (up to 250 µl of worms) were frozen in liquid nitrogen and grinded. Worm powder was added to 1.5 ml of RIPA-buffer containing protease inhibitor (Roche). The samples were mildly sonicated until worms were fairly dissolved or lysate appeared homogenous. The wormlysate was incubated for 1.5 hours on ice and then centrifuged for 20 min at 13000 rpm at 4°C. The supernatant was collected and

filtered. Sample was boiled for 5 min at 95°C and debris was collected by centrifugation before loading the SDS-page.

5.7.2. SDS page electrophoresis

Proteins with different molecular weight were separated using polyacrylamide gels. A SDS gel was composed of a 12.5 % resolving gel and 5% stacking gel. SDS-gels were prepared according standard procedures. Gel running equipment was provided by Bio-Rad. SDS gels were run in 1 x SDS running buffer (3.02 g/l Tris base, 14.4 g/l Glycine, 1.0 g/l SDS) at 30 mA per gel for 1 h at RT.

5.7.3. Western Blot analysis

Appropriate amount of sample was run on SDS polyacrylamide gel. *PageRuler Prestained Protein Lader* (Fermentas) was used as a marker. Gels were blotted using semidry blotting equipment (Bio-Rad) at 34 mA per gel for 1.5 h at RT. The PVD blotting membrane (Millipore) and blotting equipment was prepared according manufacture protocol. After the transfer, the membrane was blocked for at least 1 h at RT with 4% milk powder in TBST (TBS, 0.05% TWEEN-20). The membrane was incubated with appropriate first antibody over night at 4°C. After washing the blot was incubated with horseradish peroxidase-conjugated antibodies goat anti rabbit or goat anti mouse secondary antibody for 1 hour at RT. The blots were washed and developed using Super Signal (Thermo Scientific) for 1 to 5 min. For figure 19 the first antibody (mAB94E) was pre-incubated with 5 µg of purified antigen in TBS for 3 hours at RT.

5.8. *C. elegans* antibody staining and microscopy

For staining procedure of *phy-1(ok162) phy-2(RNAi)* using antibodies anti collagen IV and anti actin see Materials and Methods of the submitted manuscript. Images were acquired using Zeiss Axiovert 200M equipped with LSM510. Optical sections were collected 0.5 µm intervals. Images for the figure were prepared using ImageJ software.

For staining of the embryos using anti TEN-1L ICD antibody eggs of gravid hermaphrodites were released by NaOCL treatment and washed extensively with M9 and water. Cleaned eggs were transferred to object slides covered with poly-L-lysine and frozen in dry ice. The embryos were freeze cracked and immediately fixed in 3%

formaldehyde in PBS for 5 min at room temperature (RT). Embryos were washed three times for 15 min in PBS containing 0.1% TWEEN-20 (PBS-T). Samples were blocked with PBS-T containing 10% normal goat serum (PBS-T-B) for 1 hour at RT in a humidified chamber. Embryos were stained with anti TEN-1L ICD (1:10 diluted for monoclonal antibody from cell culture medium) in PBS-T-B overnight at 4°C in a humidified chamber. Samples were washed for 2 hours with several changes of PBS-T at RT and then incubated for 1 hour with secondary antibody (Alexa 488) at RT. Embryos were washed 3 times for 20 min with PBS-T followed by PBS alone and mounted with mowiol (Gibco). For staining of larvae mixed stage animals were collected in 3% formaldehyde in PBS in an Eppendorf tube and frozen in liquid nitrogen. The sample was defrosted at 37°C and refrozen 3 times. After the last cycle the sample was incubated for 10 min at RT. The following steps are identical as previously described, with the exception that the procedure was carried out in the Eppendorf tube. Images were acquired with Zeiss Axiscope and HDCam Hamamatsu 1394 ORCA-ER.

5.9. Isolation of total RNA from *C. elegans* and preparation of cDNA

Worms were intensively cleaned with M9 and ddH₂O. The worm pellet was frozen in 100 µl ddH₂O at -80°C. 400 µl Trizol Reagent (Invitrogen) was added to the frozen sample and then vortexed for 2 min. Sample was frozen in liquid nitrogen and thawed at 37°C with three cycles. 100 µl of Trizol Reagent was added and incubated for 5 min at RT. 140 µl of chloroform was added, mixed and incubated for 1 min at RT. The sample was spun for 15 min at 10000 rcf at 4°C. The liquid phase was transferred into a new tube and an equal volume of 70% ethanol was added. RNA was cleaned using Rnasy Mini Kit (Quiagen) according protocol.

1 µg of total RNA was used to generate cDNA by reverse transcription PCR (RT-PCR) using THERMOSCRIPT RT-PCR System (Invitrogen) according protocol. For quantitative real-time PCR (qRT-PCR) 10 ng of cDNA per reaction was used. SYBR QPCR SUPERMIX W/ROX (Invitrogen) was used for qRT-PCR according protocol.

5.10. List of primers

primer name	Sequence 5' → 3'	description
<i>Ten-1L_EagI_3'</i>	TTTGCGGCCG CAGTGCCA ACTTGCTGCCTTCTTC	cloning of TEN-1 ICD for expression in bacteria
<i>Ten-1L_NcoI_5'</i>	TTTCCATGGTCCAGCACAGGACCACG	
VC518_WT	TCAGTTGACCATGAGCTGAGC	genotyping of <i>ten-1(ok641)</i>
VC518_3	CAAACAGTTCCGTCTCCAGCC	
VC518_1	TGACACTGACGGAAGATGCCG	
Tm651_5`_1	GCTGAAATACCCACTCGCAGC	genotyping of <i>ten-1(tm651)</i>
Tm651_wt	GCACTCATTAGAAGAACCAGC	
Tm651_3`_2	AGTGTCACATCGTCCCCTTCC	
dpy-18(ok162)_for	GAAGAAGCTGTCGGAGGAGTA	genotyping of <i>dpy-18(ok162)</i> (<i>phy-1</i> mutant)
dpy-18(ok162)_rev	ACGGCTAGTGGGTTGAATCTC	
dpy-18(ok162)_wt_for	CGAATACCTGGCGTTTGCCTG	
<i>phy-2(ok177)_for</i>	GATCTATCGTACCTTAAGCTGG	genotyping of <i>phy-2(ok177)</i>
<i>phy-2(ok177)_rev</i>	ATAGTGCGCATTTCGGTTTCA	
<i>phy-2(ok177)_wt_for</i>	GAACATGCCACGTACCGTATCTC	
<i>phy-3_wt_for</i>	CCACCACAACA ACTGACGTAGTG	genotyping of <i>phy-3(ok199)</i>
<i>phy-3_wt_rev</i>	CGATGTCCCGAAATCTGACG	
<i>phy-3_ok199_rev</i>	CGTTGATTGTAGGCACGGATCC	
emb-9_5_727-748	TCTTATCCATGGGCTTCAAAGC	qRT-PCR for <i>emb-9</i>
emb-9_3_811-832	GTGGTCCTACTGGTCCATCAG	
let-2_new5_476-49	ATCGGATATGCTGGTGCTCC	qRT-PCR for <i>let-2</i>
let-2_new3_651-67	CCAATGCTTCCGATTCTCTGG	
ama-1_sense	CAGTGGCTCATGTCGAGT	qRT-PCR for <i>ama-1</i>
ama-1_antisense	CGACCTTCTTTCCATCAT	
M13F	TGTA AACGACGGCCAGT	sequencing RNAi clone

Table 2. Primers used in this study

5.11. List of plasmids

name	description	reference
pET-28b(+)	Protein expression vector with His tag sequence	Novagen

Table 3. Vector used in this study

5.12. List of bacteria strains

strain	genotype	reference
HB101	F ⁻ mcrB mrr hsdS20(r _B ⁻ m _B ⁻) recA13 leuB6 ara-14 proA2 lacY1 galK2 xyl-5 mtl-1 rpsL20(Sm ^R) glnV44 λ ⁻	Sigma
HT115(DE3)	F ⁻ , mcrA, mcrB, IN(rrnD-rrnE)1, lambda ⁻ , rnc14::Tn10(DE3 lysogen: lavUV5 promoter -T7 polymerase) (IPTG-inducible T7 polymerase) (RNase III minus)	CGC
ArcticExpress™ (DE3)RIL	<i>E. coli</i> B F ⁻ ompT hsdS(rB ⁻ mB ⁻) dcm ⁺ Tetr gal λ(DE3) endA Hte [cpn10cpn60 Gentr] [argU ileY leuW Strr]	Stratagene
XL10-gold	endA1 glnV44 recA1 thi-1 gyrA96 relA1 lac Hte Δ(mcrA)183 Δ(mcrCB-hsdSMRmrr)173 tetR F ⁺ [proAB lacIqZΔM15 Tn10(TetR Amy CmR)]	Stratagene

Table 4. Bacterial strains used in this study

5.13. List of worm strains

Strain name	Allele name	Genotype	description	Investigator/ reference
N2		<i>C. elegans</i> wild type var. Bristol		CGC
RU9	kdEx31	<i>ten-1b::GFP</i>		Drabikowski
RU14	kdEx32	<i>ten-1a::ICD_TM_furin::GFP</i>		Drabikowski
RU90		<i>ten-1(ok641)</i>	VC518 9x backcrossed	Trzebiatowska
RU97	kdEx41	<i>hsp::ten-1_full_ICD::GFP, rol-6</i>		Drabikowski
RU148		<i>phy-3(ok199)</i>	TP7 5x backcrossed	Topf
RU168		<i>ten-1(ok641);phy-3(ok199)</i>		Topf
RU170		<i>phy-1(ok162)</i>	JK2729 5x outcrossed	Topf
RU171		<i>ten-(ok641) phy-1(ok162)</i>		Topf
RU172		<i>ten-1(ok641) lam-1::gfp</i>		Topf
RU173		<i>phy-1(ok162) lam-1::gfp</i>		Topf
RU174		<i>phy-3(ok199) lam-1::gfp</i>		Topf
RU175		<i>ten-1(ok641);phy-3(ok199) lam-1::gfp</i>		Topf
RU176		<i>ten-(ok641) phy-1(ok162) lam-1::gfp</i>		Topf
RU177		<i>ten-(ok641) phy-1(ok162); phy-3(ok199)</i>		Topf
RU178		<i>phy-2(ok177)</i>	JK2757 5x outcrossed	Topf
RU179		<i>ten-1(ok641);phy-2(ok177)</i>		Topf
RU181		<i>phy-2(ok177);phy-3(ok199)</i>		Topf
RU182		<i>phy-2(ok177);phy-3(ok199); ten-1(ok641)</i>		Topf

Strain name	Allele name	Genotype	description	Investigator/ reference
RU184		<i>phy-2(ok177);ten-1(ok641);kdEx31</i>		Topf
RU185		<i>phy-1(ok162);kdEx31</i>		Topf
RU187		<i>phy-1(ok162) ajm-1::gfp</i>		Topf
RU188		<i>ten-1(ok641) phy-1(ok162) ajm-1::gfp</i>		Topf
RU198		<i>ten-1(ok641) ajm-1::gfp</i>		Topf
RU190		<i>ajm-1::gfp</i>	crossed with N2	Original from H. Grosshans
RU191	kdEx131	<i>myo-3p::phy-1cDNA::gfp::unc-54</i>	injection in N2, 5ng/μl kdEx131, 95ng/μl p123T	Topf
RU192		<i>ten-1(ok641) phy-1(ok162) myo-3::mCherry</i>		Topf
RU193		<i>myo-3::mCherry</i>		Topf
RU194	kdEx132	<i>phy-1p::phy-1cDNA::phy-1polyA</i>	injection in N2, 5ng/μl kdEx132, 10ng/μl unc- 122::gfp, 85ng/μl p123T	Topf
RU195		<i>ten-1(ok641) phy-1(ok162) kdEx131</i>		Topf
RU196		<i>ten-1(ok641) phy-1(ok162) kdEx132</i>		Topf
RU197		<i>ten-1(tm651) phy-1(ok162)</i>		Topf

Table 5. *C. elegans* strains used or generated in this study

6. APPENDIX

6.1. Summary of candidate genes and the observed phenotype

Enhancer of *ten-1* phenotype

gene	description	known RNAi phenotype (according „wormbase”)	knock-down in wild-type	knock-down in <i>ten-1(ok641)</i>
<i>tbb-2</i>	Beta-2-tubulin	emb	sck, pvl, ste, little progeny	adult sck, 100% emb
C36H8.1	Major sperm protein	age, slu	wt	lva, emb
<i>arx-5</i>	actin-related protein	emb	sma	sck, sma, little progeny
<i>scc-1</i>	Yeast scc (Mitotic condensin subunit) homolog protein	emb	Not 100% emb	100% emb
<i>ddb-1</i>	DNA damage-binding protein	emb, gro, unc	Not 100% emb, egl	emb, adl, ste
<i>lbp-1</i>	Fatty acid-binding protein homolog 1	wt	wt	emb, lva?, little progeny
<i>clec-167</i>	C-type lectin	ND	wt	adult arrested, emb
Y7A9A.1	Gamma-glutamyltransferase	non	wt	emb, little progeny, lva?
<i>phy-3</i>	Prolyl 4-hydroxylase subunit	wt	wt	
<i>lgc-9</i>	Ligand-Gated ion Channel	ND	wt	lva? little progeny
<i>odr-3</i>	Odorant response abnormal protein 3	ND	wt	lva? little progeny
<i>wwp-1</i>	Ww domain protein	emb	emb (not 100 %)	emb, lva?
<i>glp-1</i>	Notch receptor	emb	emb	increased emb
<i>ina-1</i>	integrin alpha	lvl, ste, stp	lva	emb, lva
<i>gei-11</i>	GEX interacting protein	sck, ste, lva, lvl	lva?	100 % lva
<i>ast-1</i>	ETS-box transcription factor	ND	WT, reduced brood size?	adult sck or let, little progeny
<i>egl-43</i>	zinc finger protein	pvl	pvl	pvl, 100 % ste
R05G6.4	DNA damage-binding protein	wt	wt	many eggs, little progeny

Suppressor of *ten-1* phenotype

gene	description	known RNAi phenotype	KD in wild type	knock-down in <i>ten-1(ok641)</i>
<i>gst-25</i>	Glutathione s-transferase	ND	wt	progeny comparable to wt
<i>col-17</i>	collagen	dpy, sck	dpy, adult burst	dpy, progeny comparable to wt
<i>pgl-1</i>	P granule protein	ND	wt	progeny comparable to wt
C36B1.11	unknown	ND	wt	progeny comparable to wt

Phenotype suppressed by *ten-1* deletion

gene	description	known RNAi phenotype (according „wormbase”)	knock-down in wild type	knock-down in <i>ten-1(ok641)</i>
Y55B1BR.3	CHROMO domain protein	emb	emb, ste	mutant phenotype
<i>hil-7</i>	histone	ND	emb, adl or arrested	mutant phenotype
<i>him-3</i>	Meiotic chromosome core protein	emb, him	emb, lva	mutant phenotype
<i>pxl-1</i>	paxillin	lva, gro, lvl	lva, ste	mutant phenotype
<i>dhs-3</i>	dehydrogenases	emb, sck	adl	mutant phenotype
<i>clp-4</i>	Calpain family protein	emb	dpy, egl, little progeny	mutant phenotype
<i>lfe-2</i>	adenylate kinase	unclassified	emb, lva	mutant phenotype
<i>unc-49</i>	inositol trisphosphate 3-kinase	ND	adult sck	mutant phenotype
<i>nex-3</i>	GABA receptor	sck, emb	emb, reduced brood size	mutant phenotype
<i>rheb-1</i>	annexin	gro, unc, stp	adl or arrested	mutant phenotype
<i>sdz-15</i>	GTPase	ND	adl, reduced brood size	mutant phenotype
<i>rpb-8</i>	F-box protein	emb	sck, ste, pvl	many eggs but progeny
C06G3.3	RNA polymerase II	ND	adl or arrested	mutant phenotype

Table 6. Putative genetic interaction partners of *ten-1*. All obtained genes of the RNAi screen are listed including the phenotype their knock-down caused in wild type and in *ten-1(ok641)* mutant. Additionally, the known RNAi phenotype of each gene is indicated as annotated in “wormbase” (www.wormbase.org). adl, adult lethal; age, extended life span; dpy, dumpy; emb, embryonic lethal; egl, egg laying defective; gro, slow growth; him, high incidence of males; lva, larval arrested; lvl, larval lethal; ND, not determined; pvl, protruding vulva; sck, sick; slu, sluggish; sma, small; stp, sterile progeny; ste, sterile; unc, uncoordinated; wt, wild type; little progeny, refers to subjective amount of F1 animals in comparison to the empty vector control and could reflect reduced brood size; mutant phenotype, refers to *ten-1* phenotype fed with empty vector RNAi

6.2. Abbreviations

°C	degree Celsius	
%	percent	
Δ	deletion	
A	app.	approximtly
		ATP	adenosine triphosphate
B	bp	base pair
C	cDNA	complementary DNA
		<i>C. elegans</i>	<i>Caenorhabditis elegans</i>
		CGC	<i>Caenorhabditis</i> Genetic Centre (Minnesota)
D	DNA	desoxyribonucleidacid
		ds	double stranded
		DTT	dithiothreitol
E	<i>E. coli</i>	<i>Escherichia coli</i>
		e.g.	for example
G	g	gravitation
		GFP	green fluorescent protein
H	h	hour
		<i>H. sapiens</i>	<i>Homo sapiens</i>
I	IPTG	isopropyl-β-D-thiogalactopyranoside

K	kDa	kilo Dalton
L	LB-Media	Luria-Bertani-Media
M	min	minute
		mRNA	messenger RNA
N	nt	nucleotide
		NGM	nematode growth media
O	OD	optical density
		ORF	open reading frame
P	PBS	phosphate buffered saline
		PCR	polymerase chain reaction
R	RNA	ribonucleic acid
		RNAi	RNA interference
		rpm	rounds per minute
S	SDS	sodium dodecyl sulphate
U	UTR	untranslated region
V	vs	versus
W	wt	wild type

7. REFERENCES

- Albertson, D. G. and Thomson, J. N.** (1976). The pharynx of *Caenorhabditis elegans*. *Philos Trans R Soc Lond B Biol Sci* **275**, 299-325.
- Bagutti, C., Forro, G., Ferralli, J., Rubin, B. and Chiquet-Ehrismann, R.** (2003). The intracellular domain of teneurin-2 has a nuclear function and represses zic-1-mediated transcription. *J Cell Sci* **116**, 2957-66.
- Baumgartner, S. and Chiquet-Ehrismann, R.** (1993). Tena, a *Drosophila* gene related to tenascin, shows selective transcript localization. *Mech Dev* **40**, 165-76.
- Baumgartner, S., Martin, D., Hagios, C. and Chiquet-Ehrismann, R.** (1994). Tenm, a *Drosophila* gene related to tenascin, is a new pair-rule gene. *EMBO J* **13**, 3728-40.
- Ben-Zur, T., Feige, E., Motro, B. and Wides, R.** (2000). The mammalian Odz gene family: homologs of a *Drosophila* pair-rule gene with expression implying distinct yet overlapping developmental roles. *Dev Biol* **217**, 107-20.
- Ben-Zur, T. and Wides, R.** (1999). Mapping homologs of *Drosophila* odd Oz (odz): Doc4/Odz4 to mouse chromosome 7, Odz1 to mouse chromosome 11; and ODZ3 to human chromosome Xq25. *Genomics* **58**, 102-3.
- Bercher, M., Wahl, J., Vogel, B. E., Lu, C., Hedgecock, E. M., Hall, D. H. and Plenefisch, J. D.** (2001). mua-3, a gene required for mechanical tissue integrity in *Caenorhabditis elegans*, encodes a novel transmembrane protein of epithelial attachment complexes. *J Cell Biol* **154**, 415-26.
- Bernassola, F., Karin, M., Ciechanover, A. and Melino, G.** (2008). The HECT family of E3 ubiquitin ligases: multiple players in cancer development. *Cancer Cell* **14**, 10-21.
- Bosher, J. M., Hahn, B. S., Legouis, R., Sookhareea, S., Weimer, R. M., Gansmuller, A., Chisholm, A. D., Rose, A. M., Bessereau, J. L. and Labouesse, M.** (2003). The *Caenorhabditis elegans* vab-10 spectraplaklin isoforms protect the epidermis against internal and external forces. *J Cell Biol* **161**, 757-68.
- Brown, N. H.** (2000). Cell-cell adhesion via the ECM: integrin genetics in fly and worm. *Matrix Biol* **19**, 191-201.
- Byrne, A. B., Weirauch, M. T., Wong, V., Koeva, M., Dixon, S. J., Stuart, J. M. and Roy, P. J.** (2007). A global analysis of genetic interactions in *Caenorhabditis elegans*. *J Biol* **6**, 8.
- Carrano, A. C., Liu, Z., Dillin, A. and Hunter, T.** (2009). A conserved ubiquitination pathway determines longevity in response to diet restriction. *Nature* **460**, 396-9.
- Chen, C., Sun, X., Guo, P., Dong, X. Y., Sethi, P., Zhou, W., Zhou, Z., Petros, J., Frierson, H. F., Jr., Vessella, R. L. et al.** (2007a). Ubiquitin E3 ligase WWP1 as an oncogenic factor in human prostate cancer. *Oncogene* **26**, 2386-94.
- Chen, C., Zhou, Z., Ross, J. S., Zhou, W. and Dong, J. T.** (2007b). The amplified WWP1 gene is a potential molecular target in breast cancer. *Int J Cancer* **121**, 80-87.
- Chin-Sang, I. D. and Chisholm, A. D.** (2000). Form of the worm: genetics of epidermal morphogenesis in *C. elegans*. *Trends Genet* **16**, 544-51.
- Chisholm, A. D. and Hardin, J.** (2005). Epidermal morphogenesis. *WormBook*, 1-22.

- Costa, M., Draper, B. W. and Priess, J. R.** (1997). The role of actin filaments in patterning the *Caenorhabditis elegans* cuticle. *Dev Biol* **184**, 373-84.
- Costa, M., Raich, W., Agbunag, C., Leung, B., Hardin, J. and Priess, J. R.** (1998). A putative catenin-cadherin system mediates morphogenesis of the *Caenorhabditis elegans* embryo. *J Cell Biol* **141**, 297-308.
- Cox, E. A. and Hardin, J.** (2004). Sticky worms: adhesion complexes in *C. elegans*. *J Cell Sci* **117**, 1885-97.
- de Pereda, J. M., Ortega, E., Alonso-Garcia, N., Gomez-Hernandez, M. and Sonnenberg, A.** (2009). Advances and perspectives of the architecture of hemidesmosomes: lessons from structural biology. *Cell Adh Migr* **3**, 361-4.
- Ding, M., Goncharov, A., Jin, Y. and Chisholm, A. D.** (2003). *C. elegans* ankyrin repeat protein VAB-19 is a component of epidermal attachment structures and is essential for epidermal morphogenesis. *Development* **130**, 5791-801.
- Ding, M., King, R. S., Berry, E. C., Wang, Y., Hardin, J. and Chisholm, A. D.** (2008). The cell signaling adaptor protein EPS-8 is essential for *C. elegans* epidermal elongation and interacts with the ankyrin repeat protein VAB-19. *PLoS One* **3**, e3346.
- Ding, M., Woo, W. M. and Chisholm, A. D.** (2004). The cytoskeleton and epidermal morphogenesis in *C. elegans*. *Exp Cell Res* **301**, 84-90.
- Dodemont, H., Riemer, D., Ledger, N. and Weber, K.** (1994). Eight genes and alternative RNA processing pathways generate an unexpectedly large diversity of cytoplasmic intermediate filament proteins in the nematode *Caenorhabditis elegans*. *EMBO J* **13**, 2625-38.
- Drabikowski, K., Trzebiatowska, A. and Chiquet-Ehrismann, R.** (2005). *ten-1*, an essential gene for germ cell development, epidermal morphogenesis, gonad migration, and neuronal pathfinding in *Caenorhabditis elegans*. *Dev Biol* **282**, 27-38.
- Fascetti, N. and Baumgartner, S.** (2002). Expression of *Drosophila* Ten-a, a dimeric receptor during embryonic development. *Mech Dev* **114**, 197-200.
- Feng, K., Zhou, X. H., Oohashi, T., Morgelin, M., Lustig, A., Hirakawa, S., Ninomiya, Y., Engel, J., Rauch, U. and Fassler, R.** (2002). All four members of the Ten-m/Odz family of transmembrane proteins form dimers. *J Biol Chem* **277**, 26128-35.
- Fessler, J. H. and Fessler, L. I.** (1978). Biosynthesis of procollagen. *Annu Rev Biochem* **47**, 129-62.
- Francis, R. and Waterston, R. H.** (1991). Muscle cell attachment in *Caenorhabditis elegans*. *J Cell Biol* **114**, 465-79.
- Friedman, L., Higgin, J. J., Moulder, G., Barstead, R., Raines, R. T. and Kimble, J.** (2000). Prolyl 4-hydroxylase is required for viability and morphogenesis in *Caenorhabditis elegans*. *Proc Natl Acad Sci U S A* **97**, 4736-41.
- Frokjaer-Jensen, C., Davis, M. W., Hopkins, C. E., Newman, B. J., Thummel, J. M., Olesen, S. P., Grunnet, M. and Jorgensen, E. M.** (2008). Single-copy insertion of transgenes in *Caenorhabditis elegans*. *Nat Genet* **40**, 1375-83.

- Gehmlich, K., Pinotsis, N., Hayess, K., van der Ven, P. F., Milting, H., El Banayosy, A., Korfer, R., Wilmanns, M., Ehler, E. and Furst, D. O.** (2007). Paxillin and ponsin interact in nascent costameres of muscle cells. *J Mol Biol* **369**, 665-82.
- Gendreau, S. B., Moskowitz, I. P., Terns, R. M. and Rothman, J. H.** (1994). The potential to differentiate epidermis is unequally distributed in the AB lineage during early embryonic development in *C. elegans*. *Dev Biol* **166**, 770-81.
- Geuijen, C. A. and Sonnenberg, A.** (2002). Dynamics of the alpha6beta4 integrin in keratinocytes. *Mol Biol Cell* **13**, 3845-58.
- Graham, P. L., Johnson, J. J., Wang, S., Sibley, M. H., Gupta, M. C. and Kramer, J. M.** (1997). Type IV collagen is detectable in most, but not all, basement membranes of *Caenorhabditis elegans* and assembles on tissues that do not express it. *J Cell Biol* **137**, 1171-83.
- Gupta, M. C., Graham, P. L. and Kramer, J. M.** (1997). Characterization of alpha1(IV) collagen mutations in *Caenorhabditis elegans* and the effects of alpha1 and alpha2(IV) mutations on type IV collagen distribution. *J Cell Biol* **137**, 1185-96.
- Hall, D. H. and Altun, Z. F.** (2008). *C. elegans Atlas*.
- Hill, K. L., Harfe, B. D., Dobbins, C. A. and L'Hernault, S. W.** (2000). dpy-18 encodes an alpha-subunit of prolyl-4-hydroxylase in *caenorhabditis elegans*. *Genetics* **155**, 1139-48.
- Holster, T., Pakkanen, O., Soininen, R., Sormunen, R., Nokelainen, M., Kivirikko, K. I. and Myllyharju, J.** (2007). Loss of assembly of the main basement membrane collagen, type IV, but not fibril-forming collagens and embryonic death in collagen prolyl 4-hydroxylase I null mice. *J Biol Chem* **282**, 2512-9.
- Hong, L., Elbl, T., Ward, J., Franzini-Armstrong, C., Rybicka, K. K., Gatewood, B. K., Baillie, D. L. and Bucher, E. A.** (2001). MUP-4 is a novel transmembrane protein with functions in epithelial cell adhesion in *Caenorhabditis elegans*. *J Cell Biol* **154**, 403-14.
- Hresko, M. C., Schriefer, L. A., Shrimankar, P. and Waterston, R. H.** (1999). Myotactin, a novel hypodermal protein involved in muscle-cell adhesion in *Caenorhabditis elegans*. *J Cell Biol* **146**, 659-72.
- Hresko, M. C., Williams, B. D. and Waterston, R. H.** (1994). Assembly of body wall muscle and muscle cell attachment structures in *Caenorhabditis elegans*. *J Cell Biol* **124**, 491-506.
- Huang, C. C., Hall, D. H., Hedgecock, E. M., Kao, G., Karantza, V., Vogel, B. E., Hutter, H., Chisholm, A. D., Yurchenco, P. D. and Wadsworth, W. G.** (2003). Laminin alpha subunits and their role in *C. elegans* development. *Development* **130**, 3343-58.
- Huang, K., Johnson, K. D., Petcherski, A. G., Vandergon, T., Mosser, E. A., Copeland, N. G., Jenkins, N. A., Kimble, J. and Bresnick, E. H.** (2000). A HECT domain ubiquitin ligase closely related to the mammalian protein WWP1 is essential for *Caenorhabditis elegans* embryogenesis. *Gene* **252**, 137-45.
- Jones, J. C., Hopkinson, S. B. and Goldfinger, L. E.** (1998). Structure and assembly of hemidesmosomes. *Bioessays* **20**, 488-94.
- Kamath, R. S. and Ahringer, J.** (2003). Genome-wide RNAi screening in *Caenorhabditis elegans*. *Methods* **30**, 313-21.

- Kaminsky, R., Denison, C., Bening-Abu-Shach, U., Chisholm, A. D., Gygi, S. P. and Broday, L.** (2009). SUMO regulates the assembly and function of a cytoplasmic intermediate filament protein in *C. elegans*. *Dev Cell* **17**, 724-35.
- Kao, G., Huang, C. C., Hedgecock, E. M., Hall, D. H. and Wadsworth, W. G.** (2006). The role of the laminin beta subunit in laminin heterotrimer assembly and basement membrane function and development in *C. elegans*. *Dev Biol* **290**, 211-9.
- Kedersha, N. L., Gupta, M., Li, W., Miller, I. and Anderson, P.** (1999). RNA-binding proteins TIA-1 and TIAR link the phosphorylation of eIF-2 alpha to the assembly of mammalian stress granules. *J Cell Biol* **147**, 1431-42.
- Kenzelmann Broz, D., Tucker, R. P., Leachman, N. T. and Chiquet-Ehrismann, R.** (2010). The expression of teneurin-4 in the avian embryo: potential roles in patterning in the limb and nervous system. *Int.J.Dev.Biol.* **in press**.
- Kenzelmann, D., Chiquet-Ehrismann, R., Leachman, N. T. and Tucker, R. P.** (2008). Teneurin-1 is expressed in interconnected regions of the developing brain and is processed in vivo. *BMC Dev Biol* **8**, 30.
- Kenzelmann, D., Chiquet-Ehrismann, R. and Tucker, R. P.** (2007). Teneurins, a transmembrane protein family involved in cell communication during neuronal development. *Cell Mol Life Sci* **64**, 1452-6.
- Keskiaho, K., Kukkola, L., Page, A. P., Winter, A. D., Vuoristo, J., Sormunen, R., Nissi, R., Riihimaa, P. and Myllyharju, J.** (2008). Characterization of a novel *Caenorhabditis elegans* prolyl 4-hydroxylase with a unique substrate specificity and restricted expression in the pharynx and excretory duct. *J Biol Chem* **283**, 10679-89.
- Kioka, N., Ueda, K. and Amachi, T.** (2002). Vinexin, CAP/ponsin, ArgBP2: a novel adaptor protein family regulating cytoskeletal organization and signal transduction. *Cell Struct Funct* **27**, 1-7.
- Labouesse, M.** (2006). Epithelial junctions and attachments. *WormBook*, 1-21.
- Leamey, C. A., Merlin, S., Lattouf, P., Sawatari, A., Zhou, X., Demel, N., Glendining, K. A., Oohashi, T., Sur, M. and Fassler, R.** (2007). Ten_m3 regulates eye-specific patterning in the mammalian visual pathway and is required for binocular vision. *PLoS Biol* **5**, e241.
- Levine, A., Bashan-Ahrend, A., Budai-Hadrian, O., Gartenberg, D., Menasherow, S. and Wides, R.** (1994). Odd Oz: a novel *Drosophila* pair rule gene. *Cell* **77**, 587-98.
- Levine, A., Weiss, C. and Wides, R.** (1997). Expression of the pair-rule gene odd Oz (odz) in imaginal tissues. *Dev Dyn* **209**, 1-14.
- Lossie, A. C., Nakamura, H., Thomas, S. E. and Justice, M. J.** (2005). Mutation of I7Rn3 shows that Odz4 is required for mouse gastrulation. *Genetics* **169**, 285-99.
- Meister, P., Towbin, B. D., Pike, B. L., Ponti, A. and Gasser, S. M.** The spatial dynamics of tissue-specific promoters during *C. elegans* development. *Genes Dev* **24**, 766-82.
- Mello, C. C., Kramer, J. M., Stinchcomb, D. and Ambros, V.** (1991). Efficient gene transfer in *C. elegans*: extrachromosomal maintenance and integration of transforming sequences. *Embo J* **10**, 3959-70.

- Mieda, M., Kikuchi, Y., Hirate, Y., Aoki, M. and Okamoto, H.** (1999). Compartmentalized expression of zebrafish ten-m3 and ten-m4, homologues of the *Drosophila* ten(m)/odd Oz gene, in the central nervous system. *Mech Dev* **87**, 223-7.
- Minet, A. D. and Chiquet-Ehrismann, R.** (2000). Phylogenetic analysis of teneurin genes and comparison to the rearrangement hot spot elements of *E. coli*. *Gene* **257**, 87-97.
- Minet, A. D., Rubin, B. P., Tucker, R. P., Baumgartner, S. and Chiquet-Ehrismann, R.** (1999). Teneurin-1, a vertebrate homologue of the *Drosophila* pair-rule gene ten-m, is a neuronal protein with a novel type of heparin-binding domain. *J Cell Sci* **112 (Pt 12)**, 2019-32.
- Morck, C., Vivekanand, V., Jafari, G. and Pilon, M.** (2010). *C. elegans* ten-1 is synthetic lethal with mutations in cytoskeleton regulators, and enhances many axon guidance defective mutants. *BMC Dev Biol* **10**, 55.
- Murakami, T., Fukunaga, T., Takeshita, N., Hiratsuka, K., Abiko, Y., Yamashiro, T. and Takano-Yamamoto, T.** (2010). Expression of Ten-m/Odz3 in the fibrous layer of mandibular condylar cartilage during postnatal growth in mice. *J Anat*.
- Myllyharju, J. and Kivirikko, K. I.** (2004). Collagens, modifying enzymes and their mutations in humans, flies and worms. *Trends Genet* **20**, 33-43.
- Myllyharju, J., Kukkola, L., Winter, A. D. and Page, A. P.** (2002). The exoskeleton collagens in *Caenorhabditis elegans* are modified by prolyl 4-hydroxylases with unique combinations of subunits. *J Biol Chem* **277**, 29187-96.
- Norman, K. R. and Moerman, D. G.** (2000). The let-268 locus of *Caenorhabditis elegans* encodes a procollagen lysyl hydroxylase that is essential for type IV collagen secretion. *Dev Biol* **227**, 690-705.
- Novelli, J., Ahmed, S. and Hodgkin, J.** (2004). Gene interactions in *Caenorhabditis elegans* define DPY-31 as a candidate procollagen C-proteinase and SQT-3/ROL-4 as its predicted major target. *Genetics* **168**, 1259-73.
- Nunes, S. M., Ferralli, J., Choi, K., Brown-Luedi, M., Minet, A. D. and Chiquet-Ehrismann, R.** (2005). The intracellular domain of teneurin-1 interacts with MBD1 and CAP/ponsin resulting in subcellular codistribution and translocation to the nuclear matrix. *Exp Cell Res* **305**, 122-32.
- Oohashi, T., Zhou, X. H., Feng, K., Richter, B., Morgelin, M., Perez, M. T., Su, W. D., Chiquet-Ehrismann, R., Rauch, U. and Fassler, R.** (1999). Mouse ten-m/Odz is a new family of dimeric type II transmembrane proteins expressed in many tissues. *J Cell Biol* **145**, 563-77.
- Page, B. D., Zhang, W., Steward, K., Blumenthal, T. and Priess, J. R.** (1997). ELT-1, a GATA-like transcription factor, is required for epidermal cell fates in *Caenorhabditis elegans* embryos. *Genes Dev* **11**, 1651-61.
- Piekny, A. J., Johnson, J. L., Cham, G. D. and Mains, P. E.** (2003). The *Caenorhabditis elegans* nonmuscle myosin genes nmy-1 and nmy-2 function as redundant components of the let-502/Rho-binding kinase and mel-11/myosin phosphatase pathway during embryonic morphogenesis. *Development* **130**, 5695-704.
- Priess, J. R. and Hirsh, D. I.** (1986). *Caenorhabditis elegans* morphogenesis: the role of the cytoskeleton in elongation of the embryo. *Dev Biol* **117**, 156-73.

- Prokop, A., Martin-Bermudo, M. D., Bate, M. and Brown, N. H.** (1998). Absence of PS integrins or laminin A affects extracellular adhesion, but not intracellular assembly, of hemiadherens and neuromuscular junctions in *Drosophila* embryos. *Dev Biol* **196**, 58-76.
- Rabinovitz, I., Tsomo, L. and Mercurio, A. M.** (2004). Protein kinase C- α phosphorylation of specific serines in the connecting segment of the beta 4 integrin regulates the dynamics of type II hemidesmosomes. *Mol Cell Biol* **24**, 4351-60.
- Rakovitsky, N., Buganim, Y., Swissa, T., Kinel-Tahan, Y., Brenner, S., Cohen, M. A., Levine, A. and Wides, R.** (2007). *Drosophila* Ten-a is a maternal pair-rule and patterning gene. *Mech Dev* **124**, 911-24.
- Riihimaa, P., Nissi, R., Page, A. P., Winter, A. D., Keskiaho, K., Kivirikko, K. I. and Myllyharju, J.** (2002). Egg shell collagen formation in *Caenorhabditis elegans* involves a novel prolyl 4-hydroxylase expressed in spermatheca and embryos and possessing many unique properties. *J Biol Chem* **277**, 18238-43.
- Roberts, B., Clucas, C. and Johnstone, I. L.** (2003). Loss of SEC-23 in *Caenorhabditis elegans* causes defects in oogenesis, morphogenesis, and extracellular matrix secretion. *Mol Biol Cell* **14**, 4414-26.
- Rubin, B. P., Tucker, R. P., Brown-Luedi, M., Martin, D. and Chiquet-Ehrismann, R.** (2002). Teneurin 2 is expressed by the neurons of the thalamofugal visual system in situ and promotes homophilic cell-cell adhesion in vitro. *Development* **129**, 4697-705.
- Rubin, B. P., Tucker, R. P., Martin, D. and Chiquet-Ehrismann, R.** (1999). Teneurins: a novel family of neuronal cell surface proteins in vertebrates, homologous to the *Drosophila* pair-rule gene product Ten-m. *Dev Biol* **216**, 195-209.
- Shakes, D. C. and Epstein, H. F.** (1995). *Caenorhabditis elegans*: Modern Biological Analysis of an Organism: Academic Press, Inc.
- Shaye, D. D. and Greenwald, I.** (2005). LIN-12/Notch trafficking and regulation of DSL ligand activity during vulval induction in *Caenorhabditis elegans*. *Development* **132**, 5081-92.
- Shen, C., Nettleton, D., Jiang, M., Kim, S. K. and Powell-Coffman, J. A.** (2005). Roles of the HIF-1 hypoxia-inducible factor during hypoxia response in *Caenorhabditis elegans*. *J Biol Chem* **280**, 20580-8.
- Simmer, F., Tijsterman, M., Parrish, S., Koushika, S. P., Nonet, M. L., Fire, A., Ahringer, J. and Plasterk, R. H.** (2002). Loss of the putative RNA-directed RNA polymerase RRF-3 makes *C. elegans* hypersensitive to RNAi. *Curr Biol* **12**, 1317-9.
- Simske, J. S. and Hardin, J.** (2001). Getting into shape: epidermal morphogenesis in *Caenorhabditis elegans* embryos. *Bioessays* **23**, 12-23.
- Simske, J. S., Koppen, M., Sims, P., Hodgkin, J., Yonkof, A. and Hardin, J.** (2003). The cell junction protein VAB-9 regulates adhesion and epidermal morphology in *C. elegans*. *Nat Cell Biol* **5**, 619-25.
- Sonawane, M., Martin-Maischein, H., Schwarz, H. and Nusslein-Volhard, C.** (2009). Lgl2 and E-cadherin act antagonistically to regulate hemidesmosome formation during epidermal development in zebrafish. *Development* **136**, 1231-40.

- Spike, C. A., Davies, A. G., Shaw, J. E. and Herman, R. K.** (2002). MEC-8 regulates alternative splicing of unc-52 transcripts in *C. elegans* hypodermal cells. *Development* **129**, 4999-5008.
- Trzebiatowska, A., Topf, U., Sauder, U., Drabikowski, K. and Chiquet-Ehrismann, R.** (2008). *Caenorhabditis elegans* teneurin, ten-1, is required for gonadal and pharyngeal basement membrane integrity and acts redundantly with integrin ina-1 and dystroglycan dgn-1. *Mol Biol Cell* **19**, 3898-908.
- Tsuruta, D., Hopkinson, S. B. and Jones, J. C.** (2003). Hemidesmosome protein dynamics in live epithelial cells. *Cell Motil Cytoskeleton* **54**, 122-34.
- Tucker, R. P. and Chiquet-Ehrismann, R.** (2006). Teneurins: a conserved family of transmembrane proteins involved in intercellular signaling during development. *Dev Biol* **290**, 237-45.
- Tucker, R. P., Chiquet-Ehrismann, R., Chevron, M. P., Martin, D., Hall, R. J. and Rubin, B. P.** (2001). Teneurin-2 is expressed in tissues that regulate limb and somite pattern formation and is induced in vitro and in situ by FGF8. *Dev Dyn* **220**, 27-39.
- Tucker, R. P., Kenzelmann, D., Trzebiatowska, A. and Chiquet-Ehrismann, R.** (2007). Teneurins: transmembrane proteins with fundamental roles in development. *Int J Biochem Cell Biol* **39**, 292-7.
- Tucker, R. P., Martin, D., Kos, R. and Chiquet-Ehrismann, R.** (2000). The expression of teneurin-4 in the avian embryo. *Mech Dev* **98**, 187-91.
- Vogel, B. E. and Hedgecock, E. M.** (2001). Hemicentin, a conserved extracellular member of the immunoglobulin superfamily, organizes epithelial and other cell attachments into oriented line-shaped junctions. *Development* **128**, 883-94.
- Wang, L., Rotzinger, S., Al Chawaf, A., Elias, C. F., Baryte-Lovejoy, D., Qian, X., Wang, N. C., De Cristofaro, A., Belsham, D., Bittencourt, J. C. et al.** (2005). Teneurin proteins possess a carboxy terminal sequence with neuromodulatory activity. *Brain Res Mol Brain Res* **133**, 253-65.
- White, J. G.** (1988). The anatomy. In "The Nematode *Caenorhabditis elegans*". NY: Cold Spring Harbor Laboratory Press, Cold Spring Harbor.
- White, J. G., Southgate, E., Thomson, J. N. and Brenner, S.** (1976). The structure of the ventral nerve cord of *Caenorhabditis elegans*. *Philos Trans R Soc Lond B Biol Sci* **275**, 327-48.
- Williams-Masson, E. M., Heid, P. J., Lavin, C. A. and Hardin, J.** (1998). The cellular mechanism of epithelial rearrangement during morphogenesis of the *Caenorhabditis elegans* dorsal hypodermis. *Dev Biol* **204**, 263-76.
- Williams-Masson, E. M., Malik, A. N. and Hardin, J.** (1997). An actin-mediated two-step mechanism is required for ventral enclosure of the *C. elegans* hypodermis. *Development* **124**, 2889-901.
- Williams, B. D. and Waterston, R. H.** (1994). Genes critical for muscle development and function in *Caenorhabditis elegans* identified through lethal mutations. *J Cell Biol* **124**, 475-90.
- Winter, A. D. and Page, A. P.** (2000). Prolyl 4-hydroxylase is an essential procollagen-modifying enzyme required for exoskeleton formation and the maintenance of body shape in the nematode *Caenorhabditis elegans*. *Mol Cell Biol* **20**, 4084-93.
- Wissmann, A., Ingles, J., McGhee, J. D. and Mains, P. E.** (1997). *Caenorhabditis elegans* LET-502 is related to Rho-binding kinases and human myotonic dystrophy kinase and interacts genetically with

a homolog of the regulatory subunit of smooth muscle myosin phosphatase to affect cell shape. *Genes Dev* **11**, 409-22.

Woo, W. M., Goncharov, A., Jin, Y. and Chisholm, A. D. (2004). Intermediate filaments are required for *C. elegans* epidermal elongation. *Dev Biol* **267**, 216-29.

Zahreddine, H., Zhang, H., Diogon, M., Nagamatsu, Y. and Labouesse, M. (2010). CRT-1/calreticulin and the E3 ligase EEL-1/HUWE1 control hemidesmosome maturation in *C. elegans* development. *Curr Biol* **20**, 322-7.

Zhang, H. and Labouesse, M. (2010). The making of hemidesmosome structures in vivo. *Dev Dyn* **239**, 1465-76.

Zhang, M., Liu, J., Cheng, A., Deyoung, S. M., Chen, X., Dold, L. H. and Saltiel, A. R. (2006). CAP interacts with cytoskeletal proteins and regulates adhesion-mediated ERK activation and motility. *EMBO J* **25**, 5284-93.

Zhou, X. H., Brandau, O., Feng, K., Oohashi, T., Ninomiya, Y., Rauch, U. and Fassler, R. (2003). The murine Ten-m/Odz genes show distinct but overlapping expression patterns during development and in adult brain. *Gene Expr Patterns* **3**, 397-405.

CURRICULUM VITAE

Name **Ulrike Topf**
Date of Birth August 17th 1982
Nationality German
Contact ulrike.topf@fmi.ch

Education

PhD (graduate studies in cell biology) Feb 2007 – Jan 2011
University of Basel, Switzerland
Master of Science (undergraduate studies in genetic, cell biology, immunology and virology) Oct 2003 – Dec 2006
Albert Ludwigs University, Freiburg i. B., Germany
Bachelor of Science (undergraduate studies in biology) Sep 2001 – Oct 2003
Johann-Wolfgang-Goethe University, Frankfurt a.M., Germany

Working experience

International PhD Program at the Friedrich Miescher Institute for Biomedical research, Basel, Switzerland Feb 2007 – present
laboratory of Prof. Dr. Ruth Chiquet-Ehrismann
Phd study: „ Investigations on the function of *ten-1* during embryonic development in *Caenorhabditis elegans*.“
Albert Ludwigs University, Freiburg i. B., Germany Nov 2005 – Dec 2006
Dept. Molecular Genetic and Bioinformatics
laboratory of Prof. Ralf Baumeister
Diploma study: “Protein modification by ubiquitin – like modifier UBL-1 in *Caenorhabditis elegans*”
Albert Ludwigs University, Freiburg i. B., Germany Nov 2004 – Dec 2006
Dept. Molecular Genetic and Bioinformatics: Student job
Albert Ludwigs University, Freiburg i. B., Germany Feb 2005 – Jun 2005
Dept. Virology: Student job

Scientific contributions

XXIInd FECTS Meeting, Davos, Switzerland

July 2010

oral and poster presentation

“*C. elegans* Teneurin, *ten-1*, genetically interacts with the collagen modifying enzyme prolyl 4-hydroxylase and maintains basement membrane integrity.”

17th International *C. elegans* meeting, LA, USA

June 2009

poster presentation

“High throughput screen for genes interacting with *ten-1*.”

Annual Meetings of the FMI

2007 – 2010

poster presentations

“High throughput RNAi screens for genes interacting with *ten-1*”

“*C. elegans* teneurin, *ten-1*, genetically interacts with genes coding for the collagen modifying enzyme prolyl 4-hydroxylase”

“*C. elegans* teneurin, *ten-1*, genetically interacts with the collagen modifying enzyme, prolyl 4-hydroxylase, and maintains basement membrane integrity”

Regional Worm meetings, Basel, Switzerland

2007 – 2010

Publications

Trzebiatowska, A., **Topf, U.**, Sauder, U., Drabikowski, K. and Chiquet-Ehrismann, R. (2008). *Caenorhabditis elegans* teneurin, *ten-1*, is required for gonadal and pharyngeal basement membrane integrity and acts redundantly with integrin *ina-1* and dystroglycan *dgn-1*. *Mol Biol Cell* 19, 3898-908.

Topf, U. and Chiquet-Ehrismann, R. (2011). Genetic interaction between *C. elegans* teneurin, *ten-1*, and the prolyl 4-hydroxylase, *phy-1*, and their function in collagen IV mediated basement membrane integrity during late elongation of the embryo. *Mol Biol Cell* (in press)